Design of Star-Shaped Organoiron Oligomers with Azo Chromophores

by

Man Ding

A THESIS SUBMITTED IN PARTIAL FULFILLMENT
OF THE REQUIREMENTS FOR THE DEGREE OF

MASTER OF SCIENCE

in

The College of Graduate Studies
(Chemistry)

THE UNIVERSITY OF BRITISH COLUMBIA
(Okanagan)

April 2011

Abstract

The synthesis and characterization of novel star-shaped oligomers containing cationic η^6-chloroarene-η^5-cyclopentadienyliron(II) complexes functionalized with azo chromophores were described in the thesis. Star-shaped macromolecules and dendrimers are of great interest for their application in light-harvesting systems, drug delivery, catalysis, and solvents. The incorporation of cationic η^6-chloroarene-η^5-cyclopentadienyliron moieties can enhance solubility and facilitate nucleophilic aromatic substitution and addition reactions due to the intense electron-withdrawing ability of the iron center. On the other hand, the azo dye chromophore in the oligomers has many applications due to its unique photophysical properties and acid-sensing capabilities.

Controlled synthetic methods involving both convergent and divergent approaches were employed to give distinct symmetrical branches that alternate between organoiron complexes and azobenzene moieties. Preparation of these molecules was achieved via metal-mediated nucleophilic aromatic substitutions and Steglich esterifications. These oligomers and their precursors were characterized through nuclear magnetic resonance spectroscopy, infrared spectroscopy, ultraviolet-visible spectroscopy and cyclic voltammetry.

Table of contents

List of figures

List of schemes

List of abbreviations

APT   attached proton test (in ^{13}C NMR spectroscopy)

Ar   aryl

*Ar   complexed aryl

ATR   attenuated total reflectance

br   broad

^{13}C carbon-13

conc.   concentrated

°C   degrees Celsius

Cp   cyclopentadienyl ring

*`Cp   non-functionalized cyclopentadienyl ring of ferrocene-1-carboxylic acid

*Cp   functionalized cyclopentadienyl ring of ferrocene-1-carboxylic acid

δ   chemical shift

d   doublet (in a spectrum)

dd   doublet of doublets(in a spectrum)

d_6 deuterium

DCC   N, N'-dicyclohexylcarbodiimide ($C_{13}H_{22}N_2$)

DCM   dichloromethane

DCU   N, N'-dicyclohexylurea ($C_{13}H_{24}N_2O$)

DMAP   4-dimethylaminopyridine ((CH_3)$_2NC_5H_4N$)

DMF   N,N-dimethylformamide

DMSO   dimethylsulfoxide

EM   Erlenmeyer

eq.   equivalents

Et	ethyl
FTIR	Fourier transform infrared
g	grams
gdqCOSY	gradient double quantum correlation spectroscopy (NMR experiment)
gHMBC	gradient heteronuclear multiple bond coherence (NMR experiment)
gHSQC	gradient heteronuclear single quantum coherence (NMR experiment)
^1H	proton
h	hours
Hz	Hertz (s^{-1})
IR	infrared spectroscopy
J	coupling constant (in spectroscopy; Hz)
L	litre (10^{-3} m^{-3})
M	molar (mol $Ł^{-1}$)
m	multiplet
Me	methyl
min	minutes
mL	millilitre (10^{-3} L)
mmol	millimole (10^{-3} mole)
mol	mole ($6.022 \cdot 10^{-23}$ particles)
nm	nanometer
NMR	nuclear magnetic resonance
o	ortho
p	para
PAMAM	poly (amidoamine)

pKa	-log of the Acid dissociation constant
POPAM	poly (propylenimine)
ppm	parts per million
q	quartet (in a spectrum)
RBF	round bottom flask
s	singlet (in a spectrum)
t	triplet (in a spectrum)
THF	tetrahydrofuran
UV	ultraviolet
UV-vis	ultraviolet-visible
λ_{max}	maximum wavelength

Acknowledgements

I owe my deepest gratitude to my supervisor, Dr. Alaa Abd-El-Aziz, whose encouragement, guidance, and support from the initial to the final level enabled me to develop an understanding of this project. I would also like to thank the members of my committee, Dr. Kevin Smith and Dr. Stephen McNeil, for teaching me about organometallic chemistry in the past two years. I would like to thank Dr. Paul Shipley for his assistance with NMR spectroscopy, and for teaching me helpful ways to run my NMR experiments more smoothly. I would also like to thank Dr. Edward Neeland for his answers to my random questions.

I am indebted to all the past and current members of the Abd-El-Aziz research group for their help. I would especially like to thank Dr. Patrick Shipman for his wisdom and patience in the lab. Thank you to Elizabeth Strohm and Sibel Sezgin for their efforts on this project. Thank you, Jessica Pilfold, for your help in editing this thesis.

Last but not least, I would like to express my thanks to my family, and all my friends for their support.

Chapter 1. Introduction

1.1 Dendrimers and star-shaped macromolecules

Traditionally, the study of macromolecular chemistry has focused on linear polymers, which are usually single, long-chain molecules with different kinds of functional groups present as repeating units. Linear polymers have been studied since the late 1700s, when chemists performed the chemical modification of linear polymer materials like natural rubber.[1] Today, many of the most famous polymers are linear polymers, such as nylon 6-6[2] and polyvinyl chloride[3], both widely seen in industry, as well as in daily life (Figure 1-1).

nylon 6-6

polyvinyl chloride
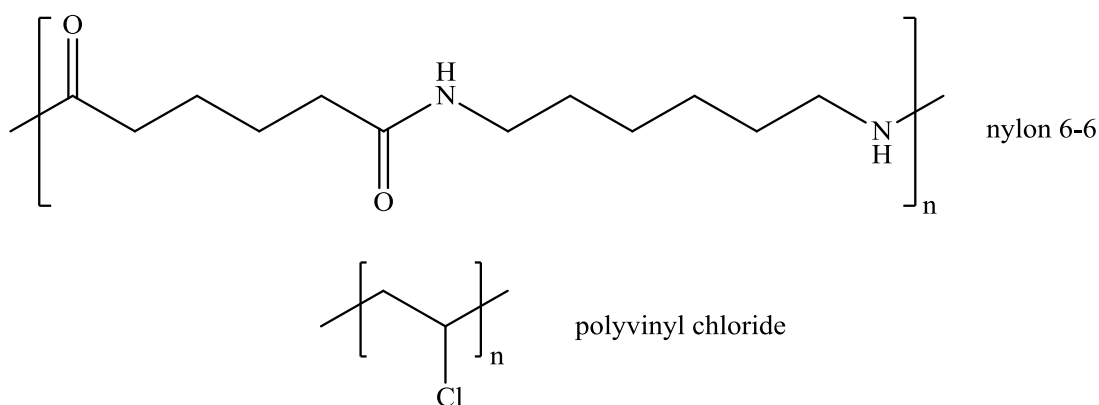
Figure 1-1: Nylon 6- 6[2] and polyvinyl chloride[3]

In fact, macromolecular chemistry is a multidisciplinary science that studies a variety of macromolecules. For example, aside from natural rubber, there are countless types of natural macromolecules, including starch and protein. In the fast-growing area of synthetic macromolecules, there are dendrimers and star-shaped macromolecules that have been studied for twenty years and are believed to have abundant applications in the future.[4] Dendrimers are a type of macromolecule that branches out in a star-shaped, three-dimensional architecture. While it is also called "arborol" or a cascade molecule, "dendrimer" is the most commonly

accepted term.[5] Figure 1-2 represents one example of polyamidoamine (PAMAM) dendrimers, today's most common class of dendrimer for applications in material science and biotechnology.[6]
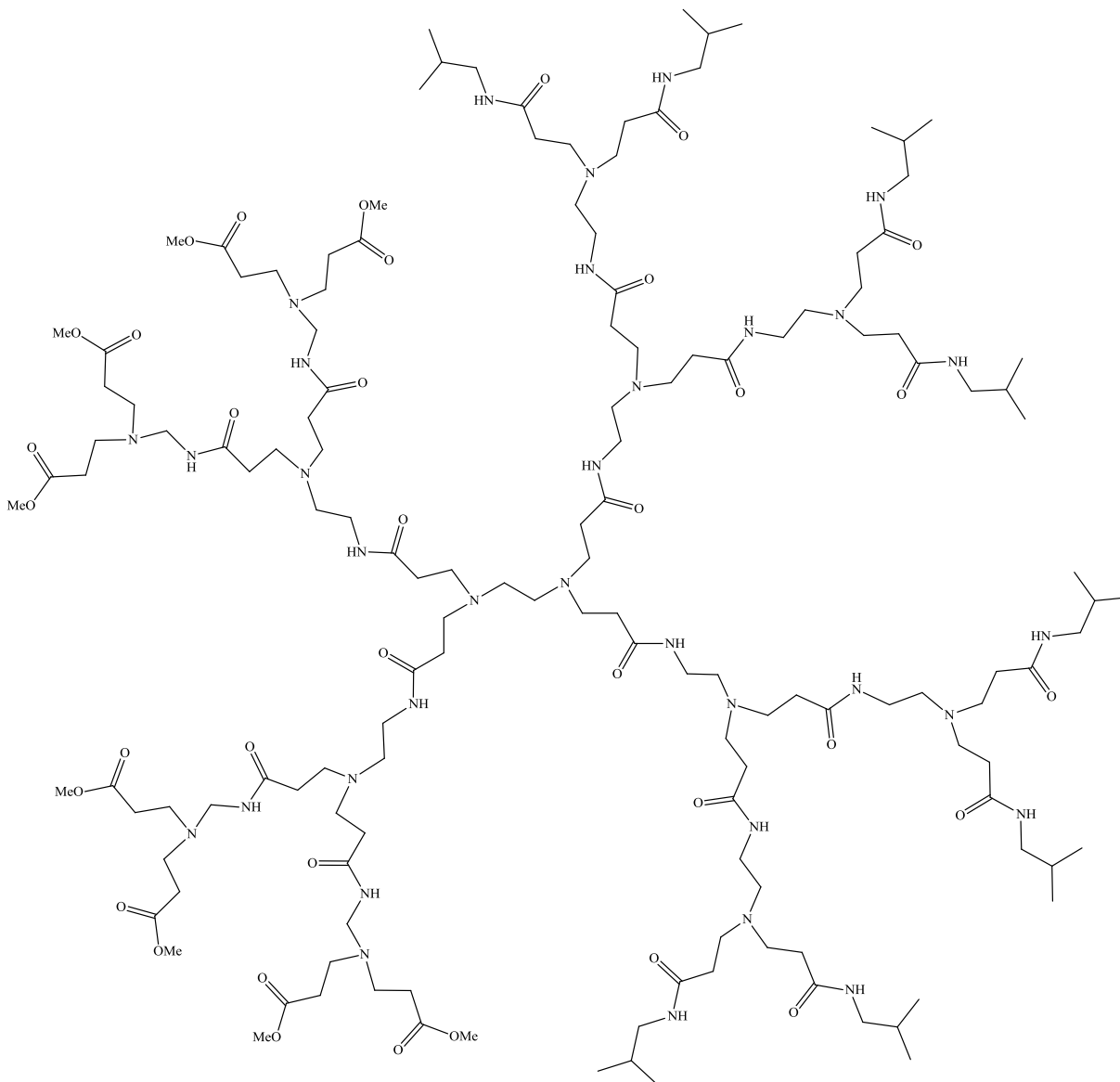
Figure 1-2: An unsymmetrical PAMAM dendrimer[6]

The star-shaped macromolecule, on the other hand, is defined by similarly-sized linear polymeric chains that originate from a central multifunctional core.[7] The structure of a star-shaped macromolecule is closer to that of linear polymers than dendrimers, but it is often linked to dendrimers, as both are classified as branched macromolecules. Figure 1-3 shows

2

one example of the star-shaped poly(ε-caprolactone), a widely studied type of star-shaped macromolecule due to its potential applications in the biomedical field.[8]
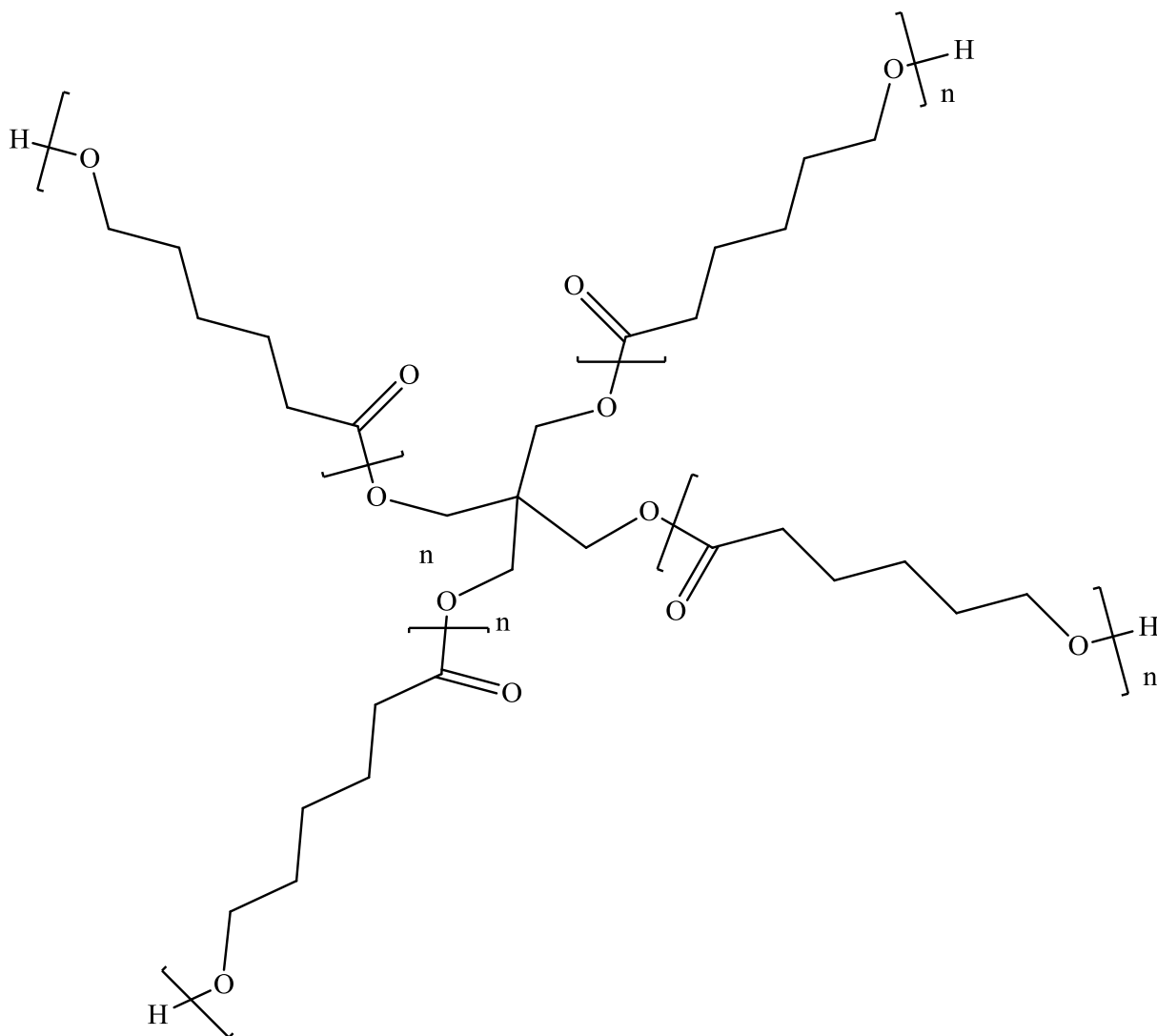
Figure 1-3: Four-arm star-shaped poly(ε-caprolactone) polymers[8]

1.2   Dendrimers and star-shaped molecule structures

The name "dendrimer" is derived from the Greek words "dendron" and "meros", meaning "tree-like branches",[5] while the star-shaped macromolecule gets its name simply because of its linear arms. The simplified structural illustrations of the dendrimer and the star-shaped macromolecule are shown in Figure 1-4. Both structures generally contain three main

3

components: an initial core, several layers, and many end groups.

(a) Dendrimer   (b) Star-shaped Macromolecule

G_0= Generation 0
G_1= Generation 1
G_2= Generation 2
G_3= Generation 3
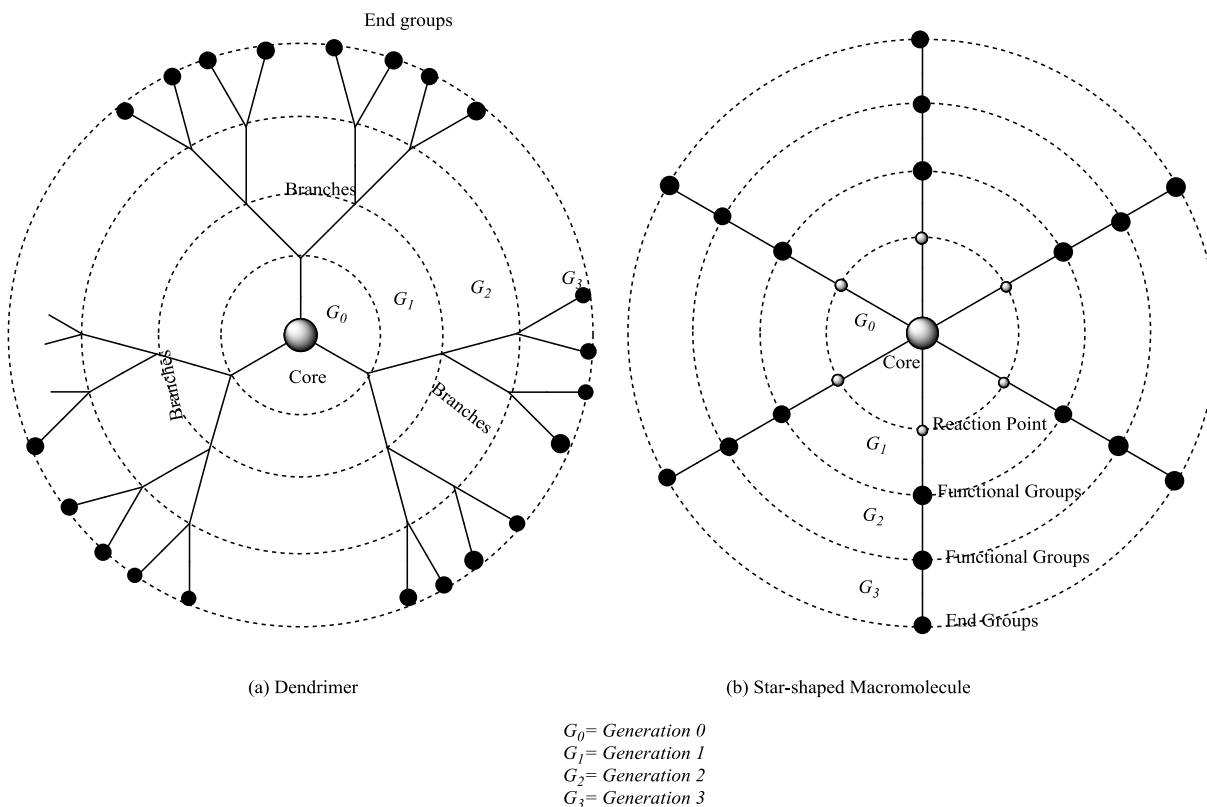
Figure 1-4: General structure of (a) dendrimer and (b) star-shaped macromolecule

The initial core is the starting point of a dendrimer or a star-shaped macromolecule. It always contains two or more of the same functional group that conduct further reactions. The core multiplicity refers to the number of functional groups present in the molecule. A higher core multiplicity will build a larger size of dendrimer or star-shaped macromolecule. Also, the core itself can exert some functionality.

The backbones of a dendrimer or a star-shaped macromolecule form different layers. For the dendrimer, each layer has branches through certain reaction points, while the star-shaped macromolecule has some functional units in each layer. Under the same layer, the branches or the functional groups are of the same repeating units. Therefore, each layer is

4

called one generation; the higher number of generations will result in a higher molecular weight if each generation contains the same type of dendrimer or star-shaped macromolecule.[5]

The end groups are located on the surface of these macromolecules, with terminal functional groups. They could be added at the last step, as in divergent synthesis, or during the first step in a convergent synthesis. These two synthetic methods are detailed in Section 1.3.

The diversity of core, branches, and end groups depends on their number of functional groups. Subsequently, each variety of dendrimer will have a different shape, stability, solubility, conformational rigidity, and viscosity. Below is a summary of the various components with different influences on the dendrimers and star-shaped macromolecules:[9]

- Core: size, shape, multiplicity, functions

- Layers: shape, size, densities/niches, guest inclusion

- End groups: shape, stability, solubility, viscosity

- Surface: shape, size, flexibility, properties

Generally, highly-branched dendrimers tend to have distinct properties in comparison with the less-branched star-shaped macromolecules. High generation dendrimers with more branches have a larger three-dimensional structure, thus demonstrating better solubility in common solvents and better guest inclusion with potential application in drug delivery and catalyst.[5] Star-shaped macromolecules, as a more simplified model, are easier to synthesize, as described in Section 1.3.2. Their symmetrical less-branched structure results in properties similar to those of linear polymers, and offer abundant application in optic and electric materials.[8]

1.3   The synthesis of dendrimers and star-shaped macromolecules

1.3.1   The synthesis of dendrimers

The pioneers of dendrimer chemistry are Fritz Vőgtle and his coworkers, who synthesized the first "cascade molecule" in 1978.[10] The reaction of the "cascade molecule" is shown in Scheme 1-1. Starting from monoamine, the synthesis used the Michael addition of acrylonitrile to produce bisnitrile, followed by the hydrogenation with sodium borohydride in the presence of Cobalt (II) ions to reduce the nitrile groups to amines. This process was repeated twice and the "cascade molecule" was produced as two tree-like branches from each of the nitrogen atoms.

This molecule opened the door for the field of dendrimers because, in theory, the repeating reaction steps are infinite. However, in reality, the process of the repeating steps is difficult due to steric hindrance, which results in a low product yield.
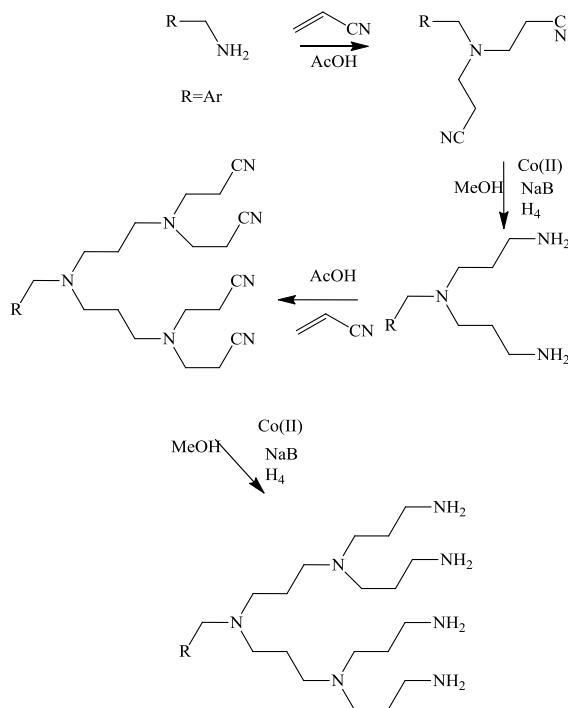
Scheme 1-1: The synthesis of a cascade molecule[10]

6

In 1985, Donald A. Tomalia synthesized and named the first idealized model of a dendrimer.[11] Similar to the "cascade molecule", the synthesis process for the PAMAM dendrimer is shown in Scheme 1-2. Firstly, the three-to-one ratio of methyl acrylate and ammonia is reacted via a Michael addition, giving a three-arm ester core. The resulting ester is then treated with an excess of ethylenediamine to give a primary triamine. This two-step process is repeated and finally results in the secondary triamine with six groups on the surface and the branches connecting though three nitrogen atoms.
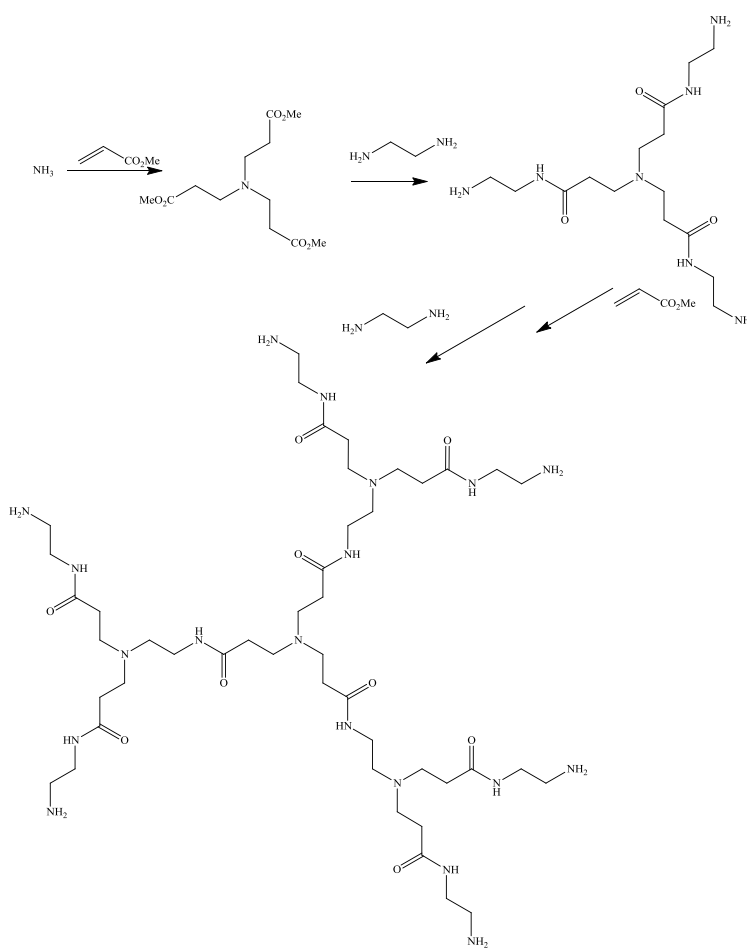
Scheme 1-2: The synthesis of a PAMAM dendrimer[11]

7

In summary, the early synthesis of the dendrimer molecule demonstrated the way that dendrimers can grow outwards from the core and diverge into space. This synthetic method is called divergent synthesis and is shown in the Scheme 1-3.[12,13]
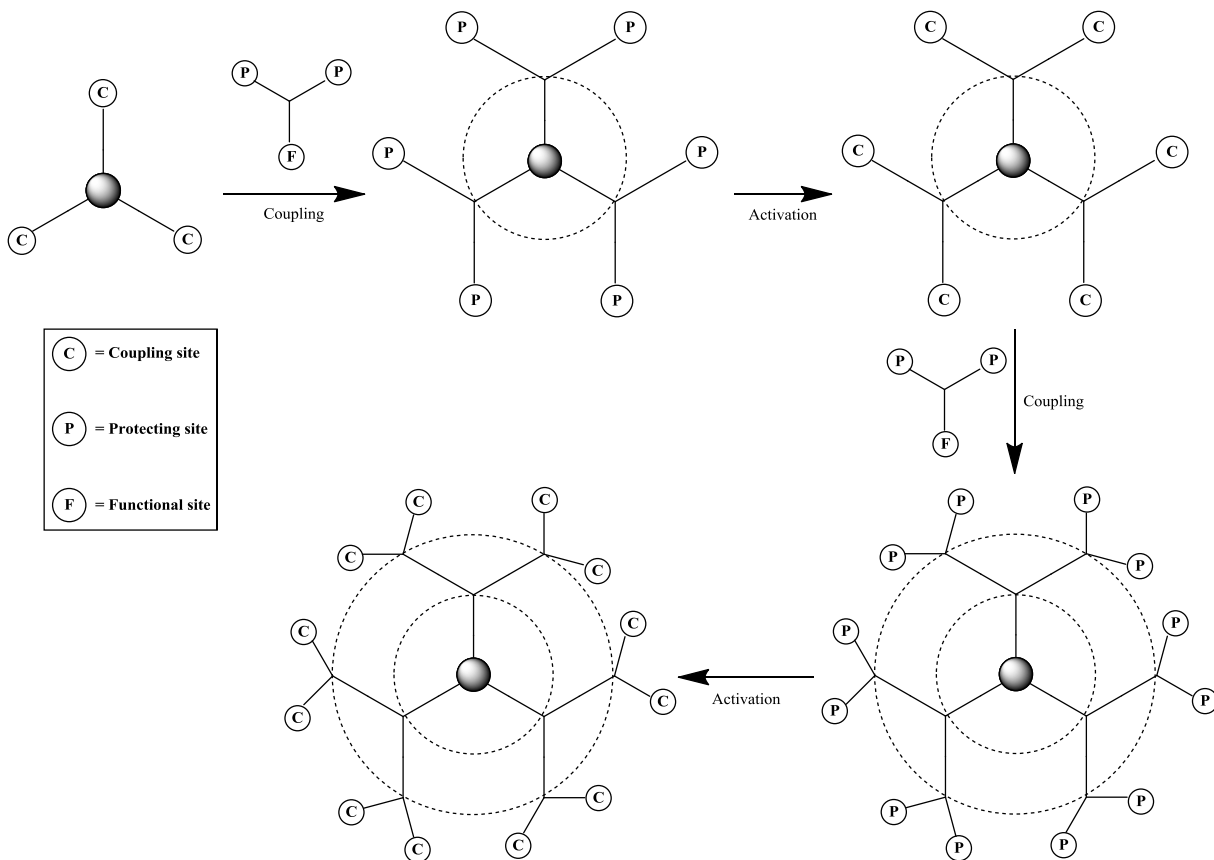
Scheme 1-3: Divergent synthesis of dendrimer

Using the divergent approach, high molecular architecture could be gained, as well as the automation of the repetitive steps. Commercially, the divergent method has been applied in preparation of POPAM and PAMAM dendrimers.[11]

There are drawbacks using the divergent approach.[11] With the increasing number of terminal functional groups, there are always increasing structural defects that exist, no matter the level of excess of reactants used. The separation and purification of one particular dendrimer would also be difficult because the different generations of the dendrimers show

very similar chemical and physical properties. In order to raise the yield of the dendrimer or lower the polydispersities in the final product, each reaction step has to be as efficient in its reactivity and purification as possible.

Several years after the success of the divergent synthetic method, an opposing method called convergent synthesis was proposed.[8,11,14] The convergent synthesis builds the surface of the dendrimer as reactive functional branches first. Then, the branches are attached to the multifunctional core from the outside layer to the inside layer. The process is shown in Scheme 1-4.
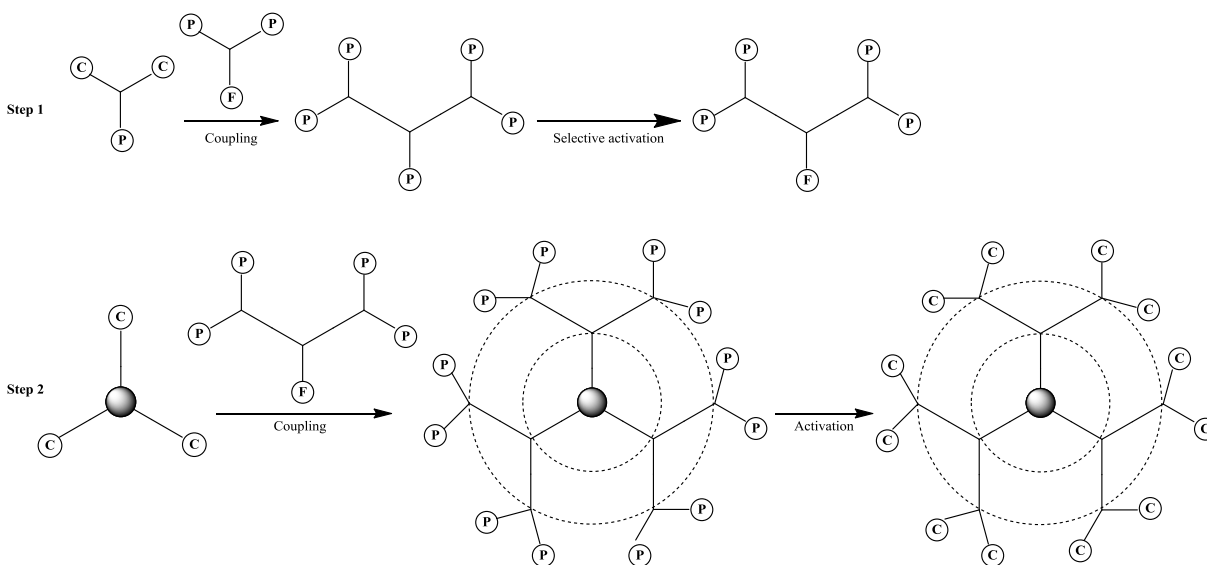
Scheme 1-4: Convergent synthesis of dendrimer

In comparison with the divergent synthetic method, convergent synthesis exhibits many advantages. Firstly, the convergent approach does not produce structural defects, as each of the branches are fully prepared before adding to the core, while the divergent method may cause some branches to miss one or two reaction steps. Secondly, a large excess of reagents is not required because multi-steps of the branches' synthesis already ensure they are fully reacted. Finally, the purification steps are done on each of the branches' synthesis, as well as the final addition of bulky branches to the core, giving fewer dendrimer-based byproducts.

9

However, there is a major disadvantage: by synthesizing the branches via the convergent method, the steric hindrance increases, which limits the growth of a high-generation dendrimer that could be produced through the divergent approach. As a result, both divergent and convergent approaches are still used in today's dendrimer synthesis, complimentary with each other.

Based on these two traditional synthetic approaches, new methods of dendrimer synthesis have emerged in recent years, namely orthogonal synthesis,[5, 15] double stage convergent method,[16] double-exponential method,[17] and hypermonomer method.[18] However, these methods are currently being studied, none of which can be applied widely thus far. Under certain structural conditions, these modern methods offer short routes and diverse products, which appeals to chemists. Therefore, the synthesis of the dendrimer is always modified according to different structural conditions in current research.

1.3.2   The synthesis of star-shaped macromolecules

The synthesis of star-shaped macromolecules is similar to the synthesis of dendrimers, but the process is relatively simpler, as there are fewer branching units from the multifunctional core. "Arm first" method is similar to the convergent approach in that a linear chain can be synthesized first, which is subsequently reacted with a multifunctional core through a reactive group placed at the terminal end of each chain. "Core first" method is like the divergent method of dendrimer synthesis, in which a multifunctional core is used as an initiator for the attachment of monomers to form the star-shaped macromolecule.

For a star-shaped oligomer with a limited number of generations, the synthesis involves step-wise reactions via the two approaches described above. On the other hand, a star-shaped polymer could be obtained through different polymerization methods, namely

anionic, cationic, controlled radical atom transfer radical polymerization (ATRP), reversible addition-fragmentation transfer (RAFT), and group transfer polymerization (GTP).[8]

1.4   The synthesis and application of metallodendrimers

Dendrimers that have acquired metal ions in their structures are called metallodendrimers.[19] These types of dendrimers have attracted research interest in recent years because of their redox properties, and they can be used in catalysts and molecular recognition.[20] In metallodendrimers, metal ions can be precisely placed in the core, branches, or end groups (Figure 1-5).

Metal ion

(a)   (b)   (c)
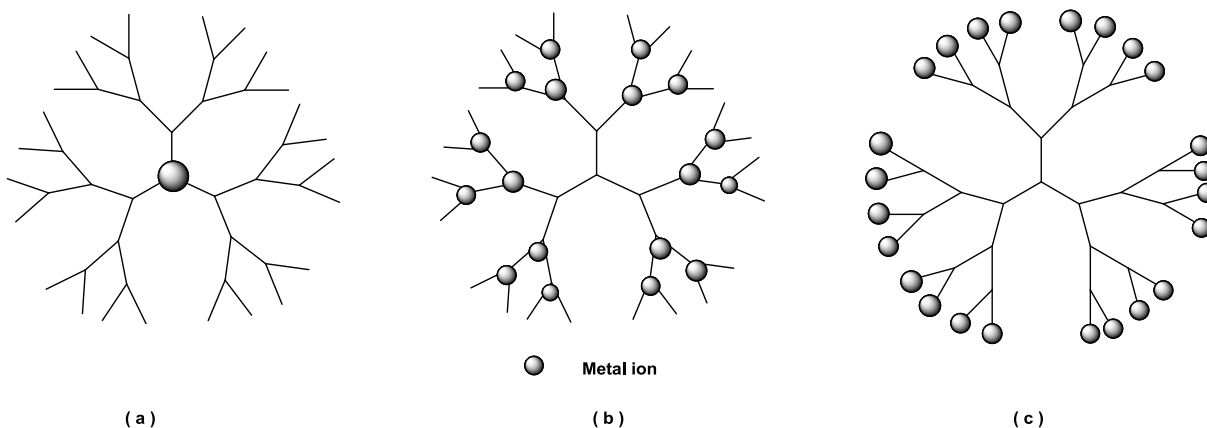
Figure 1-5: Different positions of metals in metallodendrimers: (a) metal ions in the core; (b) metal ions in the branches; (c) metal ions in the end group

1.4.1   Metal ions in the core

Usually, the incorporation of metal ions into the dendrimer core only requires a one-step reaction, meaning the dendritic groups can react with the existing metal complex through a ligand, or a metal cation can directly complex with a dendritic ligand. For example, the representative zinc dendrimer [21] **(a)** originates from the reaction of a Zn^{II}-porphyrin tetracarboxylic acid complex and some dendritic branches, while the representative ruthenium

dendrimer [22] **(b)** results from the ruthenium ion directly complexed with the dendritic-substituted bipyridine ligand (Figure 1-6).
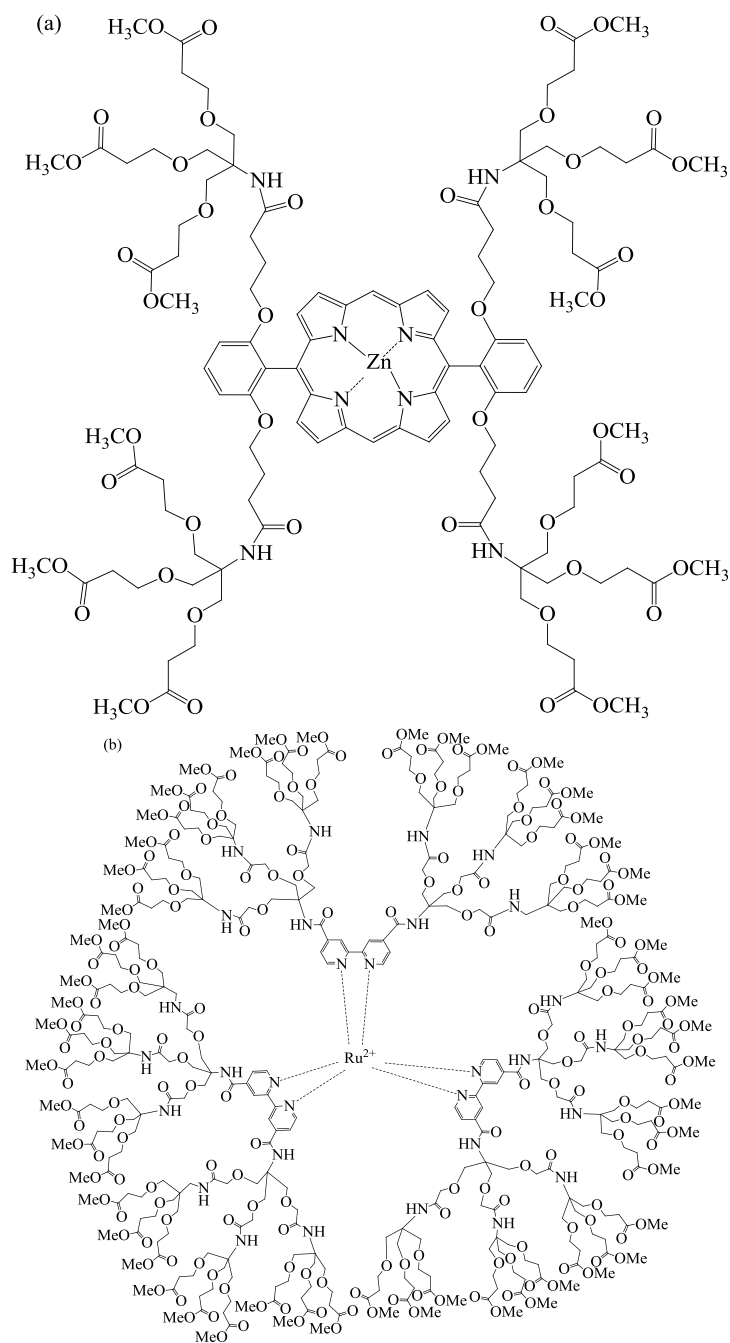
Figure 1-6: Examples of metal-cored metallodendrimers: (a) zinc(II)-porphyrin dendrimer[21] and (b) ruthenium bipyridine dendrimer[22]

1.4.2 Metal in the branches

The metal-coordinated dendritic branches can be synthesized both from the convergent and divergent synthetic methods using different ligands and metals. Figure 1-7 shows one example of a metallodendrimer derived from polypyridine and Ru^{2+} or Os^{2+}.[23] This kind of metallodendrimer finds application in artificial light-harvesting antennae. Firstly, its dendritic structure permits the formation of the light-active subunits by a limited number of synthetic steps. Furthermore, the divergent and convergent synthetic strategies allow modifications in the various layers.

$M^{2+}= Ru^{2+}, Os^{2+}$
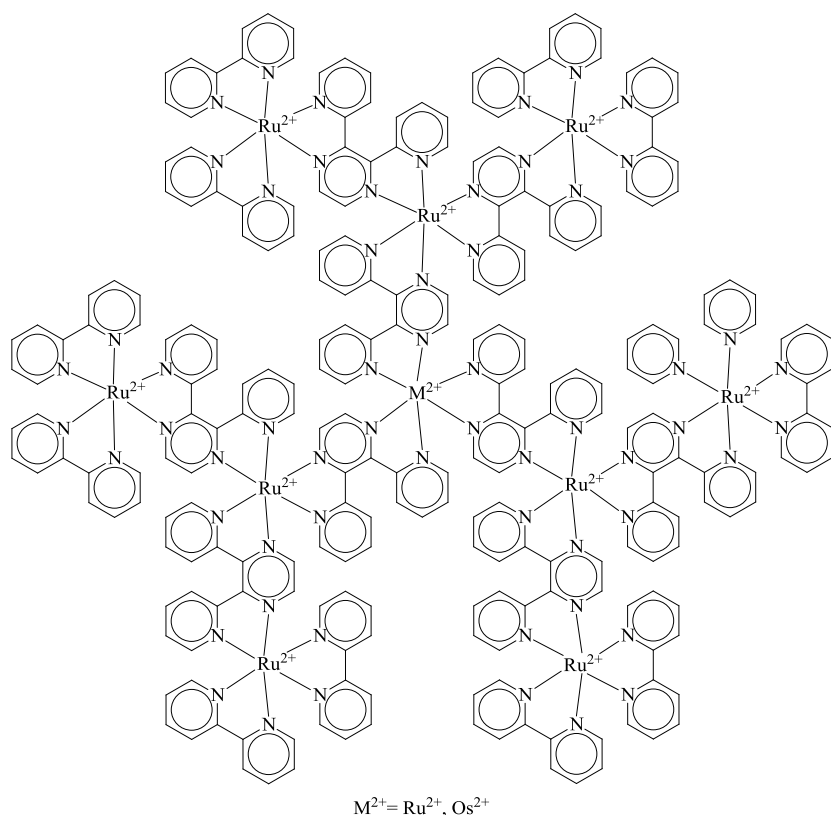
Figure 1-7: Ru^{2+} ion placed in branches of the dendrimer[23]

1.4.3 Metal in the end groups

To place metal ions in the end groups, a previously synthesized dendrimer can be added with suitable ligands as terminal groups, and then reacted with a metal complex.[24] If a dendrimer is terminated with amines or carboxylic acids, it can directly react with a metal

complex. Figure 1-8 shows a bimetallic dendrimer containing ferrocenyl and cobaltocenium unit[25] that is yielded from the reaction of dendritic polyamine with chlorocarbonylferrocene and chlorocarbonylcobaltocenium hexafluorophosphate. This dendrimer shows comprehensive electrochemical activity for application as an enzyme electrode sensor: under anaerobic conditions, the ferrocene units act as mediators in enzymatic processes, while in the presence of oxygen, the cobaltocenium moieties take part in electrocatalytic processes.
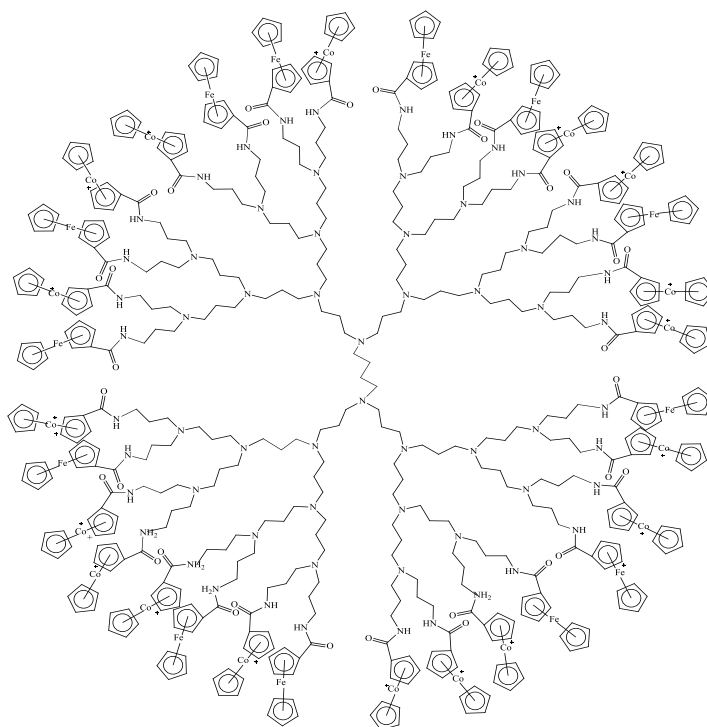
Figure 1-8: Cobaltocene as the end group of a PAMAM dendrimer[25]

1.5 Organoiron-containing star-shaped macromolecules

Compared with many other metals, iron has a unique advantage in that it is usually described as environmentally-friendly and economical. Without radioactivity, iron can form stable complexes with a wide range of ligands. Iron can directly bond to carbon and the resulting compound is called an organoiron compound. The history of organoiron chemistry dates back to 1891, when pentacarbonyliron, $[Fe(CO)_5]$, was discovered by Mond and

14

Berthelot as a yellow, musty-smelling liquid which resulted from a direct reaction between finely-divided iron and carbon monoxide.[26] Different synthetic methods account for other iron carbonyl compounds, whose structures are shown in Figure 1-9.[27]
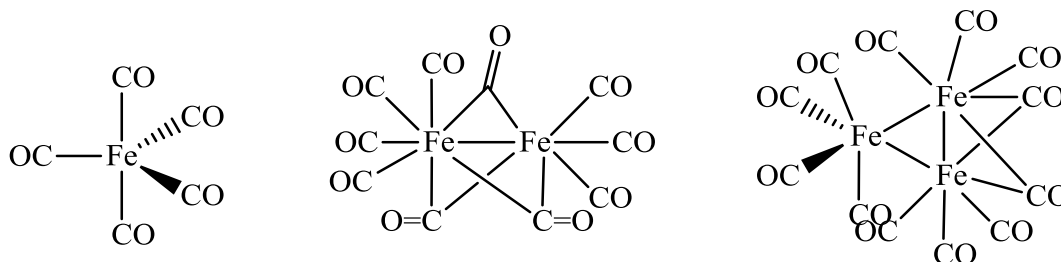
Figure 1-9: Iron carbonyls[27]

These compounds contain either metal-metal bonds or bridging carbonyl ligands, which can be replaced by a variety of other ligands such as alkenes, dienes, and phosphines.[27] They are potentially useful as reagents for affecting functional group interconversions, utilizing iron(0) as a reducing agent, as well as the nucleophilic character of iron.

In 1951, Kealy and Pauson discovered ferrocene,[28] one of the most important discoveries in the field of organometallic chemistry. Prior to this, transition metal-carbon bonds were rare and thought to be unstable. Although there were a number of metal complexes that had been reported, the lack of suitable tools for characterization and structural determination delayed the development of the area. Since then, these ideas were proved false, and ferrocene was discovered to be stable at high temperatures with a well-defined structure. Therefore, organoiron chemistry became more appealing to numerous chemists due to the useful way the complexes could be applied to material sciences and general synthetic chemistry. Countless studies on organoiron complexes were published every year thereafter.

When working with dendrimers and star-shaped macromolecules, cationic iron complexes, [FeCp(arene)][PF$_6$], offer an easy and accessible pathway in the synthesis. In a classical study, the one-pot hexasubstitution of [FeCp(C$_6$Me$_6$)][PF$_6$] [29] was conducted

15

smoothly using an excess of ^{t}BuOK and methyl iodide in THF at a very fast reaction rate (Scheme 1-5). The reaction proceeds because of the strong electron-withdrawing character of the cationic complex. In terms of acidity, the pKa of FeCp(C$_6$Me$_6$)][PF$_6$] in DMSO was found to be approximately 14 units lower for the 18-electron complexes [FeCp(η^6-C$_6$Me$_6$)][PF$_6$] (pKa = 29) than for the free arene (pKa = 43).[30,31]
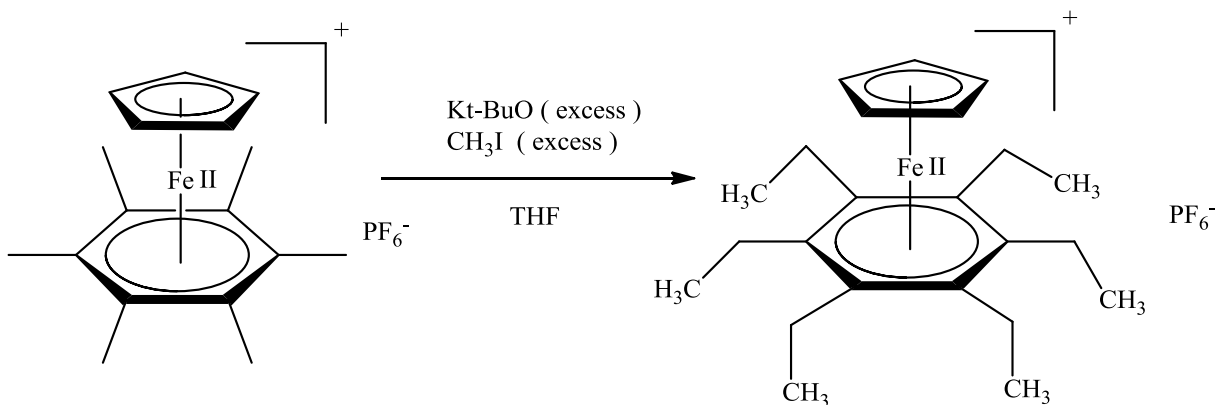
Scheme 1-5: One-pot hexasubstitution of [FeCp(C$_6$Me$_6$)][PF$_6$][29]

The reaction was later improved using other functional groups, which resulted in the hexaferrocenyl alkylation complex becoming the initial core of some dendrimers and star-shaped macromolecules.[32,33,34] Figure 1-10 shows one hexa-branched star derived from the hexaferrocenyl alkylation complex reacting with linear organic halides through a convergent approach.[35]
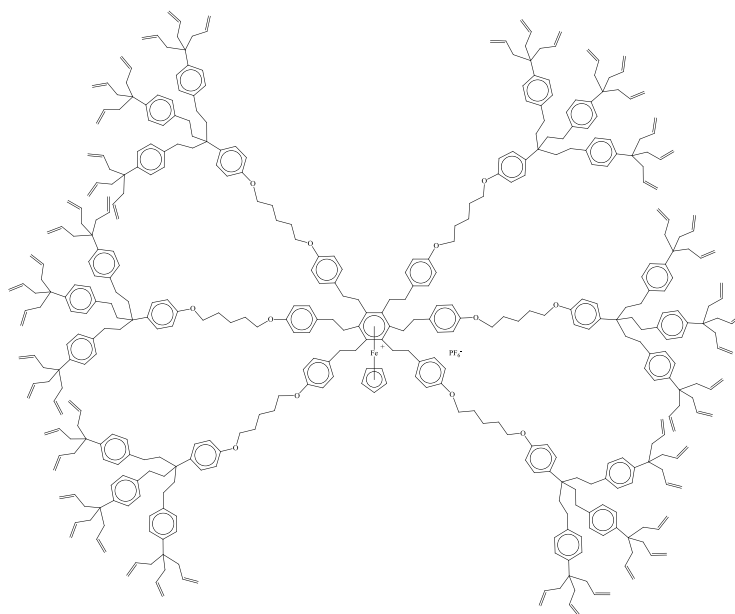
Figure 1-10: Hexa-branched star-shaped macromolecules with oranoiron core[35]

Figure 1-11 demonstrates that organoiron can also be introduced to the branches.[36] This star-shaped polyether was achieved though nucleophilic aromatic substitution and Steglish esterification, and characterized using electrochemistry, which demonstrated their potential uses as sensors and molecular batteries.

n=1,2
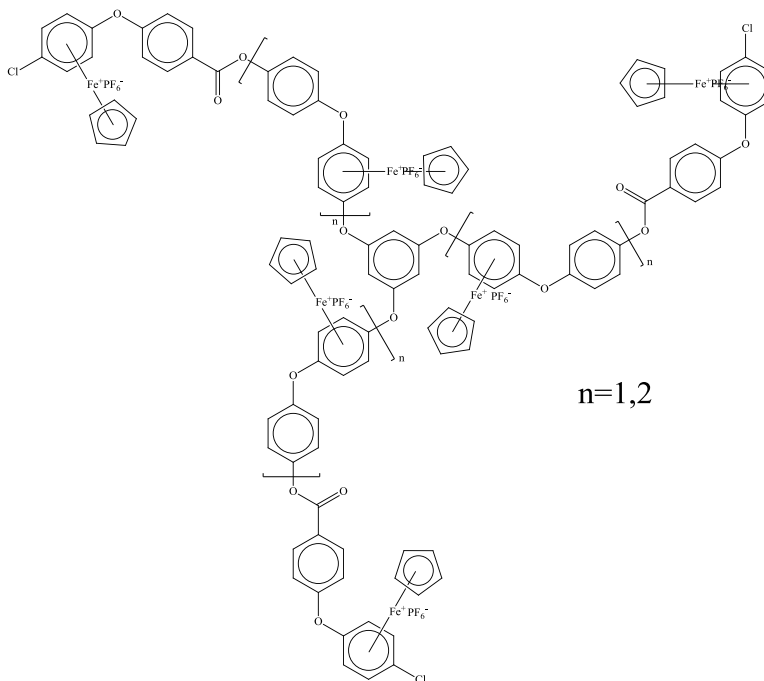
Figure 1-11: Star-shaped organoiron oligomer containing ester/ether linkages [36]

1.6　Azo-containing dendrimers and star-shaped macromolecules

Similar to metal complexes, dye molecules can interact with some part of the dendrimer as well, through its core, branches, or the end groups. This interaction results in the change of the luminescence and absorption spectra of dyes. Meanwhile, due to the addition of dyes, dendrimers can become sensitive to light and display energy transfers.[37]

Different dyes display different types of photochemistry. Among them, an azo dye is a great example of a dye that can conduct photoisomerization.[38,39,40] The detailed synthesis and chemistry of azo dyes will be explained in Chapter 2. Essentially, the azo molecule isomerizes from its planar *trans* form to the non-planar *cis* form after exposed to UV light irradiation with a wavelength between 300 nm and 400 nm. Under visible light, the *cis* form can fully isomerize back to the *trans* form without any decomposition, as shown in Scheme 1-6. There is also thermoisomerization[41] taking place during the temperature change, but usually photoisomerization is preferred because UV light is a "green" source, which does not contaminate any reaction system. Also, one can get the precise measurement of different excitation wavelengths. Finally, the irradiation of UV light is efficient with a minimal economic cost.
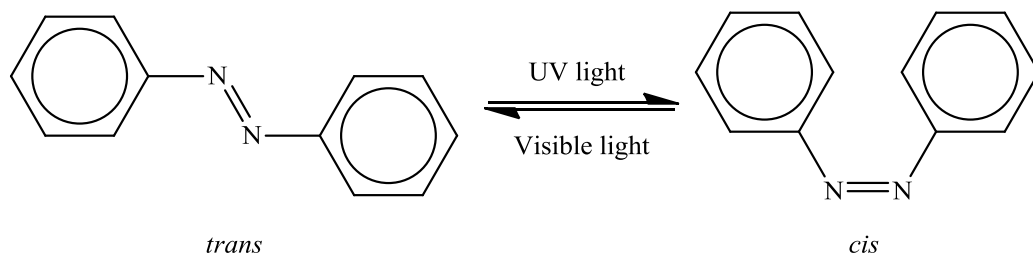
Scheme 1-6: Photoisomerization of azobenzene[38]

The incorporation of the azo chromophore into the polymers is fascinating because the resulting new, functional material is believed to have efficient photoisomerization, as well as photoinduced anisotropy.[42,43] There are reports of azobenzene-containing polymers that have

applications in laser-induced surface relief gratings, [44] liquid crystalline films, [45] and photoresponsive material. [46] As for dendrimers, the incorporation of azo chromophores would be even more exciting because their rigid structures and good solubility in common organic solvents may offer more of their potential applications.

Figure 1-12 shows a dendrimer with azobenzene end groups. [47] The main components of this dendrimer can be seen as two separate parts reacting together: the inner poly(propylene imine) dendrimers with amino groups, and the azobenzene acid. The synthesis utilizes the esterification of the poly(propylene imine) dendrimers at the periphery using 4-(phenylazo)benzoic acid, which results in a good yield of the product.
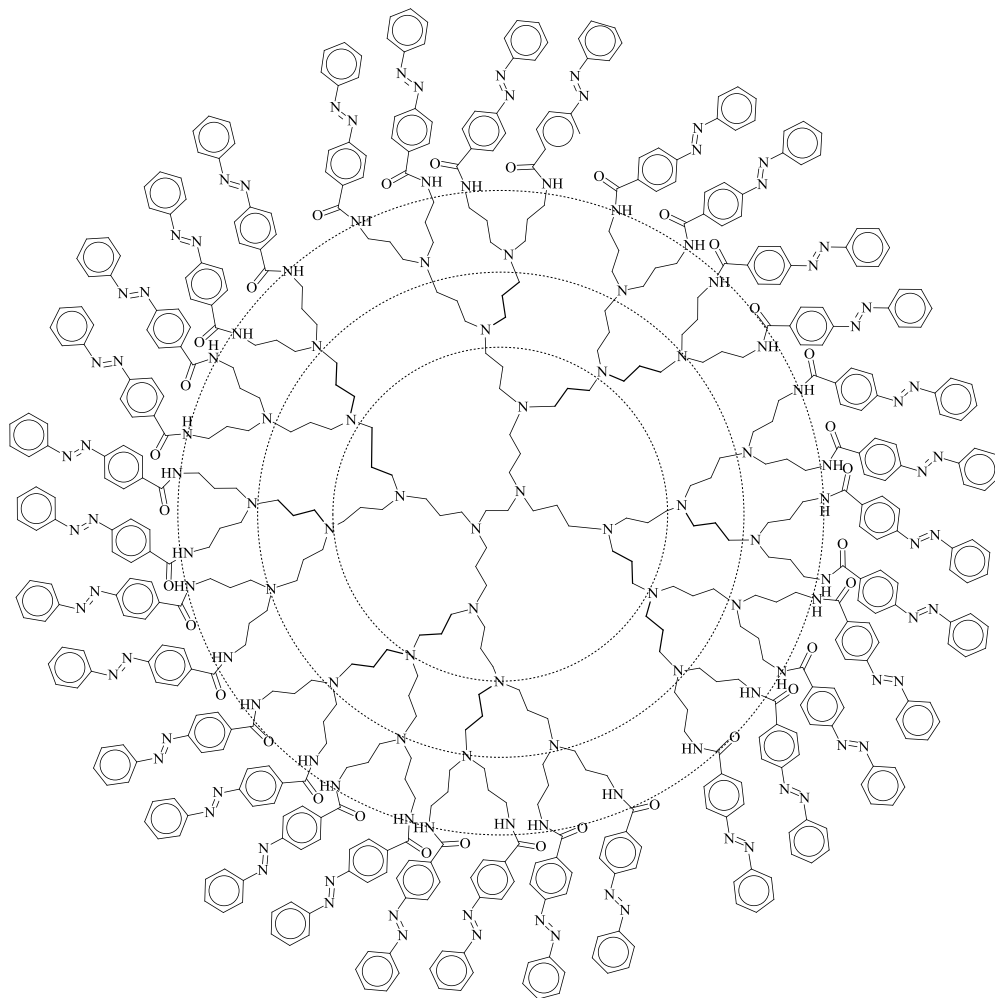
Figure 1-12: Dendrimer with azobenzene end groups[47]

The photochemistry confirms the shape of this dendrimer can be reversibly switched by UV light without losing properties of the original dendrimers. This photoresponsive dendrimer demonstrates its potential use as a material for holographic data storage.[46]

Scheme 1-7 shows a working mechanism for the opening and closure of the azo-containing dendrimer using UV light.[48] In the dark or under the visible light, the azo groups are in the *trans* form. This leaves the surface of the dendrimer open so that guest molecules can enter the dendrimer. When UV light is applied, all of the azo end groups isomerize into the *cis* forms, causing steric hindrance at the surface and results in the closure of the dendrimer, thus trapping the guest molecules. In conclusion, this working mechanism shows the potential application of azo-containing dendrimers in catalysis and drug delivery.
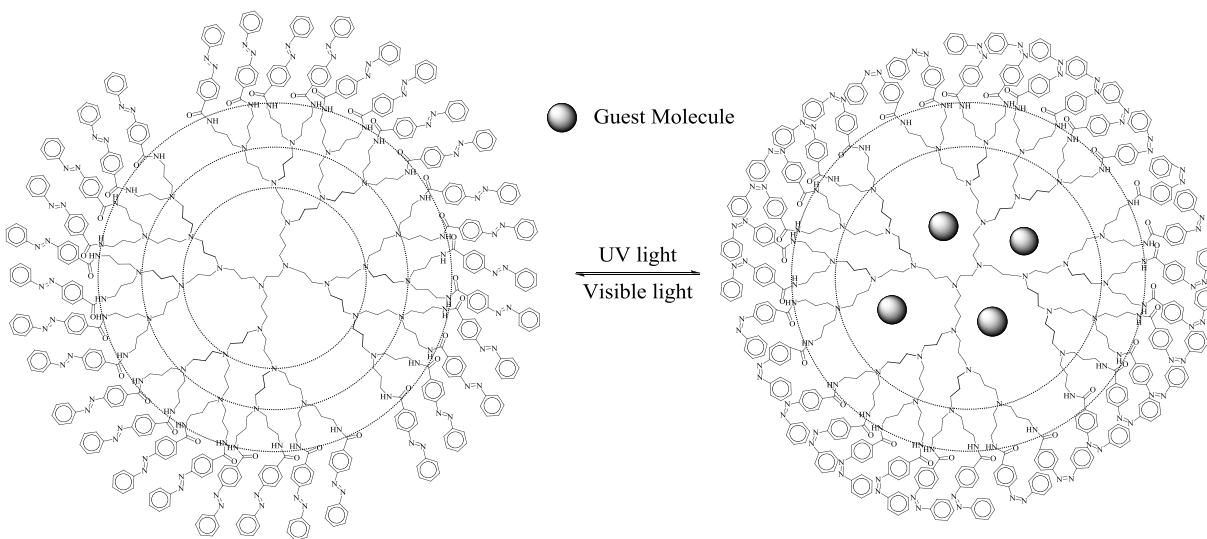
Scheme 1-7: The opening and closure of an azobenzene-containing dendrimer for guest molecules[48]

Figure 1-13 shows an example of a star-shaped azobenzene-based chromophore.[49] This chromophore could later be incorporated into polycarbonate using guest-host chemistry to achieve an NLO (non-linear optical) polymer, a type of polymer studied in recent years because of its application in high bandwidth optical switches and modulators, as well as in

wavelength filters, small-angle beam steering, remote sensing, photonic control of phased arrays, and a variety of other optical circuits.[49]
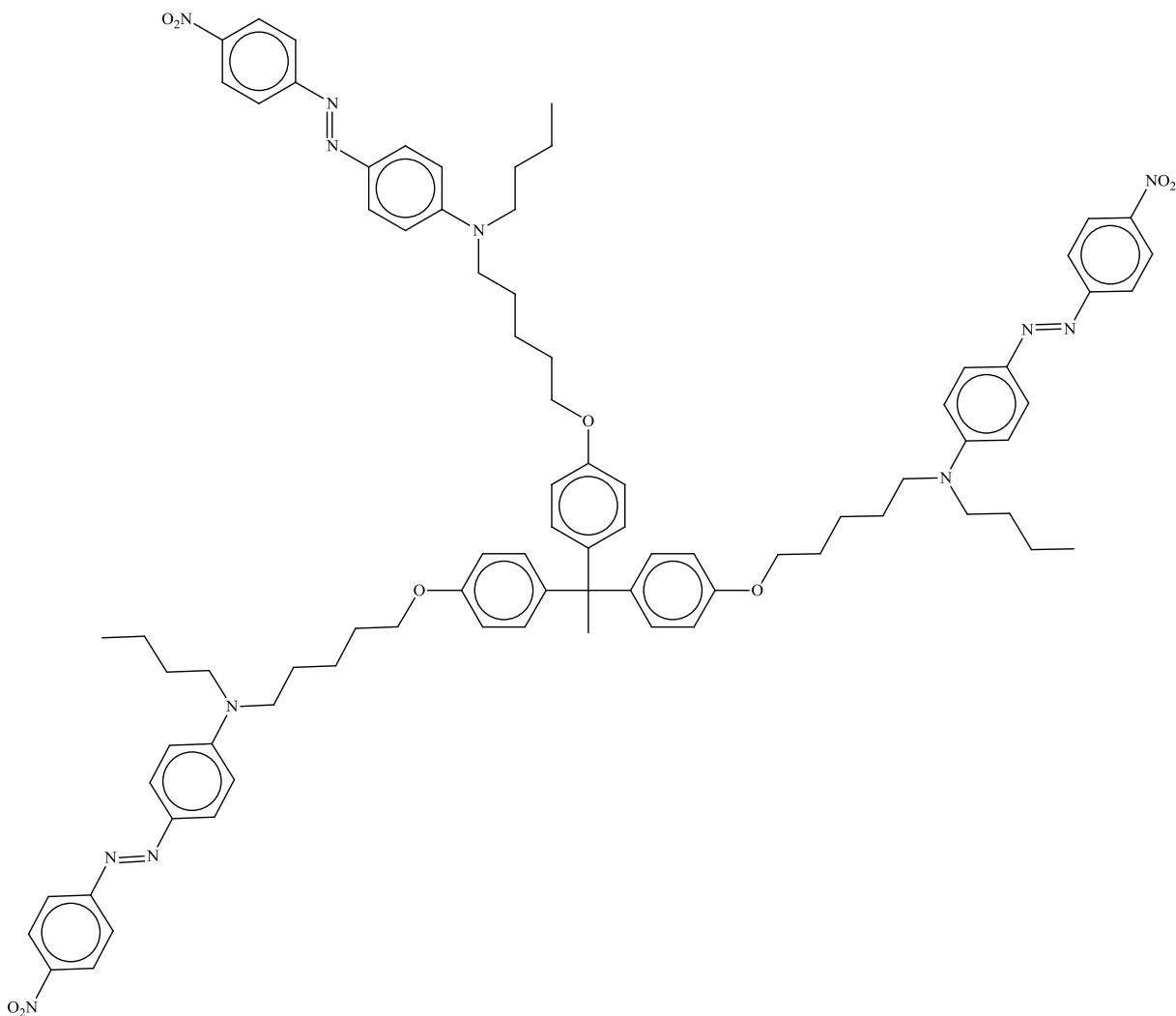
Figure 1-13: Star-shaped azobenzene-based EO chromophores[49]

In general, star-shaped macromolecules and dendrimers based on organorion moieties and azo dyes have been reported separately. However, there are a few publications regarding dendrimers and stars with both of these two functional units. Due to the individual potential applications of both the functionalized dendrimer and star-shaped molecule, it would be interesting and worthwhile to design a dendrimer or a star-shaped macromolecule with both organometallic moieties and azo dye groups.

Previously, the Abd-El-Aziz research group has reported the syntheses of various polymers containing neutral and cationic cyclopentadienyliron moieties with azo dyes either in the side chains or directly in their backbone.[50,51,52,53] More recently, the research group was the first to communicate the synthesis of polymers and azo dye-containing dendritic species based on upper rim functionalized organoiron metallocalix[4]arenes.[54] The azo dye-containing metallocalix[4]arenes demonstrated visible and reversible colour change in the presence of both acid and base, making them excellent candidates for reusable acid sensors.

Based on these previous works, this thesis describes the synthesis and characterization of star-shaped oligomers containing cationic η^6-chloroarene-η^5-cyclopentadienyliron (II) complexes functionalized with azo chromophores. Controlled methods involving both convergent and divergent approaches were employed to give distinct symmetrical branches that alternate between organoiron complexes and azobenzene moieties. Chapter 2 will focus on the synthesis and characterization of various organoiron complexes and azo dyes, along with their ability to be linked together as the building blocks for stars and dendrimers. Chapter 3 will discuss the results of the reactions of the stars and dendrimers containing both functional groups.

Chapter 2. Synthesis of star-shaped oligomers as building components

2.1   Introduction

In preparation for star-shaped oligomers containing cationic η^6-chloroarene-η^5-cyclopentadienyliron complexes functionalized with azo chromophores, this chapter will focus on the detailed synthesis and chemistry of organoiron moiety and azo dyes, including some theories and reaction mechanisms. Although most of these components are synthesized according to the published methods, this chapter reports a new example of an organoiron star that can conduct further reactions and a new azo dye which can be seen as the functional core for the oligomers synthesis in next chapter.

The organoiron moieties used in this chapter are η^6-chloroarene-η^5-cyclopentadienyliron(II) hexafluorophosphate complexes. Because of the nucleophilic character, η^6-chloroarene-η^5-cyclopentadienyliron(II) hexafluorophosphate complexes are able to conduct metal-mediated nucleophilic substitution. Therefore, organoiron moieties are connected to many functional groups that serve as the building components in the synthesis of dual-functionalized star-shaped oligomers.

On the other hand, various azo dyes were synthesized with functional groups that can connect to the organorion moieties. For example, an azo dye with a phenolic group can conduct nucleophilic substitution with η^6-chloroarene-η^5-cyclopentadienyliron(II) hexafluorophosphate complexes, while an azo dye with a hydroxyl group can conduct a condensation reaction with η^6-chloroarene-η^5-cyclopentadienyliron(II) hexafluorophosphate carboxylic complexes. As a result, these azo dyes become the core, branches, and end groups in the structure of dual-functionalized star-shaped oligomers.

2.2 The synthesis and chemistry of the η^6-haloarene-η^5-cyclopentadienyliron(II) hexafluorophosphate complex

The discovery of ferrocene in 1951 marks the rebirth of organometallic chemistry and since then, numerous studies of organoiron complexes are reported every year.[28] These complexes are derived from the rich chemistry of ferrocene, as cyclopentadienyl(Cp) rings are able to conduct reactions with numerous electrophiles. Moreover, one of the Cp rings of ferrocene can be displaced by an arene, resulting in a cationic η^6-arene-η^5-cyclopentadienyliron complex. The displacement of one Cp ring by an arene is described as a ligand exchange reaction, first reported in 1963 by Nesmeyanov, Vol'kenau and Bolesova.[55,56,57] Scheme 2-1 shows one example of the ligand exchange reaction of ferrocene and 1,4-dichlorobenzene. Using $AlCl_3$ in the presence of powdered aluminum at temperatures between 80-165 $^\circ$C for 5 hours, the reaction gives η^6-dichlorobenzene-η^5-cyclopentadienyliron complex as the product, which can be subsequently treated with ammonium tetrafluoraborate or ammonium hexafluorophosphate and isolated as a neutral salt. The aluminum is used to prevent the ferrocene from being oxidized to the ferrocinium cation and no additional solvent is required, as 1,4-dichlorobenzene is liquid under reaction temperatures.

2.1   **2.2**   **2.3**
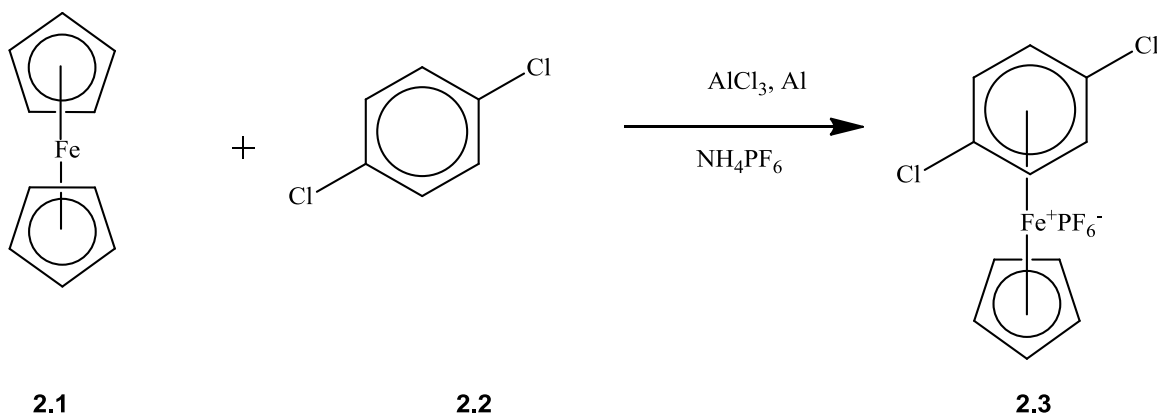
Scheme 2-1: Ligand exchange reaction of ferrocene

The proposed mechanism for this ligand exchange reaction is shown in Scheme 2-2 as a Friedel-Crafts reaction. Firstly, $AlCl_3$ coordinates to one of the Cp rings from ferrocene and disrupts the bond between the ring and the iron. The resulting cyclopentadienyliron cation is then coordinated with dichlorobenzene and gives the η^6-dichlorobenzene-η^5-cyclopentadienyliron complex.[58,59]
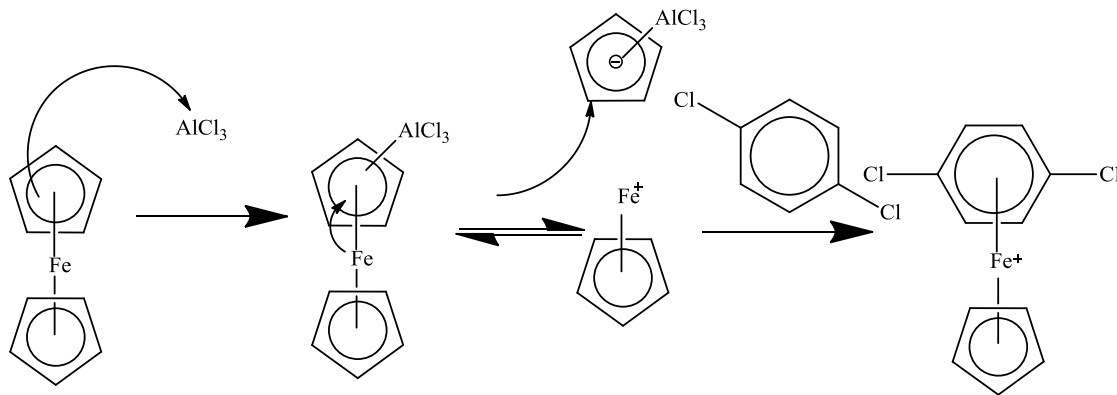
Scheme 2-2: Proposed mechanism for the ligand exchange reaction of ferrocene[59]

The introduction of the organoiron moiety to an arene offers convenient characterization in ^{1}H NMR and ^{13}C NMR spectroscopy. In both NMR spectroscopic methods, the resonance representing the complexed arene appears at a significantly lower chemical shift than that of the non-complexed arene ring. For example, in the η^6-dichlorobenzene-η^5-cyclopentadienyliron(II) hexafluorophosphate complex **2.3**, there is a resonance at 7.02 ppm

of the complexed arene, while in dichlorobenzene **2.2** the non-complexed arene resonance appears at 7.42 ppm. This unique upfield chemical shift of the complexed arene is due to the destabilization of anisotropy for the arene with the coordination of the π-system to the iron centre. Accordingly, this phenomenon can be applied to the assignment of a macromolecule containing a complexed multi-arene ring system.
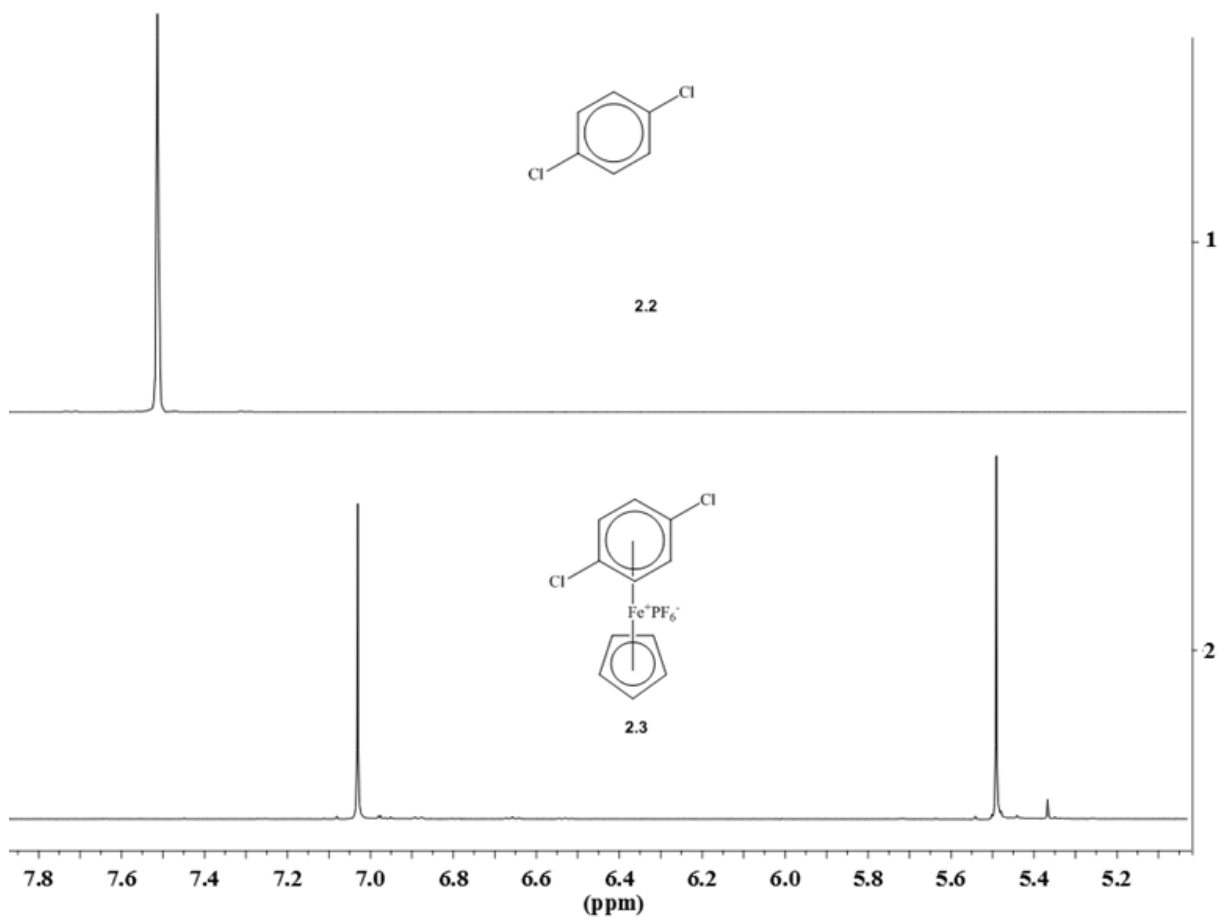
Figure 2-1: Comparison of 400 MHz ^{1}H NMR of dichlorobenzene 2.2 (spectrum 1) and complex 2.3 (spectrum 2)

Another advantage of the ligand exchange reaction is the ability to characterize the unique electrochemical properties of the resulting complex due to the different potential oxidation states. As shown in Scheme 2-3[60], for ferrocene, only single-electron oxidations can be performed to result in the reduction of the ferrocene to the 16-, 17-, 18-, and 19-electron

26

states.[61,62] The cationic arene-coordinated cyclopentadienyliron complexes produce both one- and two-electron reversible oxidations, providing oxidation states of 17-, 18-, 19- and 20-electron. The neutral 19-electron complexes are fully reversible to either the 18-electron or 20-electron state, and 18-electron complexes are fully reversible to either the 17-electron or 19-electron state.[63] Due to the increased electron delocalization, the electron-withdrawing group on the complexed arene will result in the complex undergoing reduction at more positive voltages than those with electron-donating groups.
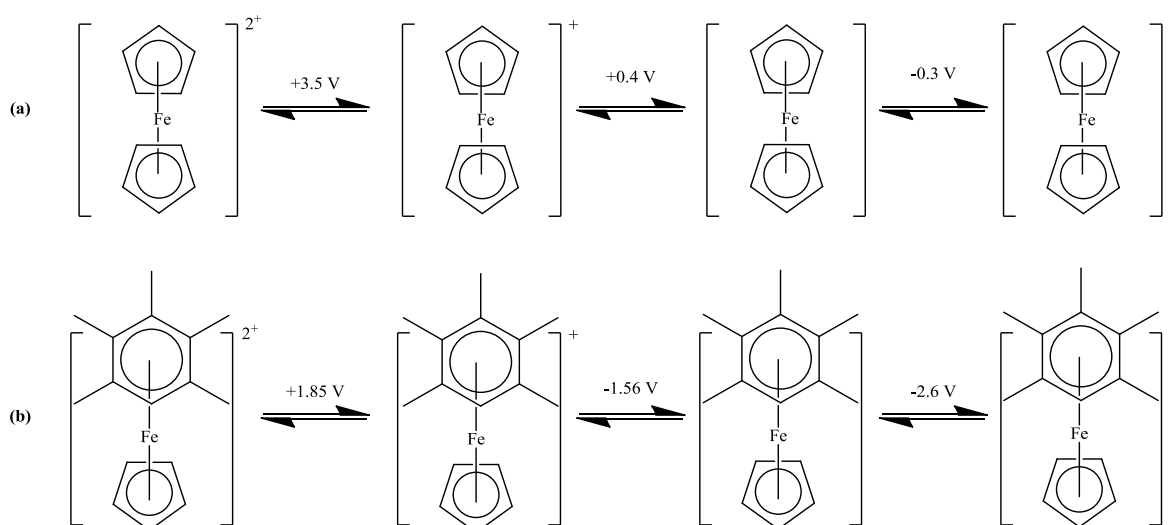
Scheme 2-3: Potentials for the oxidation states determined by cyclic voltammetry of (a) ferrocene and (b) η^6-hexamethylbenzene-η^5-cyclopentadienyliron(II); potentials are given versus a saturated calomel reference electrode[60]

Because the arene derivatives can be functionalized for further reaction, the resulting η^6-haloarene-η^5-cyclopentadienyliron complex became a bridge between synthetic organic chemistry and organometallic chemistry.[58,59] For example, the mono- and dichloro of η^6-haloarene-η^6-cyclopentadienyliron(II) compounds can undergo a metal-mediated nucleophilic reaction. The strong electron-withdrawing capabilities of the cyclopentadienyliron ring make the haloarene slightly positively-charged and easily attacked by a nucleophile. With the

addition of a weak base like K_2CO_3, the arene is easily dehalogenated and substituted with the nucleophile. Scheme 2-4 demonstrates the mechanism of an η^6-dichloroarene-η^5-cyclopentadienyliron(II) complex attacked by a nucleophile Nu-H to give the Nu-substituted η^6-chloroarene-η^5-cyclopentadienyliron(II) hexafluorophosphate complex. More excitingly, this reaction occurs under mild condition at room temperature, whereas the nucleophilic substitution of chlorobenzene with phenolic groups requires long reaction times, high temperature, high pressure, or harsh catalysts.[58,59]

Nu-H = ROH, R_2NH, or RSH
B: = K_2CO_3 or R_2NH
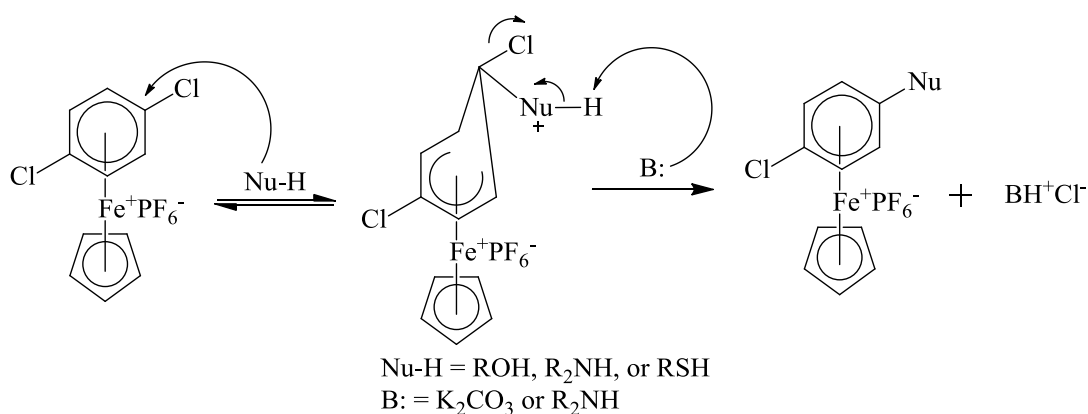
Scheme 2-4: Metal-mediated nucleophilic substitution of an η^6-dichloroarene-η^5-cyclopentadienyliron(II) hexafluorophosphate complex[59]

2.2.1 The synthesis and chemistry of the η^6-haloarene-η^5-cyclopentadienyliron(II) hexafluorophosphate complex with carboxylic groups

Utilizing the nucleophilic substitution of the η^6-chlorosubstitutedarene-η^5-cyclopentadienyliron complexes, the Abd-El-Aziz group has prepared a series of carboxylic acid-functionalized organoiron complexes. In the synthesis of dual-functionalized star-shaped oligomers with both organoiron moieties and azo groups, two carboxylic acid complexes functionalized by organoiron are first prepared in order to conduct further condensation reactions: a monometallic acid complex and a bimetallic acid complex.

According to previous publication,[64] the monometallic acid complex **2.5** is synthesized from the reaction of *p*-dichlorobenzecyclopentadienyliron hexafluorophosphate (*p*-dichloro complex, **2.3**) with 4-hydroxybenzoic acid (Scheme 2-5). This reaction is a typical example of a metal-mediated nucleophilic aromatic substitution reaction in the presence of K_2CO_3. It was carried out in DMF for 12 hours at room temperature.
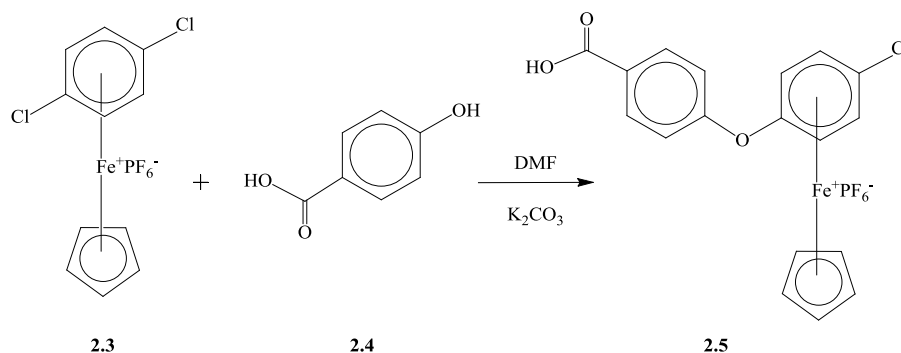
Scheme 2-5: Synthesis of monometallic acid complex 2.5[64]

Similarly, the previously reported[64] bimetallic acid complex **2.7** was synthesized by the reaction of 4,4-bis(4-hydroxyphenyl)valeric acid with *p*-dichloro complex **2.3** (Scheme 2-6). The reaction conditions are similar to the monometallic acid complex using K_2CO_3 in DMF at room temperature. However, because of the ratio of the reagents, a longer reaction time of 36 hours is required to make sure both phenolic groups are metal-mediated.
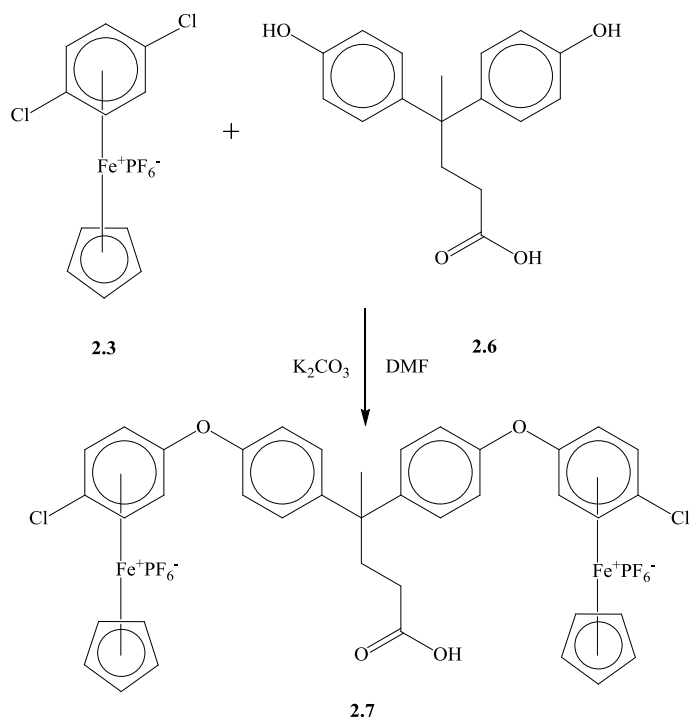
Scheme 2-6: Synthesis of bimetallic carboxylic acid complex 2.7 [64]

2.3 Steglich esterification of bimetallic carboxylic acid complex 2.7

There are many useful and reliable methods for the esterification of carboxylic acids, such as reacting their sodium, potassium, or calcium salts with alkyl halides, or following the Fischer-Speier procedure in the presence of mineral acids.[65] Among those methods, Steglich esterification is an efficient way that is widely used under mild conditions. Steglich esterification is the condensation reaction of carboxylic acids and alcohols, yielding esters; the reaction utilizes dicyclohexylcarbodiimide (DCC) as a coupling reagent and 4-dimethylaminopyridine (DMAP) as a catalyst.[66] The general reaction proceeds at 0 °C for the first five minutes, and room temperature for the duration of the reaction for 3 hours (Scheme 2-7).
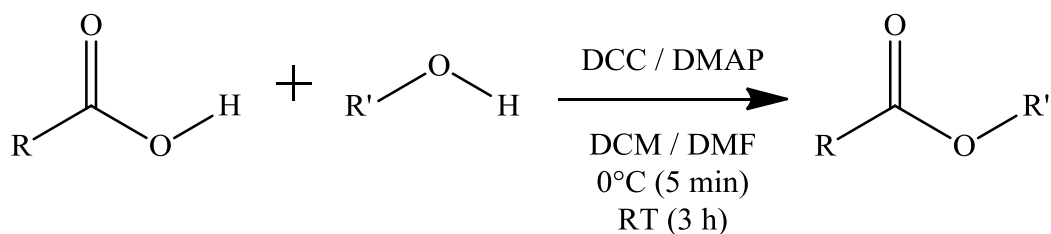
Scheme 2-7: A simplified Steglich esterification[69]

The general mechanism of the DCC/DMAP esterification reaction is shown in Scheme 2-8. Firstly, the carboxylic acid is dehydrated by a strong nucleophile (DMAP) and subsequently reacted with DCC to form an *o*-acylisourea intermediate. This intermediate shows some similarity with the corresponding carboxylic acid anhydride in that it is more reactive than the free acid. Next, the protonated DMAP acts as an acyl transfer reagent, leading to a reactive amide, or "active ester". This amide intermediate cannot form intramolecular side products but reacts rapidly with the alcohol. Finally, the corresponding ester and the stable byproduct, dicyclohexylurea (DCU), are formed. The side product DCU demonstrates low solubility in most common solvents, such as water, dichloromethane, and acetone. Therefore, it is easily removed from the system through filtration as white precipitate.
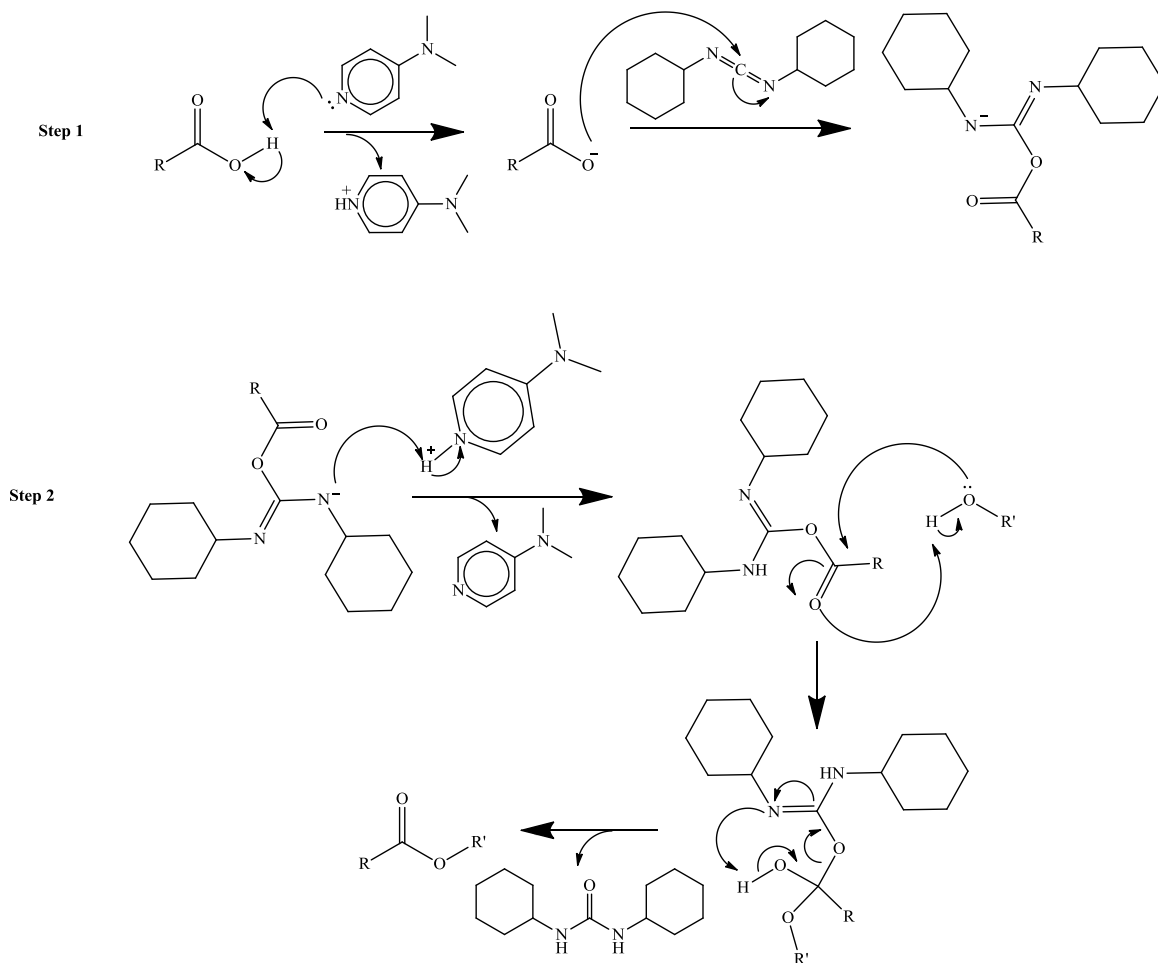
Scheme 2-8: The mechanism of the Steglich esterification using DCC/DMAP

In previous reports, esterification of acid complex **2.7** was accomplished via condensation reactions to afford various esters.[67,68,69] The formation of novel ester complex **2.9** was achieved by reacting the bimetallic carboxylic acid complex **2.7** with 1,12-dodecanediol to exclusively afford the monosubstituted diiron complex **2.9** in a 96% yield (Scheme 2-9). Longer reaction time than the general method was used (48h) with improved purity in ^{1}HNMR characterization. 1, 12-dodecanediol was selected due to its long alkyl chain, which enhances the solubility of polymers in organic solvents by including long chain alkyls.[70,71,72]
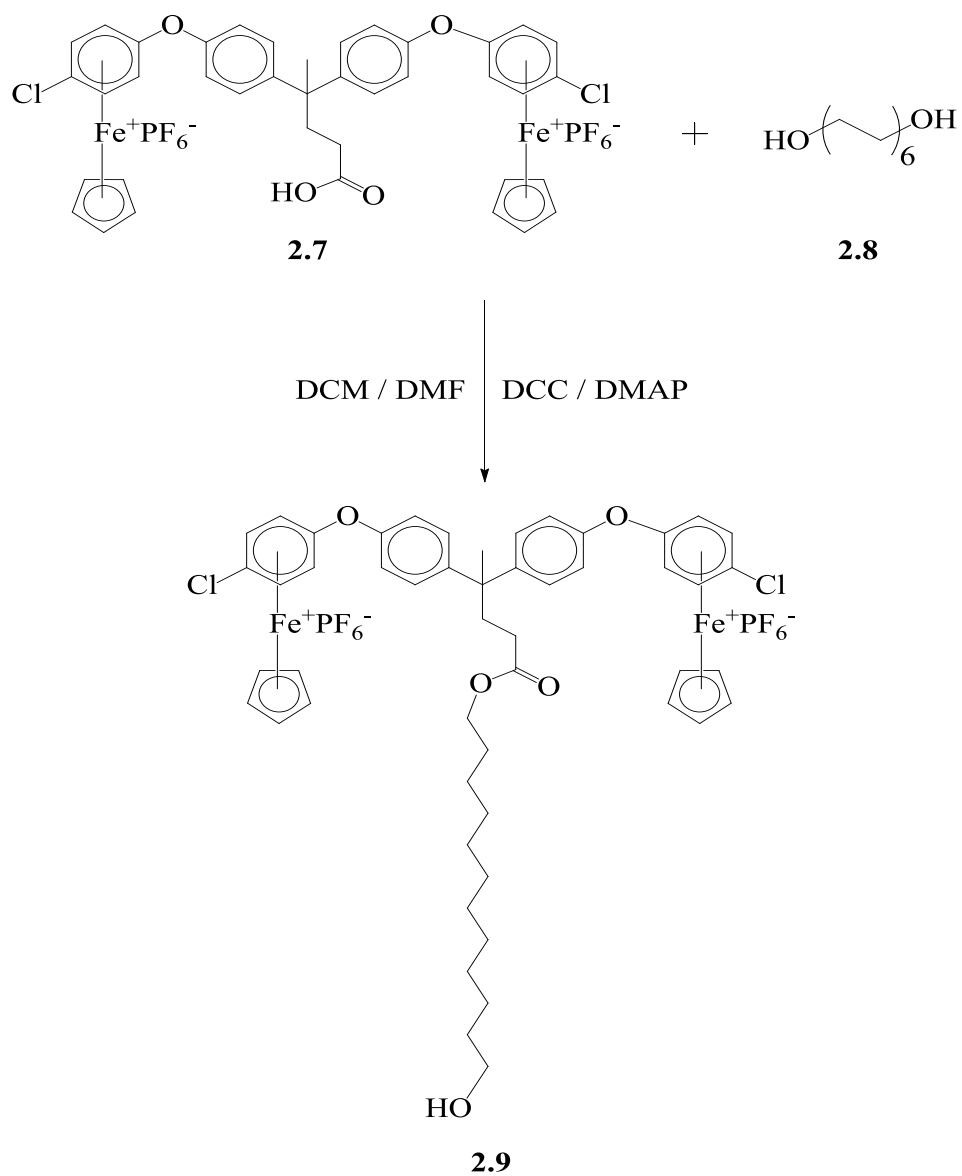
Scheme 2-9: Steglich esterification of bimetallic carboxylic acid complex with 1,12-dodecanediol
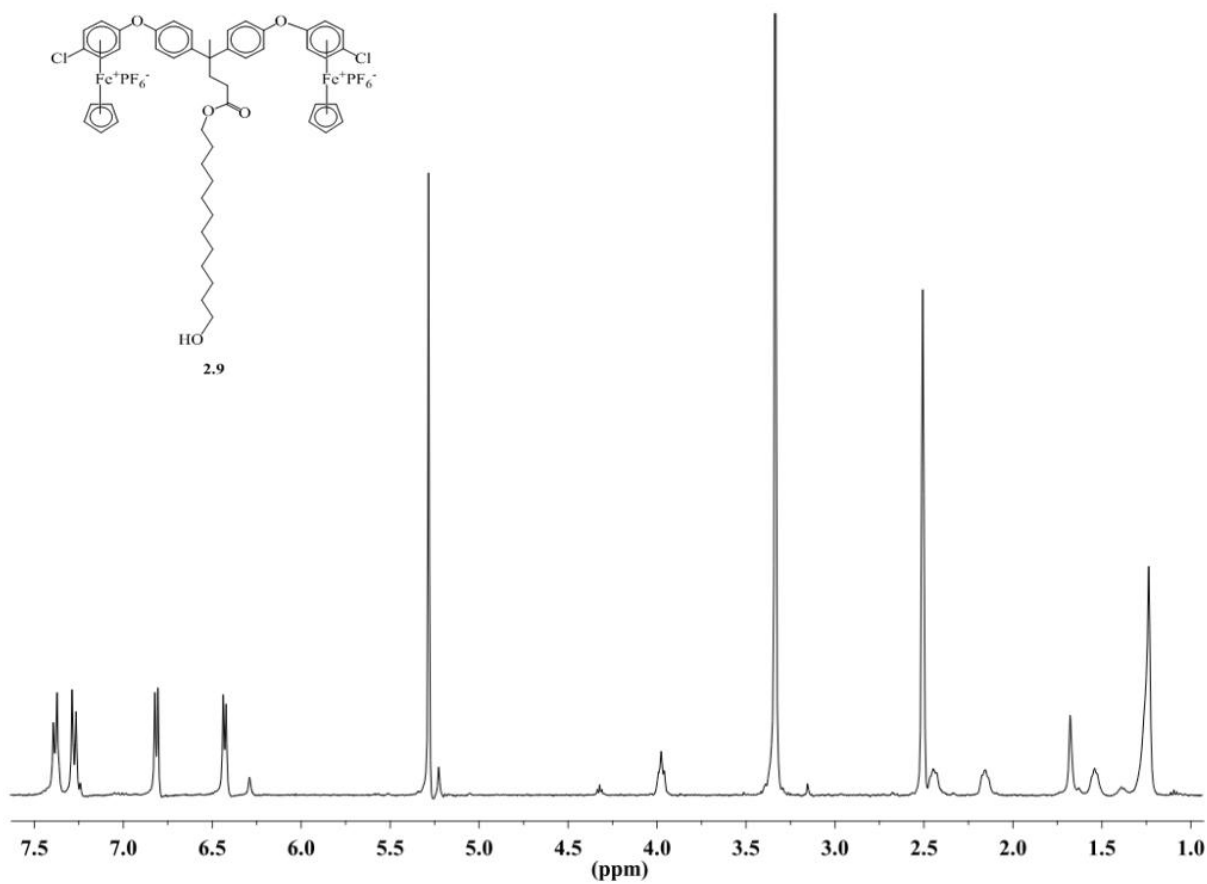
Figure 2-2: 400 MHz ^{1}H NMR spectrum of complex 2.9

The ^{1}H NMR spectrum (Figure 2-2) indicates the formation of complex **2.9** successfully. The incorporation of the iron complex gave rise to the non-complexed arene resonances at 7.38 and 7.26 ppm, and the complexed arene resonances at 6.81 and 6.42 ppm. The cyclopentadiene (Cp) resonance appears at 5.27 ppm as a single peak, which shows the purity of the product. The broad peak at 4.38 ppm integrated to one proton is the alcohol proton. The methylene proton resonance at 3.96 ppm indicates the formation of the ester bond. Furthermore, the methylenes adjacent to the carbonyl carbon appear at 2.44 and 2.15 ppm. The methyl group resonates as a singlet at 1.67 ppm. Lastly, the broad peaks at 1.53 and 1.23 are derived from the long chain methylene protons.
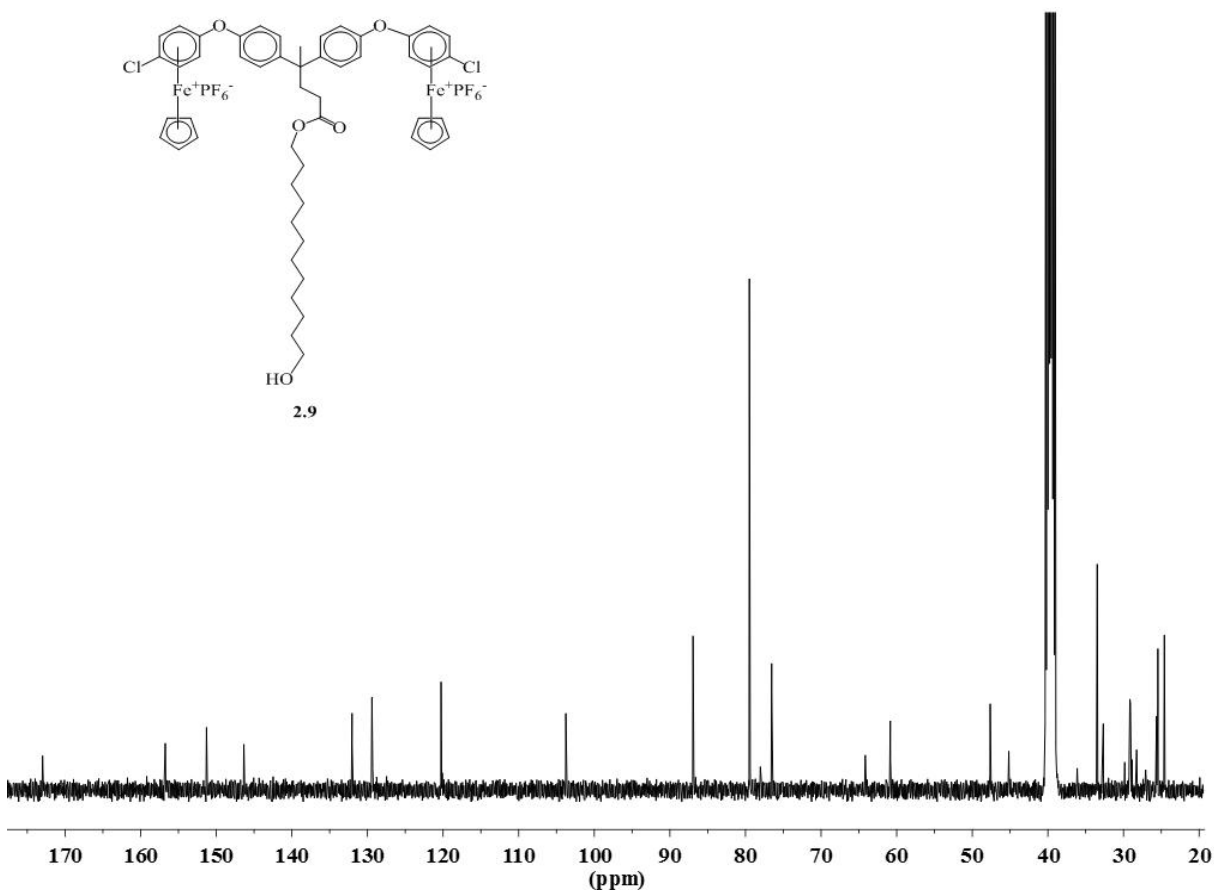
Figure 2-3: 101 MHz ^{13}C NMR spectrum of complex 2.9

The ^{13}C NMR spectrum also confirms the expected structure (Figure 2-3). The carbonyl carbon resonance is visible at 172.8 ppm. There are four quaternary carbon resonances at 156.6, 151.1, 146.2, and 131.9 ppm. The next four resonances representing the non-complexed arene, appear at 129.2, 120.1, 129.2, and 120.1 ppm. The resonance at 79.3 ppm corresponds to the Cp moiety and the resonances at 86.8 and 76.4 ppm correspond to the complexed arene, which are shielded by the iron. On the alkyl chain, the methylene carbons near the ester and hydroxyl groups appear at 64.0 and 60.7 ppm, respectively. The methylene carbons resulting from bimetallic carboxylic complex **2.7** are shown at 47.5 and 45.0 ppm. The other carbons of the long chain show resonances at 33.4, 32.5, 29.7, 29.1, 29.0, 28.9, 28.7, 28.1, 25.5, and 25.3 ppm, while the methyl carbon appears at 24.4 ppm.

35

The same experimental conditions can be applied to form a novel tetrairon star core containing an aliphatic bridge, as shown in Scheme 2-10.
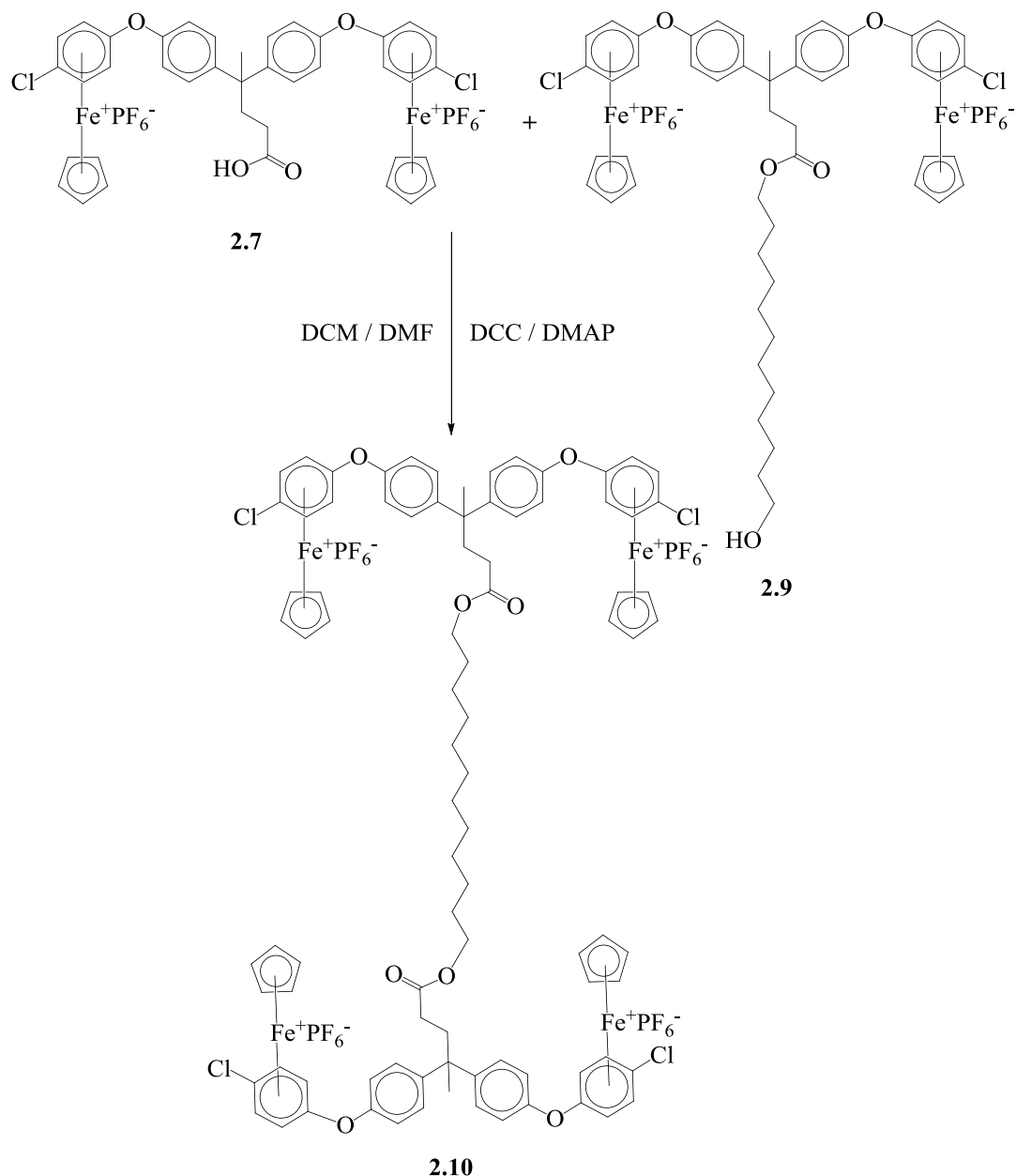
Scheme 2-10: The formation of the tetrairon star core containing an aliphatic bridge

The ^{1}H and ^{13}C NMR spectra of complex **2.10** indicate its symmetric nature. In ^{1}H NMR spectrum (Figure 2-4), the shift of the methylene group attached to the hydroxyl group to 3.97 ppm is an indication for the formation of complex **2.10** as well as the disappearance of the alcohol proton peak. Furthermore, the appearance of only one resonance (5.28 ppm)

36

corresponding to the Cp protons indicates that the monosubstituted complex **2.9** was fully reacted to yield the disubstituted complex **2.10**.
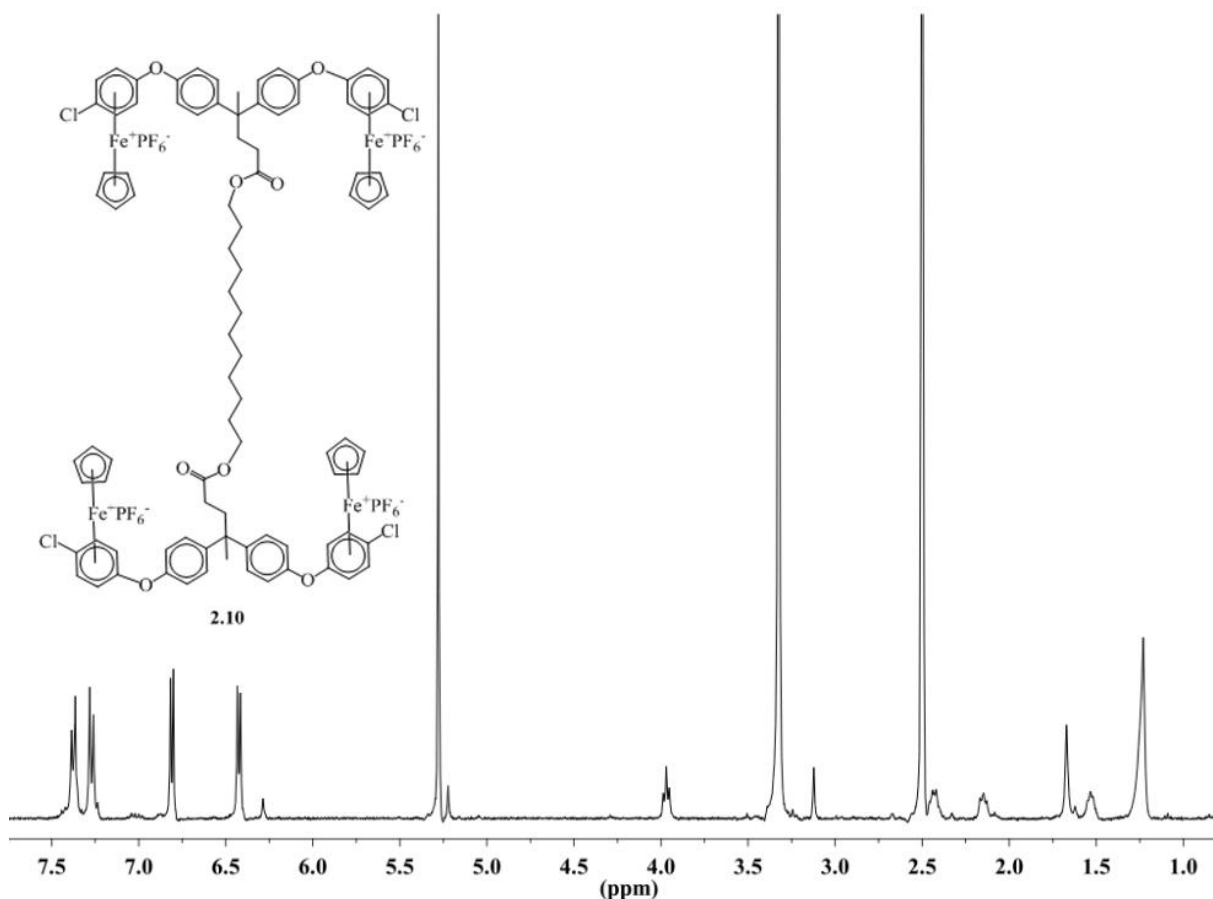
Figure 2-4: 400 MHz ^{1}H NMR spectrum of complex 2.10

The APT ^{13}C NMR further supports the formation of the ester functionality, as seen from the disappearance of the carbon peak at 60.7 ppm that corresponds to the methylene carbon adjacent to the hydroxyl group of complex **2.9** (Figure 2-5). Furthermore, the appearance of only one resonance (79.3 ppm) corresponding to the Cp protons indicates that the monosubstituted complex **2.9** was fully reacted to yield the disubstituted complex **2.10**.
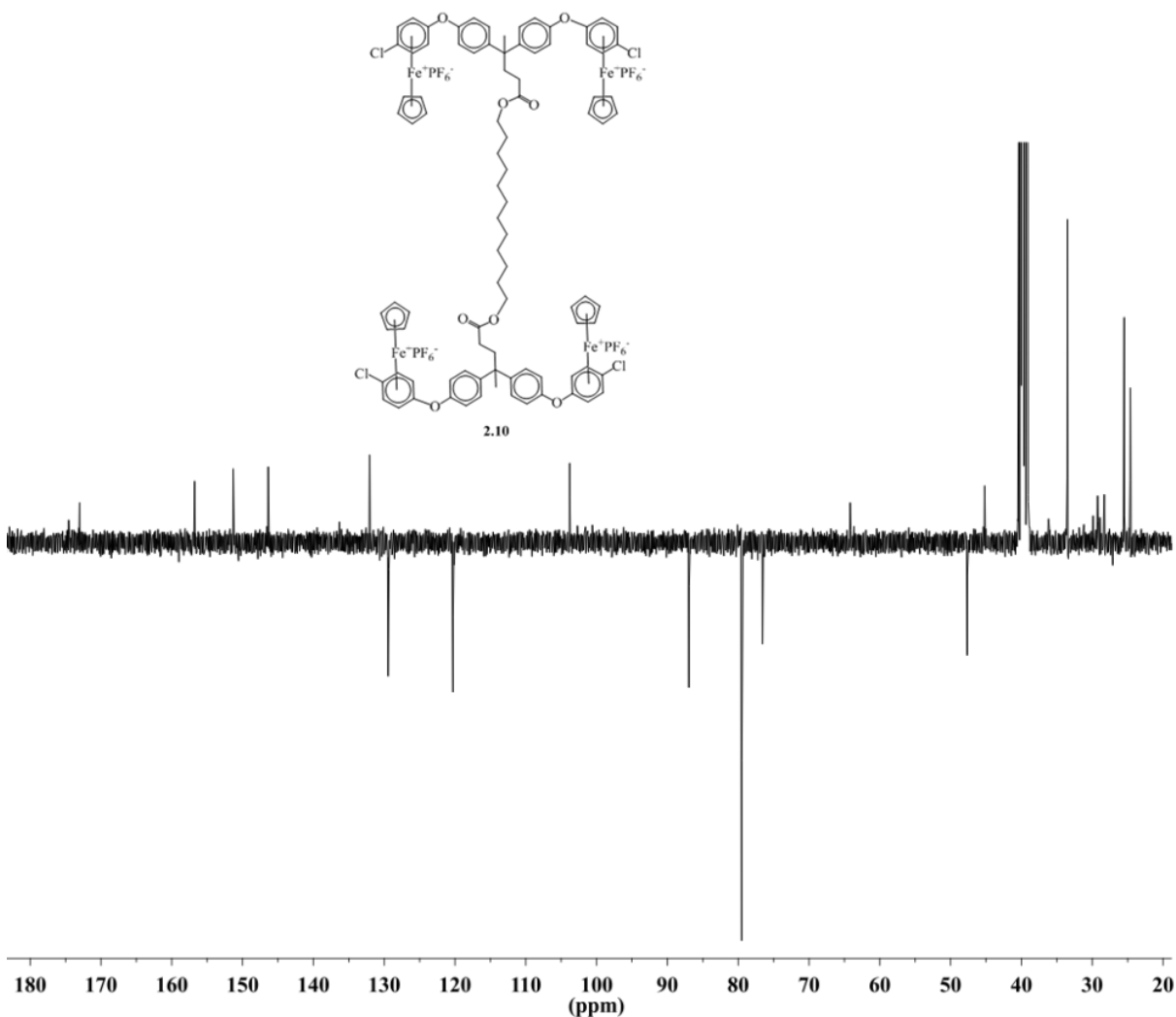
Figure 2-5: 101 MHz APT ^{13}C NMR spectrum of complex 2.10

The synthesis of an another organoiron star core was achieved via metal-mediated nucleophilic aromatic substitution reaction using three molar equivalents of *p*-dichloro complex **2.3** to one molar equivalent of phloroglucinol (Scheme 2-11). The triiron star was synthesized and purified using the previously published method.[36] After purification, the yield was fairly low due to the loss of product during column chromatography.
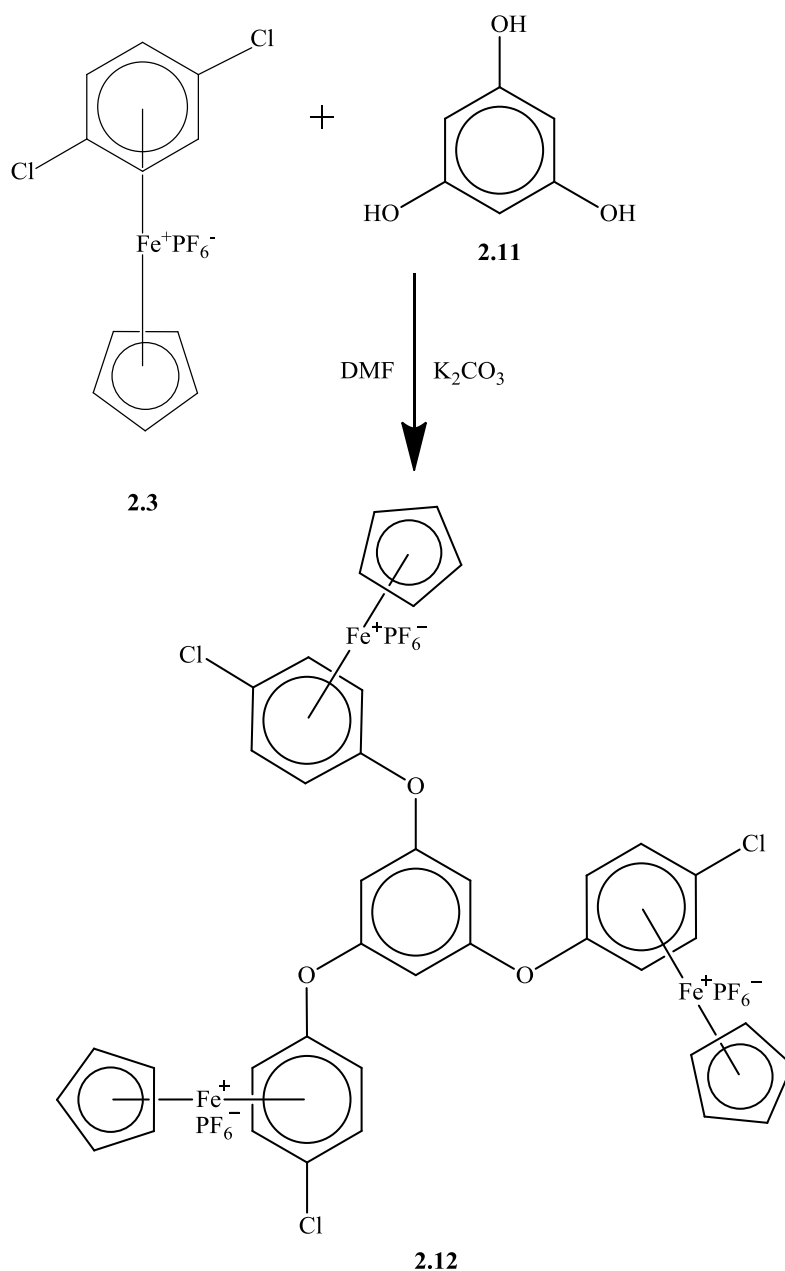
Scheme 2-11: Synthesis of triiron core via metal-mediated nucleophilic substitution[36]

2.4 The synthesis and chemistry of azo dyes

Over the centuries, some stable natural dyes have been identified and developed for their synthetic methods.[73,74] Accordingly, some dyes that do not occur naturally were designed and synthesized. For instance, azo dyes are one type of dyes that can supply a complete rainbow of colors,[75,76] and find extensive use in the food and textile industries.[77,78,79] The

structure of azo dyes are usually the derivatives of diazene(diimide), HN=NH, wherein both hydrogens are substituted by hydrocarbon groups, such as PhN=NPh.[75]

Azo dyes were first prepared by Peter Griess in 1858 as one of the most significant discoveries in color chemistry.[71] It marks the beginning of a new age, where synthetic dyes were of lower cost, higher yield, and gave better technical performance than natural dyes extracted by traditional methods. Shortly after the discovery, one of Griess' azo compounds, 4-aminoazobenzene, become commercially available under the name of Aniline Yellow.[74] (Figure 2-6)
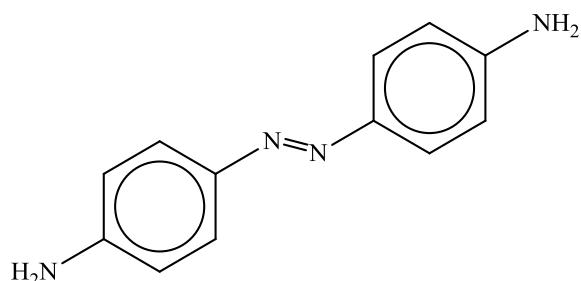
Figure 2-6: One of the first synthesized azo dyes, 4-aminoazobenzene[74]

Generally, the synthesis of azo dyes includes two steps: diazotization and azo coupling in solution (or suspension).[73,74] The choice of solution is based on the type of coupling component used. A basic medium is used if the coupler is phenolic or carboxylic in nature, and an acidic solution is used if the coupler is amino-phenyl in nature.[73] The first step involves the reaction of a primary aromatic amine ($ArNH_2$) with nitrous acid (HNO_2) to form a diazonium salt ($ArN_2^+Cl^-$). Because nitrious acid is unstable and decomposes easily into oxides of nitrogen, it is usually generated by the treatment of sodium nitrite ($NaNO_2$) and hydrochloric acid (HCl). The excess nitrous acid can be removed through the addition of sulfamic acid or urea. Once the diazonium cation forms, it can easily decompose. Therefore, it is essential to maintain the reaction system at a low temperature, usually between 0-5 °C. The second step, azo coupling, is the reaction of the diazotized amine with another aromatic

compound. The aromatic compound used in azo coupling reactions is called the coupling reagent. This coupler can be functionalized with a variety of groups such as N-alkyl groups, halogens, or nitro groups. The overall synthesis is illustrated in Scheme 2-12.

R_1 = N-alkyl, halogen, nitro, H

R_2 = N-alkyl, halogen, nitro, H
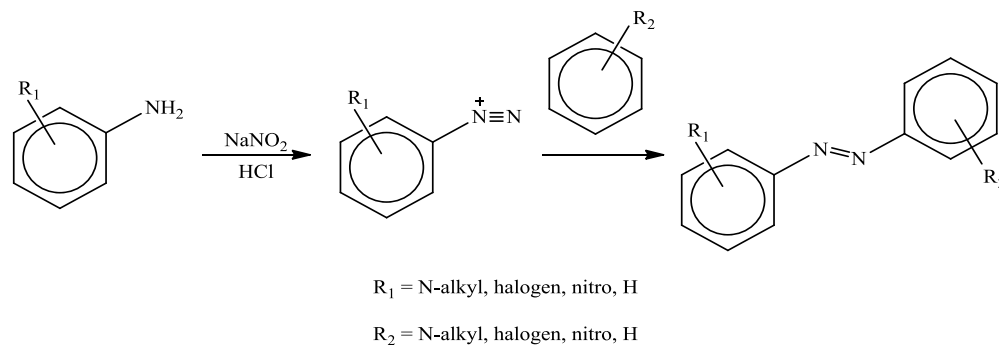
Scheme 2-12: The general synthesis of an azo dye

The general two step mechanism for azo dye formation, using aniline and phenol as example reagents, is illustrated in Scheme 2-13.
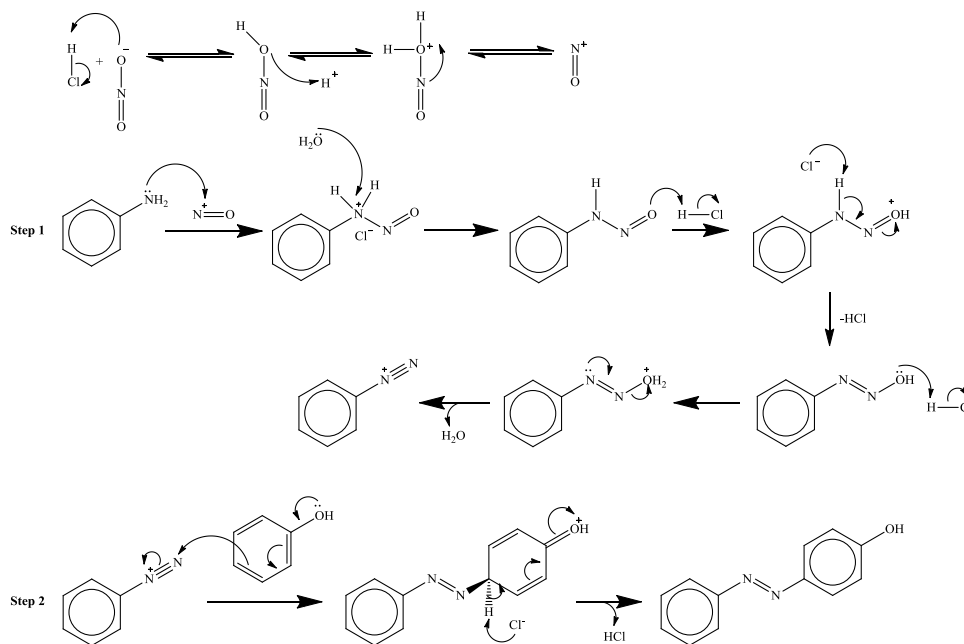
Scheme 2-13: Mechanism of an azo dye synthesis: (step 1) diazotization, (step 2) azo coupling

Depending on the aromatic rings and different substituents, there are two main kinds of azo dyes: aryl- and hetarylazo dyes.[80-85] Arylazo dyes are composed of carbon-based arenes

41

like the aminobenzenes and azobenzenes.[80,81,82] Hetarylazo dyes, such as benzothiazole and thiophene, are composed of heteroaromatic rings with heteroatoms such as sulfur or nitrogen.[83,84,85]

With respect to color properties, azo dyes are capable of providing virtually a complete range of hues.[73-75] The color of azo dyes originates from their selective absorption of incident light. The absorption of different wavelengths of light is based on their conjugation of π-systems. Usually, arylazo dyes have high levels of conjugation, thus producing deep colors like red and purple[80], whereas hetarylazo dyes, such as pyridine and thiophene systems, have less conjugation, resulting in brighter colors like yellow and orange.[83-85] The substituents on the aromatic rings play a role in the electron delocalization. For example, electron-withdrawing groups will delocalize the π-systems, causing a red shift in the absorption spectra, while electron-donating groups have the opposite effect, causing a blue shift in the absorption spectra. The shift in absorption spectra will accordingly result in the change of colors.[74] As discussed in Chapter 1, the azo groups –N=N– in the azo dye conduct photon-responsive isomerization. In the visible light or in the dark, azo compounds exist in the *trans* form; under the irradiation of UV light, the *trans* form undergoes conversion to the *cis* form. This feature is utilized in applications such as optical storage media, photo-optic switches, and liquid crystals.[73]

2.4.1 The synthesis of mono- and disazo dyes

Azo dyes that contain functional substituents, such as phenols or hydroxyl groups are useful for reactions with various complexed organoiron moieties. Such reactions yield complexes that contain both azo chromophore and organoiron functional units. These complexes are particularly useful for forming functional cores of star-shaped oligomers. As a result, azo dyes containing phenolic groups were synthesized followed by subsequent

nucleophilic aromatic substitution with organoiron complexes to form metal-azo dye complexes. Moreover, azo dyes containing hydroxyl groups were also prepared, since these dyes can undergo condensation reactions with metal-based carboxylic acids to form metal-azo dye esters.

One such azo dye synthesis has been previously reported and is shown in Scheme 2-14, using 4-hydroxyl aniline and 2-(N-ethylanilino) ethanol.[86] The suspension solution of 4-hydroxyl aniline in concentrated HCl was added to $NaNO_2$ for the diazotization, followed by the azo coupling reaction of 2-(N-ethylanilino) ethanol. The resulting azo dye contains two functional groups: the phenolic -OH and the hydroxyl group. Both functional groups can serve as reacting sites for further reactions with organoiron moieties (Figure 2-7).
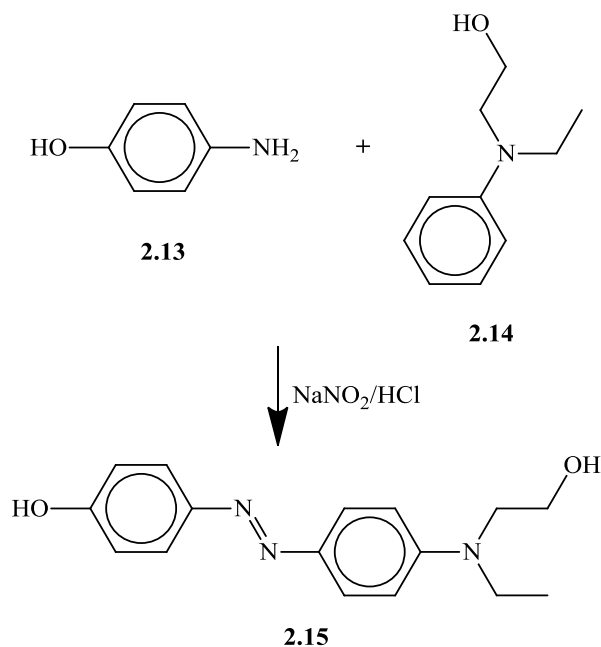
Scheme 2-14: Synthesis of azo dye 2.15[86]
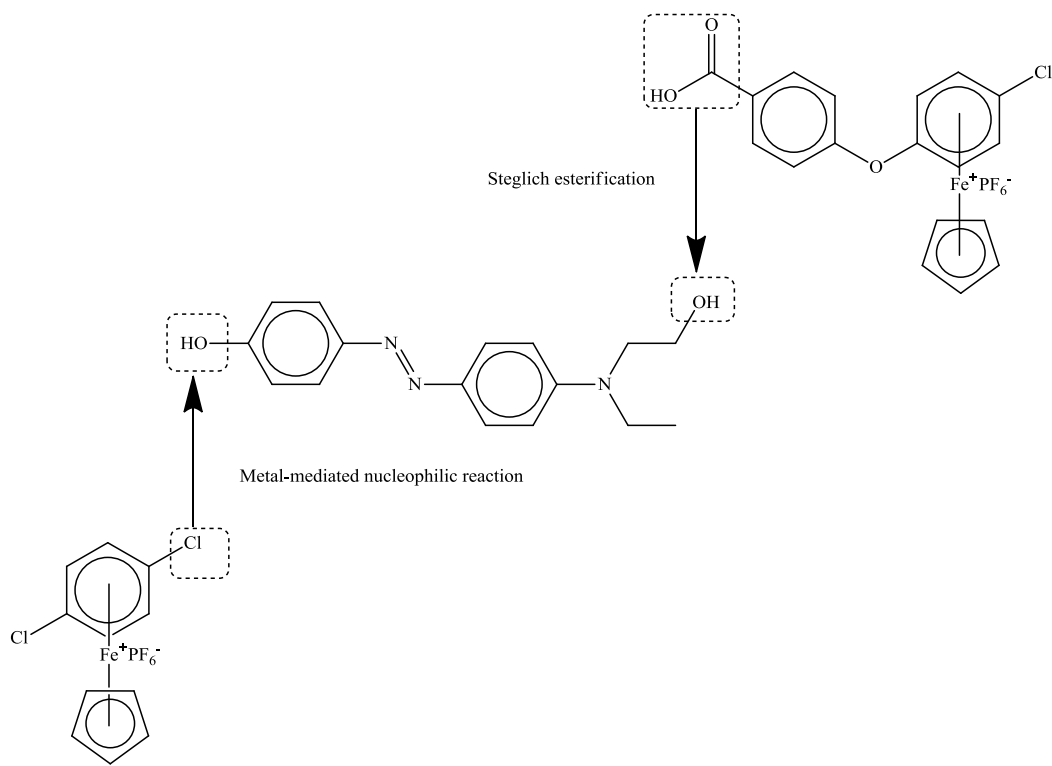
Figure 2-7: Reactivity of arylazo dye 2.15

A novel dye, similar to azo dye **2.15**, containing two terminal hydroxyl groups (**2.17**) was synthesized using standard methods.[87] The incorporation of two hydroxyl groups gives two potential reaction sites for Steglish Esterification.
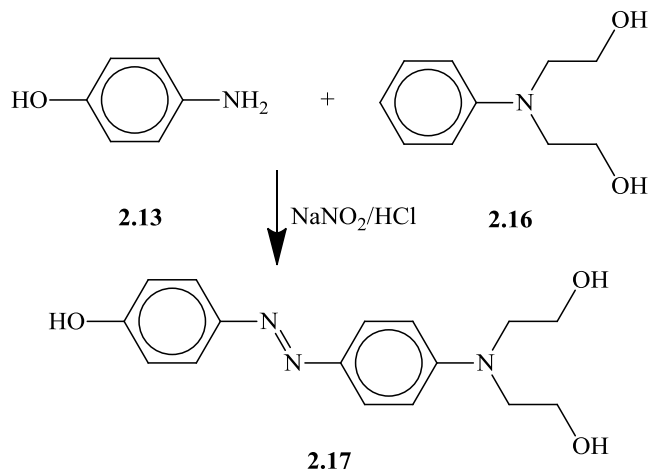
Scheme 2-15: Synthesis of arylazo dye 2.17 with two hydroxyl groups

The ^{1}H NMR of arylazodye **2.17** is shown in Figure 2-8. The aromatic resonances appear as four sets of doublets at 7.76, 7.74, 6.96, 6.86 ppm. The aliphatic methylenes appear as a triplet at 3.68 ppm for the CH_2 alpha to the alcohol group and a multiplet at 3.82 ppm integrating for 4H, two protons for each CH_2 attached to the nitrogen.
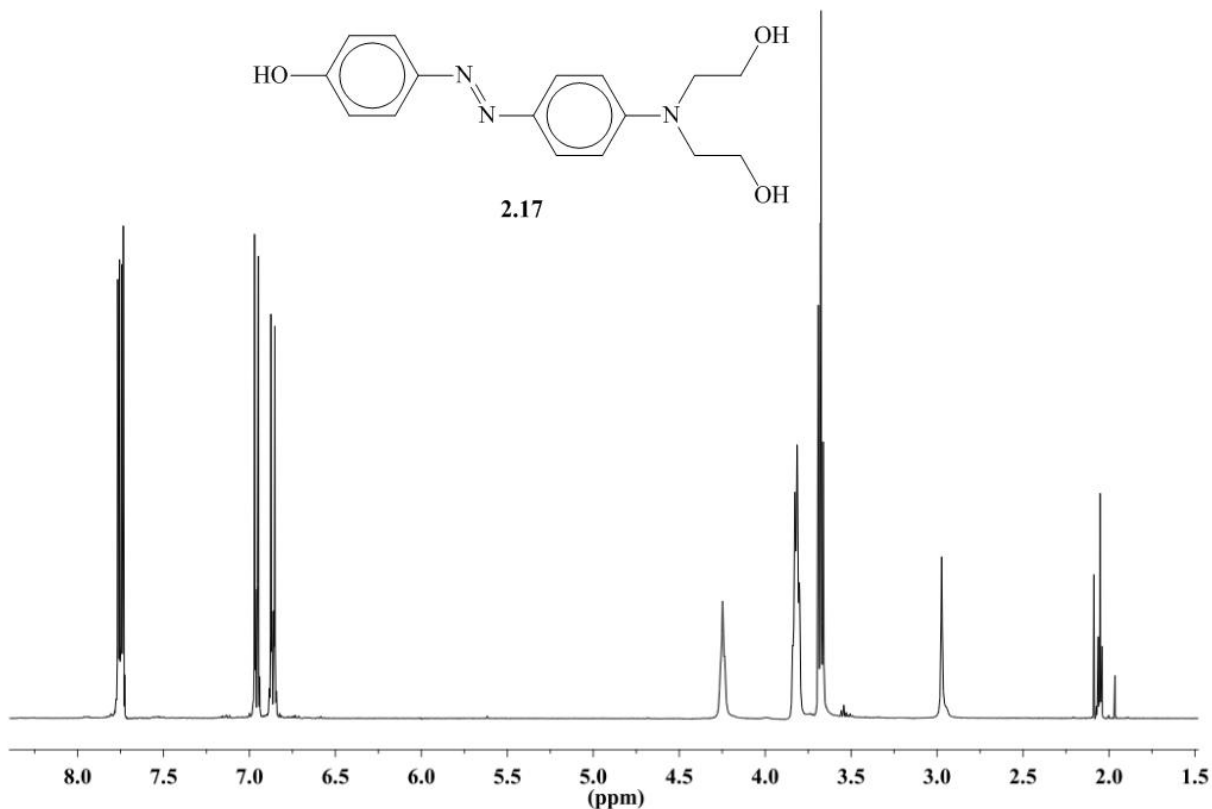
Figure 2-8: 400 MHz ^{1}H NMR spectrum of azo dye 2.17

The ^{13}C NMR NMR spectrum also shows peaks as expected. (Figure 2-9)The quaternary carbon peaks appear at 160.0, 151.4, 147.6 and 144.3 ppm, while the aromatic CH carbon resonances show at 125.2, 124.8, 116.5 and 112.5 ppm. The two methylene carbon resonances show at 60.3 and 55.1ppm. However, these two hydroxyl groups are too close to each that steric hindrance is introduced when conducting Steglish esterification.
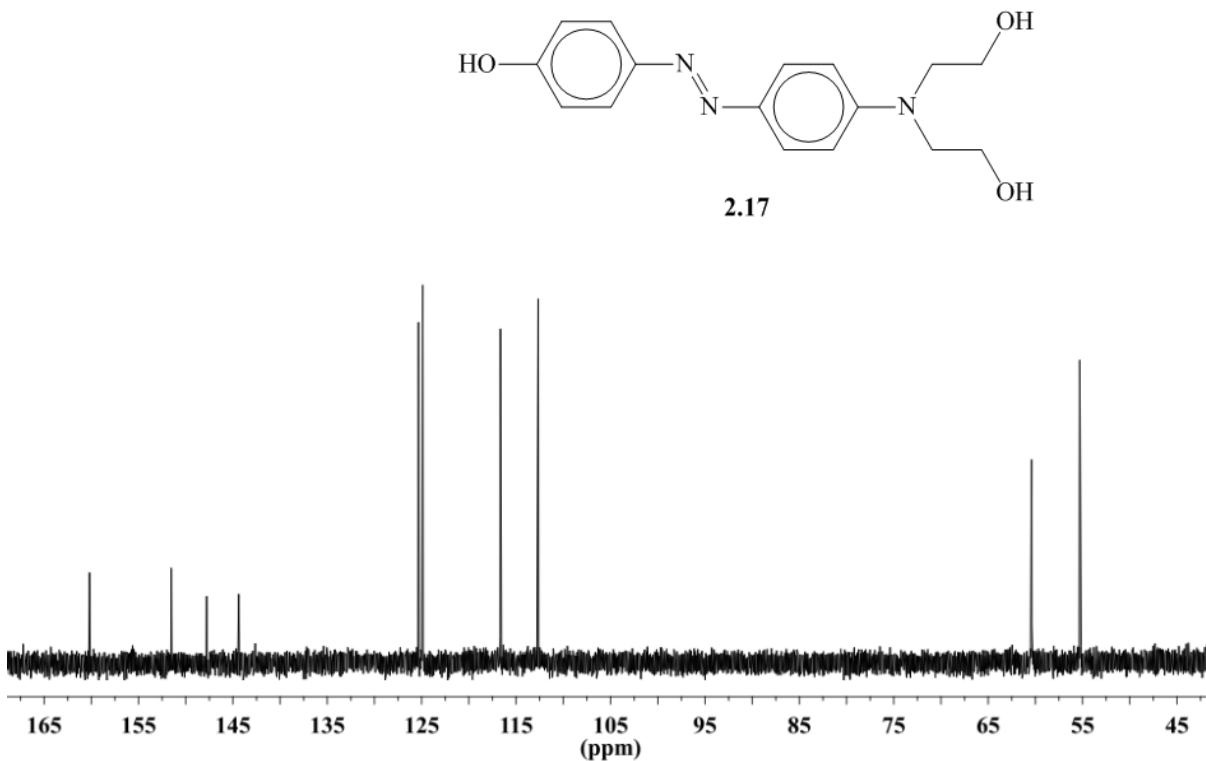
Figure 2-9: 101 MHz ^{13}C NMR spectrum of azo dye 2.17

Most commercially important azo dyes contain one single azo group and are therefore referred to as monoazo dyes. There are also many kinds of azo dyes that contain two or more azo groups called disazo dyes, which have been found to enhance dye-fiber interactions by hydrogen bonding, thus presenting better dyeing properties than the monoazo dye.[88,89,90] For the design of azo components for star-shaped oligomers, a disazo dye would offer a more efficient route, as there is one reaction site connecting each azo group. More excitingly, a disazo dye can become the initial core of a star or dendrimer itself.

Figure 2-10 shows the structure of C.I. Disperse Yellow 68[90] , a candidate for the initial core in the structure of stars or dendrimers. This molecule is a disazo dye that bears two phenol groups that can potentially conduct metal-mediated nucleophilic reactions from both ends of the molecule. However, the synthesis of this disazo dye requires multiple steps of diazotization and azo coupling. Firstly, a monoazo dye must be synthesized with one phenol

46

end and one amine end. Next, another round of diazotization and azo coupling reaction must be conducted to the monoazo dye to synthesize the disazo dye.[90]
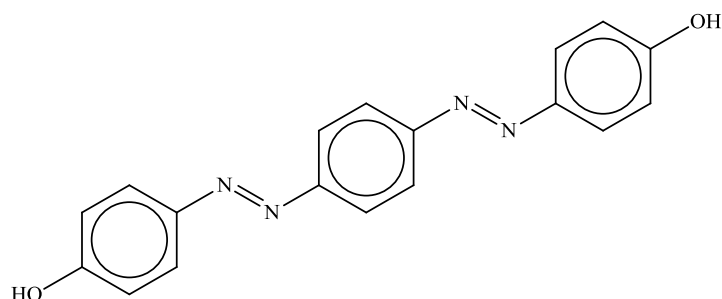
Figure 2-10: C.I. Disperse Yellow 68[90]

An alternative novel disazo dye with two hydroxyl groups (**2.19**) has been prepared in one step (Scheme 2-16). The incorporation of two terminal hydroxyl groups on disazo dye **2.19** allows two points of reactivity in one reaction, thus lowering the number of steps for further reactivity. A simplified synthetic route, compared to that used for C.I. Disperse Yellow 68, to form disazo dye **2.19** was carried out using a symmetrical starting material with two amine ends, 4,4'-diaminodiphenyl sulfide (**2.18**), in order to conduct a one-pot reaction with two molar equivalents of the coupling reagent, **2.14** (Scheme 2-16).
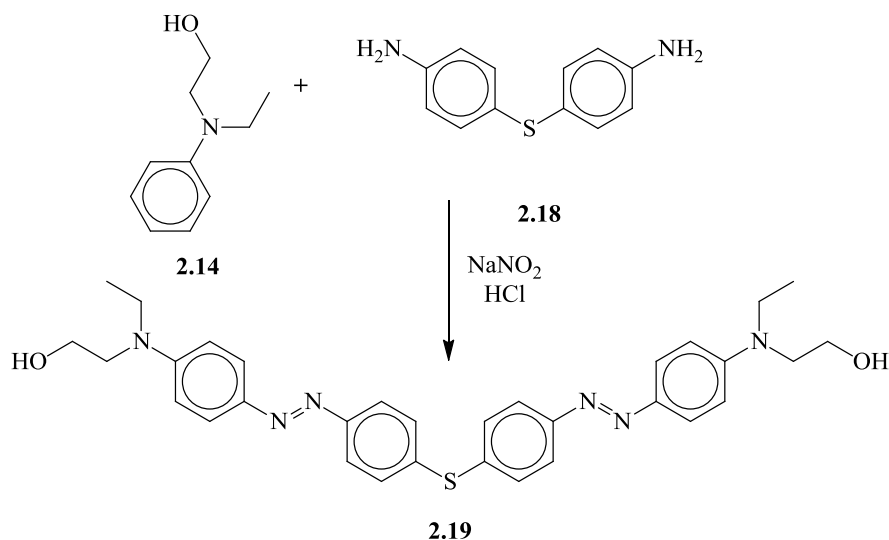
Scheme 2-16: The synthesis of disazo dye 2.19

The synthesis was performed via the general method of azo dye preparation. In the first step for diazotization, two molar equivalents of NaNO$_2$ were added and four molar equivalents of concentrated HCl were used. In the azo coupling step, two molar equivalents of 2-(N-ethylanilino) ethanol was used. The total reaction time was doubled to allow for the full diazotization and azo coupling to afford the novel red disazo dye **2.19** in a 67% yield.

2.19
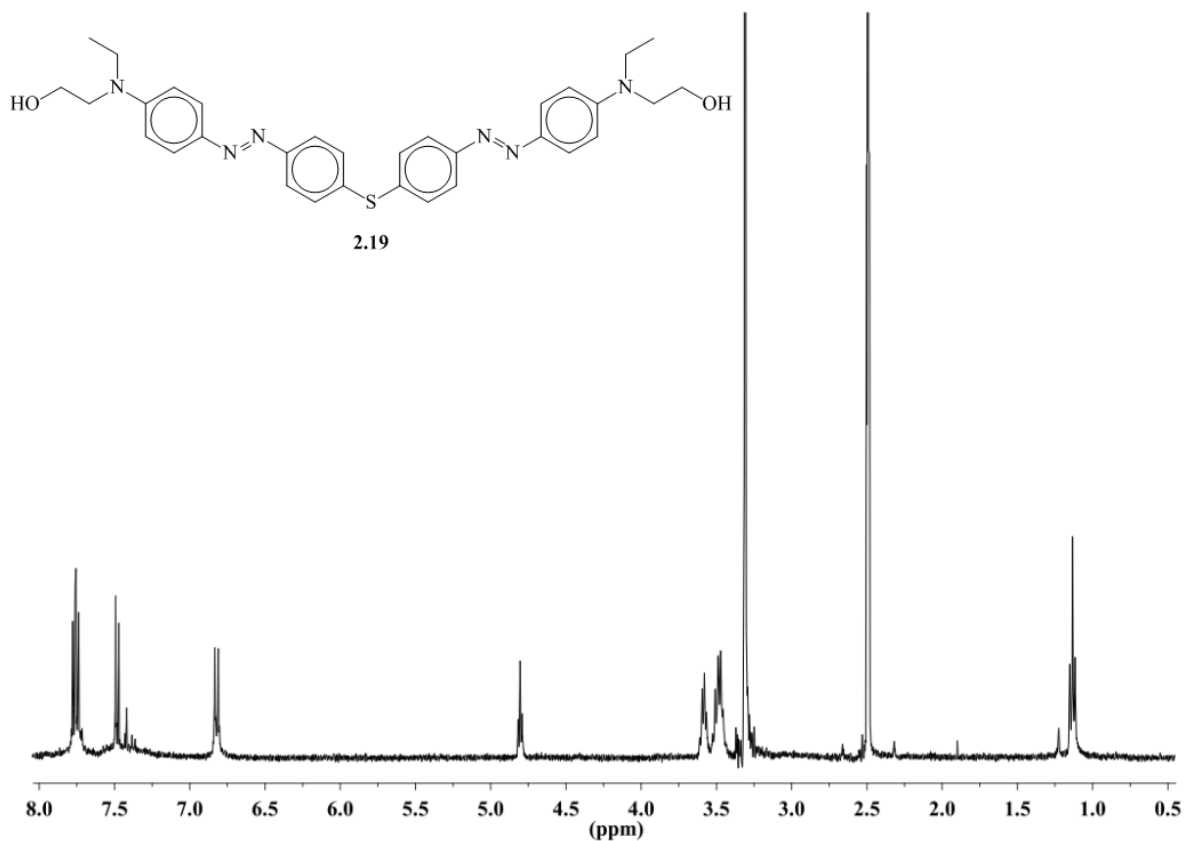
Figure 2-11: 400 MHz ^{1}H NMR spectrum of disazo dye 2.19

Figure 2-11 shows the ^{1}H NMR spectrum of the novel disazo dye **2.19**. The aromatic resonances appear as four sets of doublets at 7.78, 7.76, 7.49, and 6.83ppm. The hydroxyl groups appear at 4.76 ppm as a multiplet. The methylene protons next to the hydroxyl group appear as a multiplet at 3.59 ppm. The peaks corresponding to the methylene protons adjacent to the nitrogen are overlapping and appear as a multiplet at 3.49 ppm. The aliphatic CH$_3$ appears as a triplet at 1.14 ppm.

Also, in the ^{13}C NMR spectrum (Figure 2-12), all the peaks are present as expected. Due to the symmetric structure, there are only four peaks corresponding to the quaternary carbons at 151.6, 150.8, 142.2, 135.7 ppm. The resonances of the aromatic (CH) carbons appear at 131.3, 125.2, 122.8, and 111.2 ppm, while the aliphatic methylene carbon resonances appear at 58.3, 52.1, and 45.1 ppm. Finally, the methyl group resonance appears at 12.0 ppm.

2.19
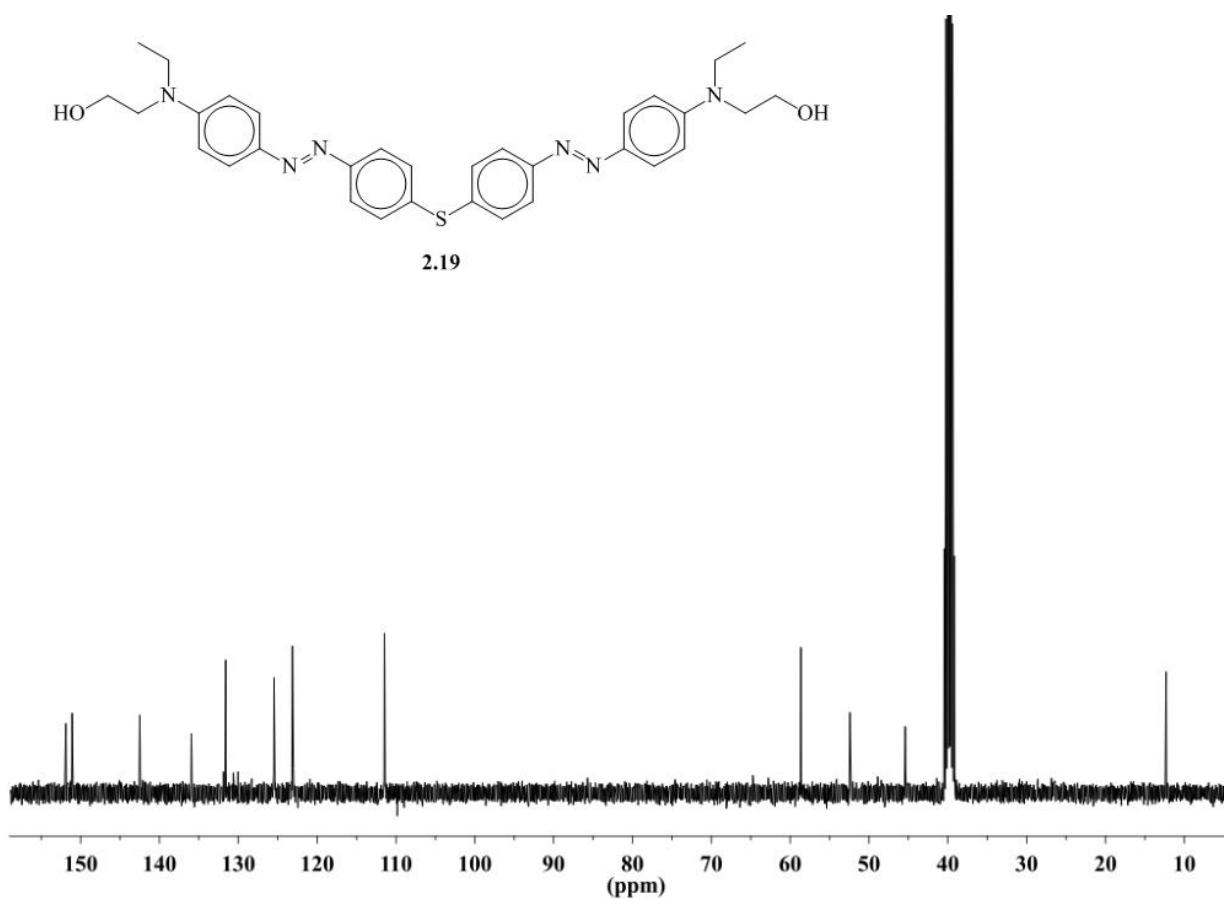
Figure 2-12: 101 MHz ^{13}C NMR spectrum of disazo dye 2.19

In the structures of stars and dendrimers, there are end groups that terminate the chain. In the design of star-shaped organoiron oligomers functionalized with azo chromophores, azo dyes can serve as end groups. Scheme 2-17 shows the synthesis of a previously reported hetarylazo dye[91] **2.22** which can react through the phenol group to the terminal chlorine group

49

on the complexed aromatic ring. This hetarylazo dye was prepared according to the published method from A.K. Prajapat *et al.*[91] The first step involves diazotization of 2-amino-6-methoxybenzothiazole using an aqueous solution of 50% H_2SO_4 and $NaNO_2$, stirring at 0 ℃. Subsequently, the diazonium ion was coupled to phenol, dissolved in an aqueous solution of 10% HCl and stirred at 0 ℃. An orange precipitate was isolated by filtration and dried under reduced pressure. The resulting pure product was confirmed spectroscopically via ^{1}H NMR and was compared to the previously reported spectral results.[91]
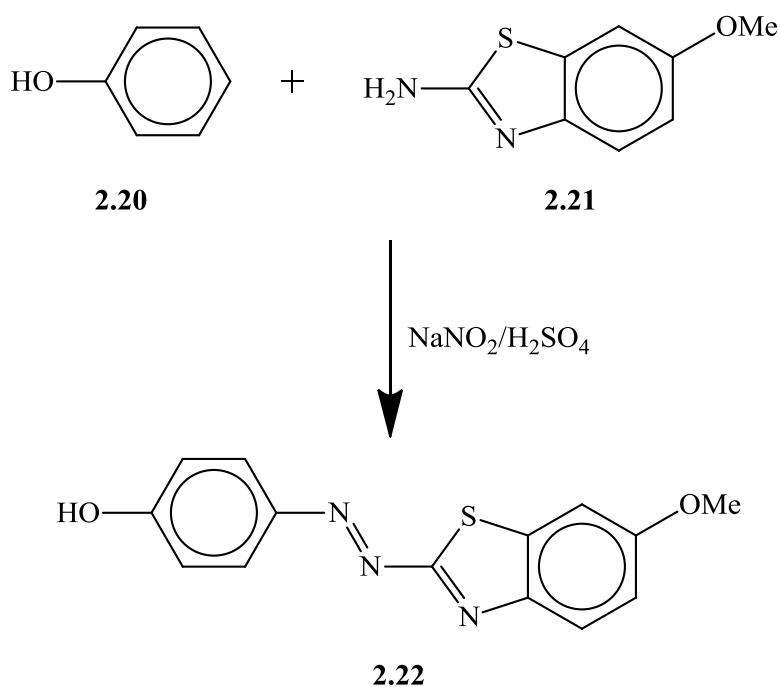
Scheme 2-17: The synthesis of hetarylazo dye 2.22[91]

Because of its low solubility in common solvents such as acetone and dichloromethane, hetarylazo dye **2.22** offers an effective purification method. In the divergent approach, since the oligomers are believed to have good solubility in common organic solvents, any excess of hetarylazo dye **2.22** can be easily removed through filtration as an undissolved solid.

2.4.2 Synthesis of complexed arylazo dyes

The previously reported[52] complexed arylazo dye was synthesized via metal-mediated nucleophilic substitution with *p*-dichloro complex **2.3**. As shown in Scheme 2-18, a one-to-one molar ratio of *p*-dichloro complex **2.3** and arylazo dye **2.15** were stirred in DMF in the presence of K_2CO_3 at room temperature, following the general method of the metal-mediated nucleophilic substitution. The resulting complexed azo dye has two reacting sites: (1) terminal chlorine group on the complexed aromatic ring to conduct metal-mediated nucleophilic substitution, and (2) the hydroxyl group to conduct esterification reactions.
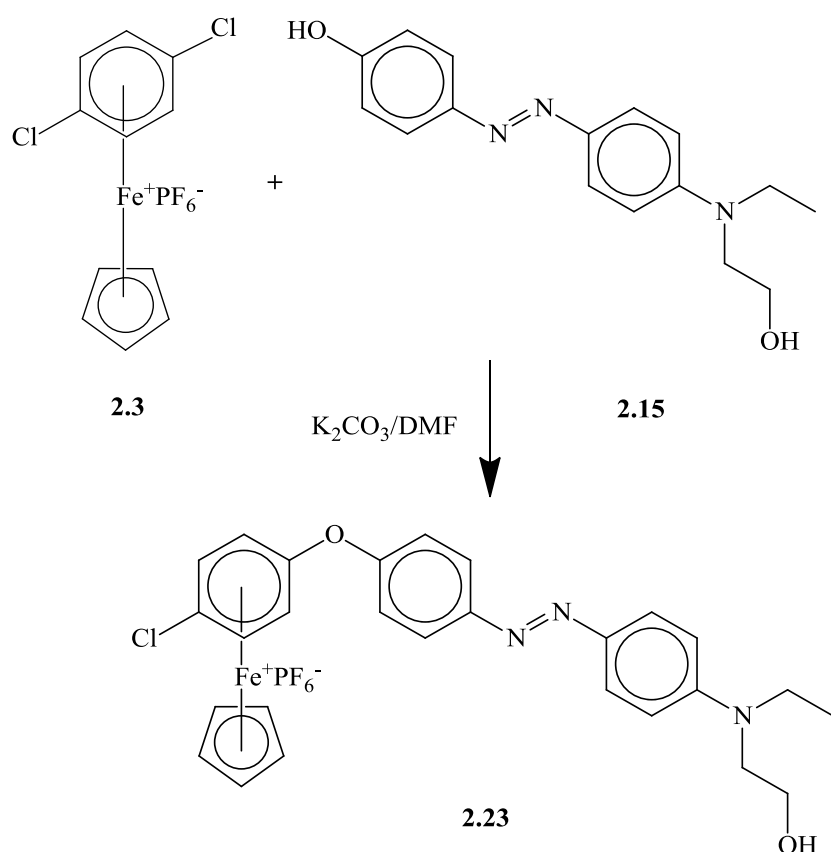
Scheme 2-18: Synthesis of metal-complexed azo dye 2.23[52]

Scheme 2-19 shows one example of the reaction utilizing the terminal chlorine group on the complexed aromatic ring for further metal-mediated nucleophilic substitution.[53] One more molar equivalent of azo dye **2.15** is added to the complexed azo dye **2.23**, using the same

reaction conditions as the monosubstituted complexed azo dye **2.24** to afford the disubstituted

azo dye **2.24**. The synthesis could also be conducted using a 1:2 molar ratio of *p*-dichloro

complex **2. 3** and azo dye **2.15**.
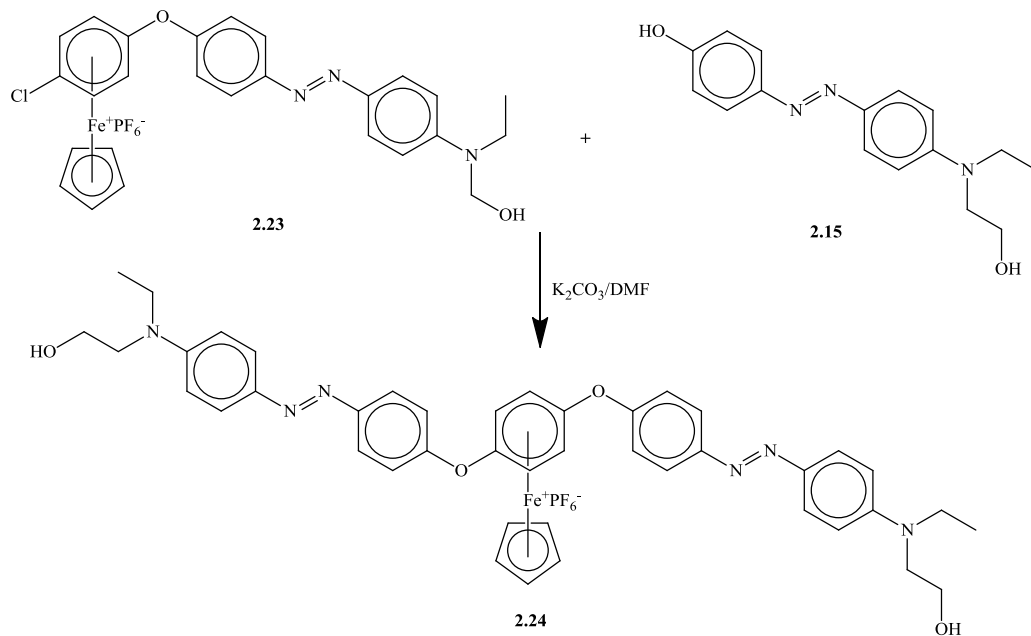
Scheme 2-19: Synthesis of disubstituted complexed azo dye 2.24[53]

Chapter 3. The synthesis of organoiron stars and dendrimers with azo dye bridges

3.1 Introduction

In Chapter 2, both organoiron moieties and azo dyes were synthesized as the building blocks for oligomers. This chapter will discuss the synthesis and characterization of the dual-functionalized oligomers bearing both organoiron moieties and azo dyes. To incorporate the organoiron complexes and azo dyes into the stars and dendrimers through their functional units, both metal-meditated nucleophilic substitution and Steglich esterification reactions are used. With reference to the dendrimer or star synthesis, both convergent and divergent approaches may be employed.

Figure 3-1 demonstrates two examples of proposed oligomers where both the organoiron moiety and azo dyes are introduced. In Figure 3-1 a), complex **2.3** was connected to an azo dye first and attached to the organic core following the convergent approach. In Figure 3-1 b), a core containing both an azo dye and complex **2.3** was designed first, and then attached with four of the organoiron moieties, as per the divergent approach. The preparation of these molecules can be achieved via metal-mediated nucleophilic aromatic substitutions and ester condensation reactions.
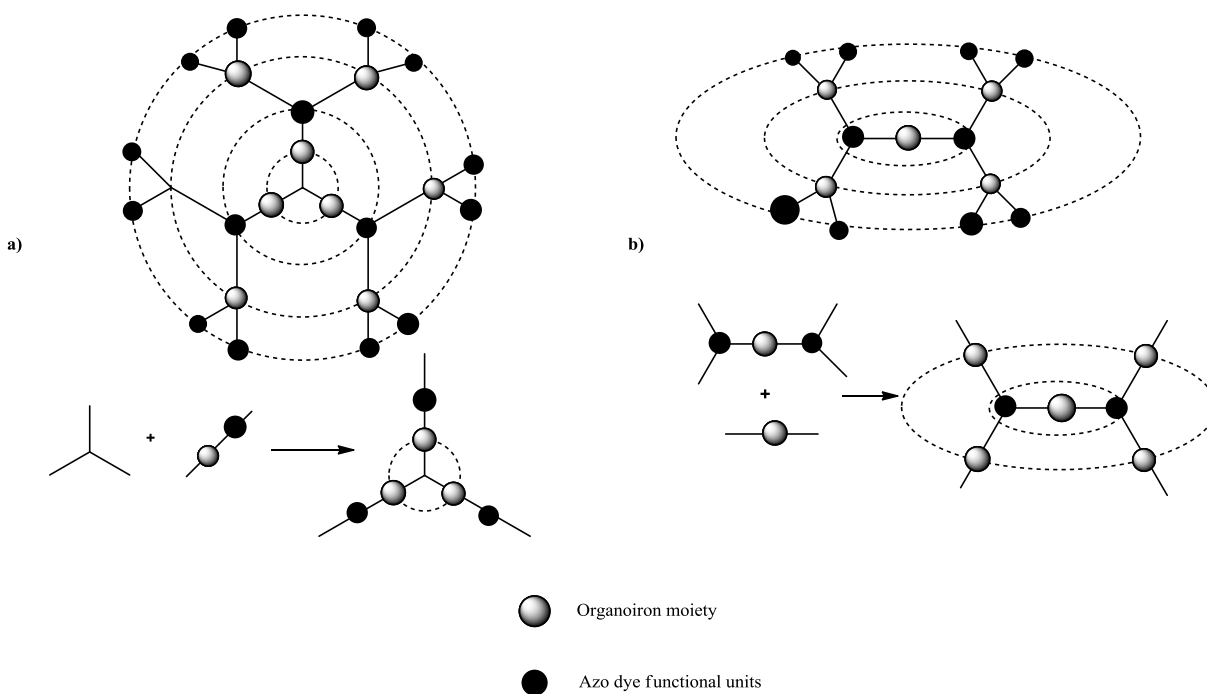
Figure 3-1: Proposed oligomers containing organoiron moieties and azo groups

3.2   Results and discussion

3.2.1   The synthesis and characterization of three-arm star-shaped oligomers

The design of star-shaped organoiron oligomers containing azo chromophores has been achieved via both convergent and divergent methods using metal-mediated nucleophilic aromatic substitution and esterification reactions. Reaction of metal complexed azo dye **2.23** with 1,3,5-benzene tricarboxylic acid (**3.1**) led to the formation of the three-arm triiron star containing three azo dye moieties (**3.2**).Compound **3.2** was synthesized in cooperation with Elizabeth Strohm.[92,93]
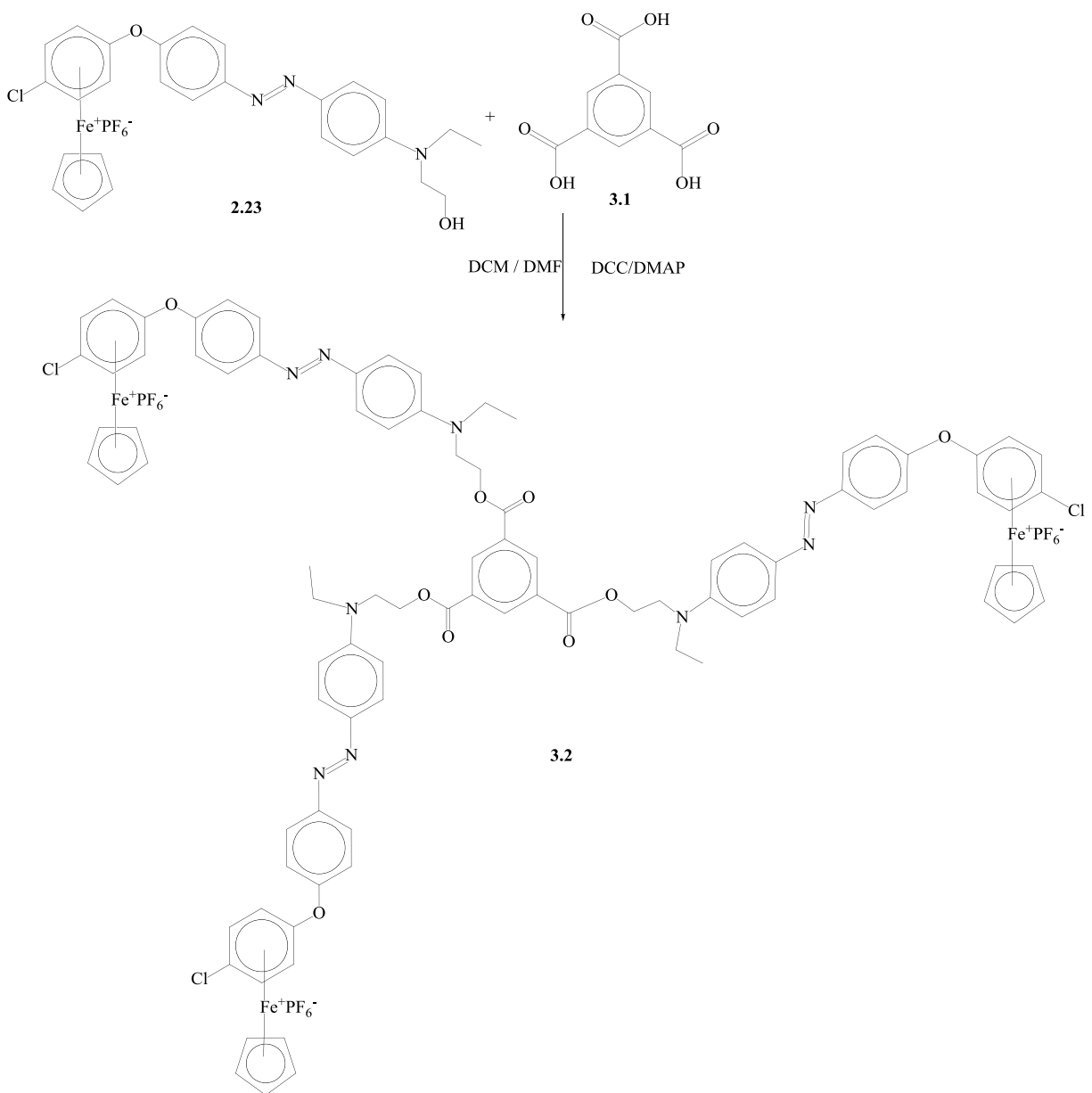
Scheme 3-1: The preparation of triiron complex 3.2

Figure 3-2 shows the ^{1}H NMR spectrum of complex **3.2**. Compared to complex **2.23**, there is a clear shift in the hydroxyl methyl resonance from 3.80 ppm in complex **2.23** to 4.57 ppm in complex **3.2**.
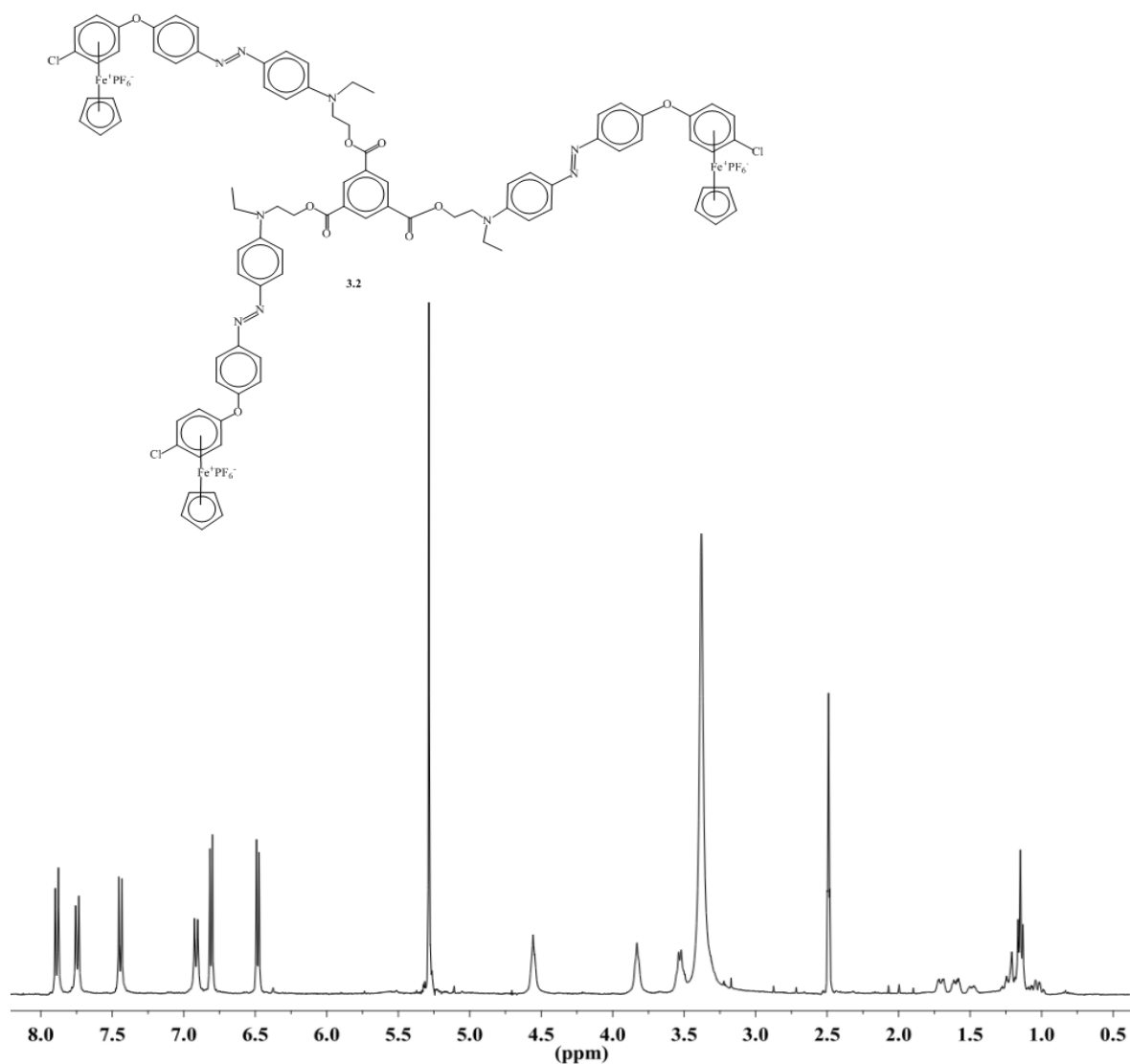
Figure 3-2: 400 MHz ^{1}H NMR spectrum of star-shaped complex 3.2

The gDQCOSY confirmed the ^3J correlation between the CH$_2$O- protons (4.57 ppm) and the NCH$_2$- protons at 3.84 ppm (Figure 3-3). The formation of the ester was further confirmed by similar shifts in the ^{13}C spectrum; in particular, the appearance of the carbonyl ^{13}C peak corresponding to the ester functionality at 164.1 ppm. The gHMBC spectrum also confirmed the structure of oligomer **3.2** by showing ^3J correlations between the CH$_2$O- (4.57 ppm), the ester core aromatic hydrogens (8.60 ppm), and the ester carbonyl carbon (164.1 ppm). IR spectroscopy supported the formation of the ester linkages with a C=O stretching frequency of 1734 cm^{-1}.
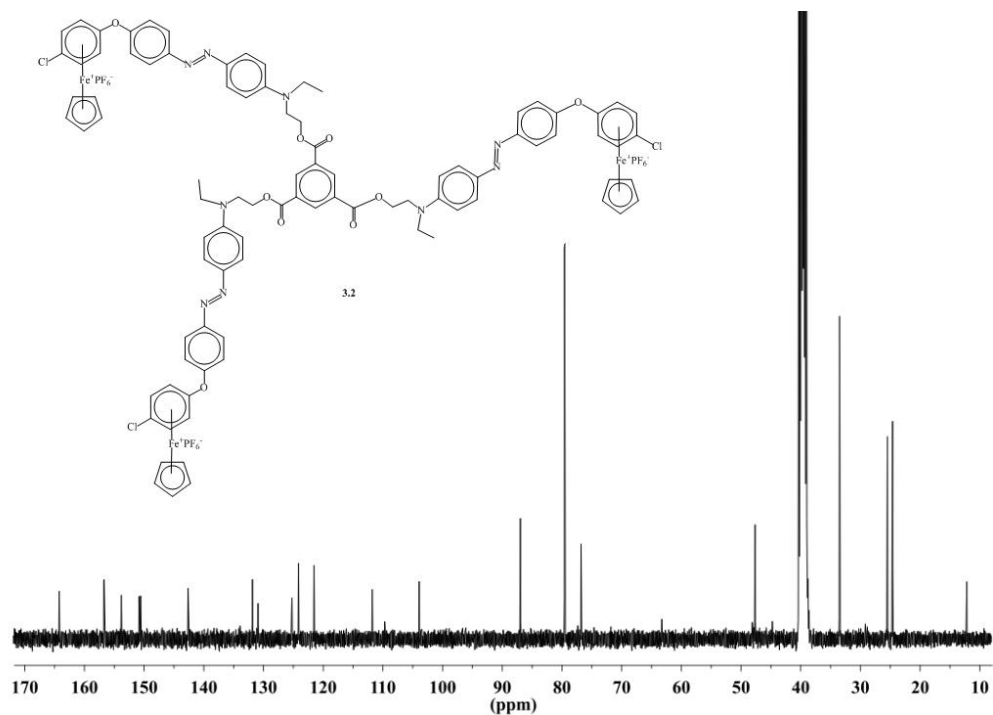
Figure 3-3: 101 MHz ^{13}C NMR spectrum of star-shaped complex 3.2
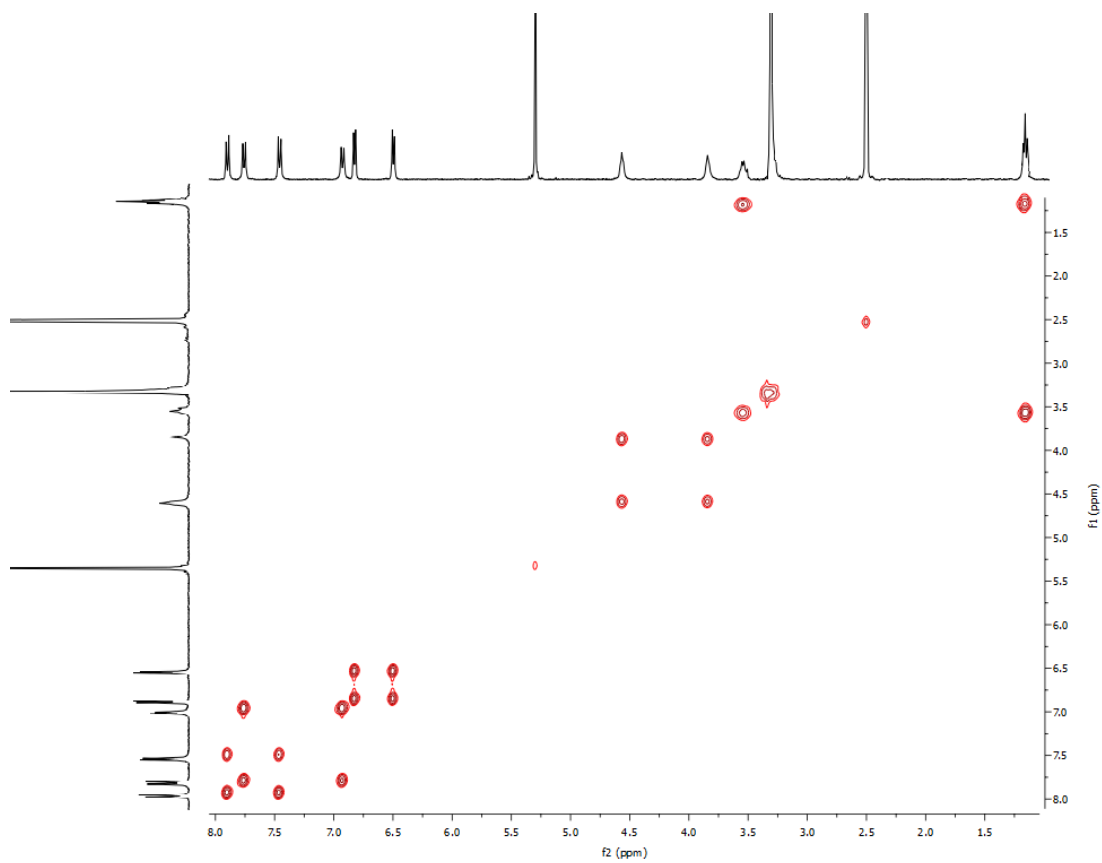
Figure 3-4: ^{1}H-^{1}H gDQCOSY NMR spectrum of star-shaped complex 3.2
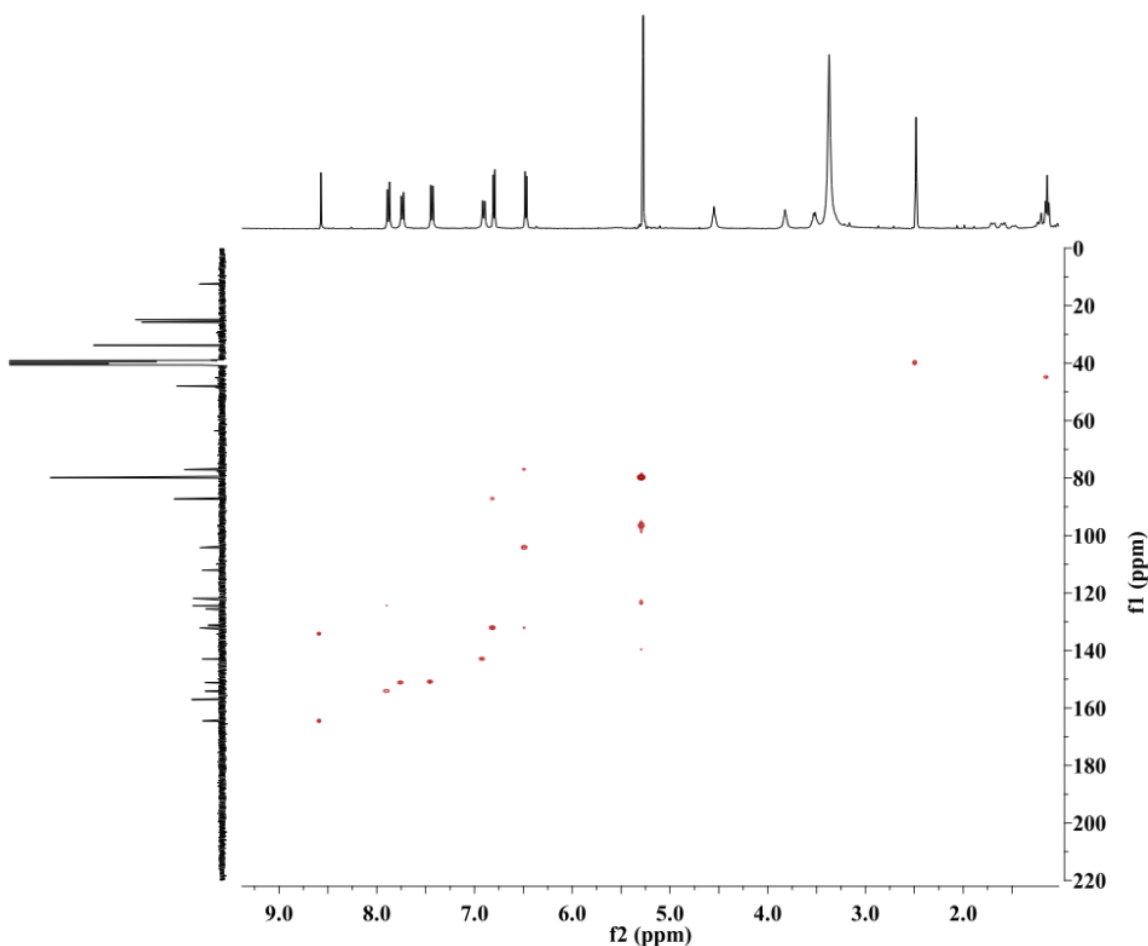
Figure 3-5: ^{1}H-^{13}C gHMBC NMR spectrum of star-shaped complex **3.2**

In compound **3.2**, the presence of three terminal aryl chloro groups that are complexed to the cyclopentadienyliron moiety allow for further reactions to extend the size of the star-shaped oligomers via a divergent approach. To illustrate this point, complex **3.2** underwent a nucleophilic aromatic substitution reaction with phenolic hetarylazo dye **2.22** to give rise to the triiron core with an arylazo dye bridge and terminal hetarylazo dye (Scheme 3-2). It is important to note that through the divergent approach, the inclusion of an arylazo dye forms the first generation, while the addition of a hetarylazo dye forms the second generation. The divergent method was chosen because it employs less structural hindrance compared to the convergent method, and can therefore be utilized to grow higher generation.
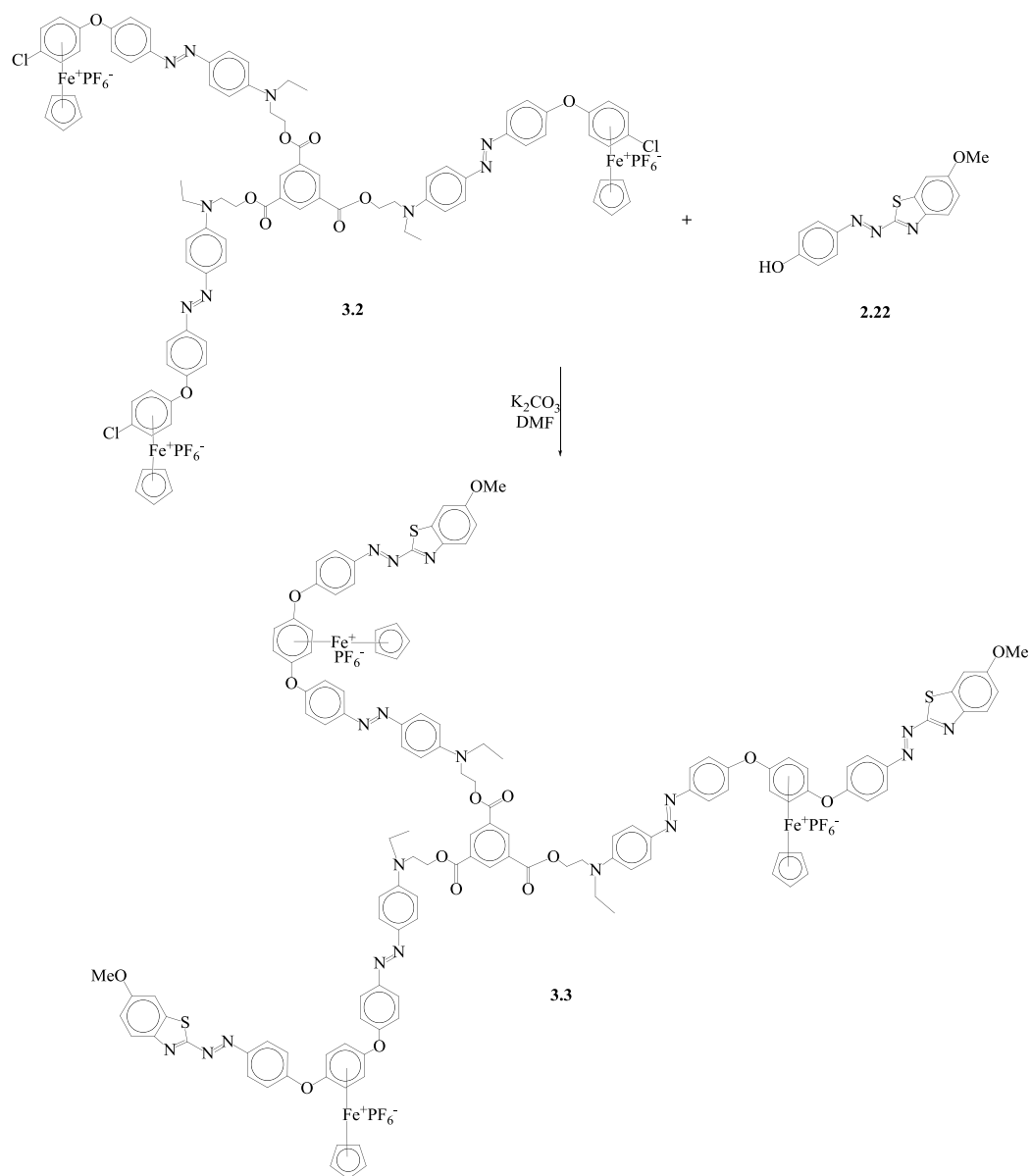
Scheme 3-2: Nucleophilic aromatic substitution of complex 3.2

In the preparation of star-shaped molecule **3.3**, excess amount of phenolic hetarylazo dye **2.22** is used to make sure all three terminal aryl chloro groups of complex **3.2** are reacted. For purification, the crude product was dissolved in acetone and the excess hetarylazo dye **2.22** remained as a suspended solid. The solid suspension was removed via filtration and the filtrate, containing the product, was collected. Due to the three dimensional structure, star-

shaped molecule **3.3** shows enhanced solubility in acetone compared to its starting materials **3.2** and **2.22**.

The formation of star-shaped molecule **3.3** is confirmed by both ^{1}H and ^{13}C NMR spectroscopy. In the ^{1}H NMR spectrum (Figure 3-5), the non-complexed arene peaks at 7.92, 7.33, 7.39, 6.98 ppm result from phenolic hetarylazo dye **2.22**, while the non-complexed arene peaks at 8.50, 7.69, 7.39, and 6.86 ppm result from oligomer **3.2**. The region of 7.87-7.82 ppm appears as a multiplet due to the overlapping aromatic protons of complex **3.2** and hetarylazodye **2.22**. The complexed arene peaks appearing at 6.76 and 6.43 ppm in the ^{1}H NMR spectrum of complex **3.3** are shifted from 6.82 and 6.50 ppm from oligomer **3.2**. Similarly, the cyclopendiene peak shifted from 5.30 ppm to 5.24 ppm. The methoxy peak appears at 3.35 ppm as a singlet, while the methyl peak appears at 1.10 ppm as a triplet. Finally, all the methylene proton resonances occur at 4.51 and 3.78 ppm. All integrations were as expected as well. The ^{13}C NMR spectrum (Figure 3-7) further confirms the successful synthesis of complex **3.3**. The single Cp peak appears at 79.5 ppm indicating the purity of product. Furthermore, the methoxy carbon resonance appears at 55.0 ppm.
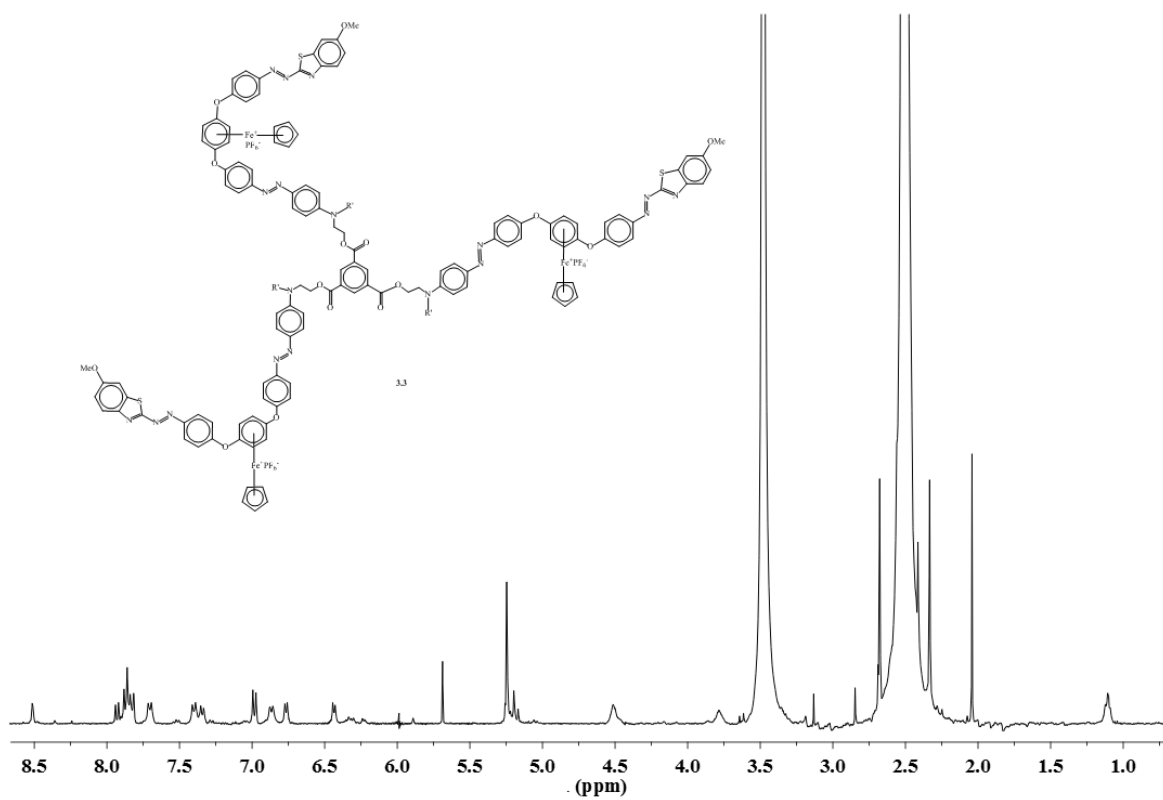
Figure 3-6: 400 MHz ^{1}H NMR spectrum of star-shaped molecule 3.3
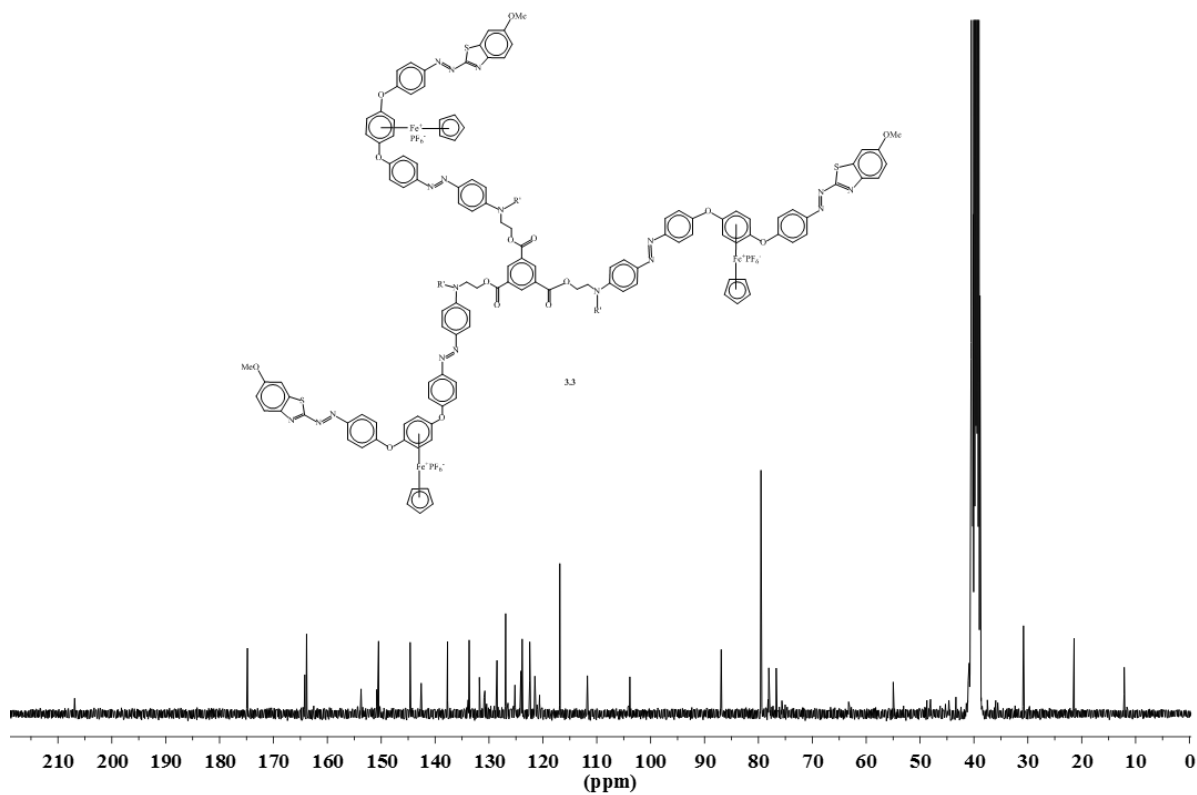
Figure 3-7: 101 MHz ^{13}C NMR spectrum of star-shaped molecule 3.3

61

With the same starting material in the synthesis of the triiron ester core star, the tri-ether core analogue was also prepared via the reaction of complexed azo dye **2.23** with phloroglucinol (**2.11**) to produce the triiron ether core (**3.4**) containing azo groups with terminal alcohol functionalities (Scheme 3-3). This reaction proceeded at room temperature in the presence of base via metal-mediated nucleophilic substitution to give the star-shaped oligomer **3.4** in 80% yield.
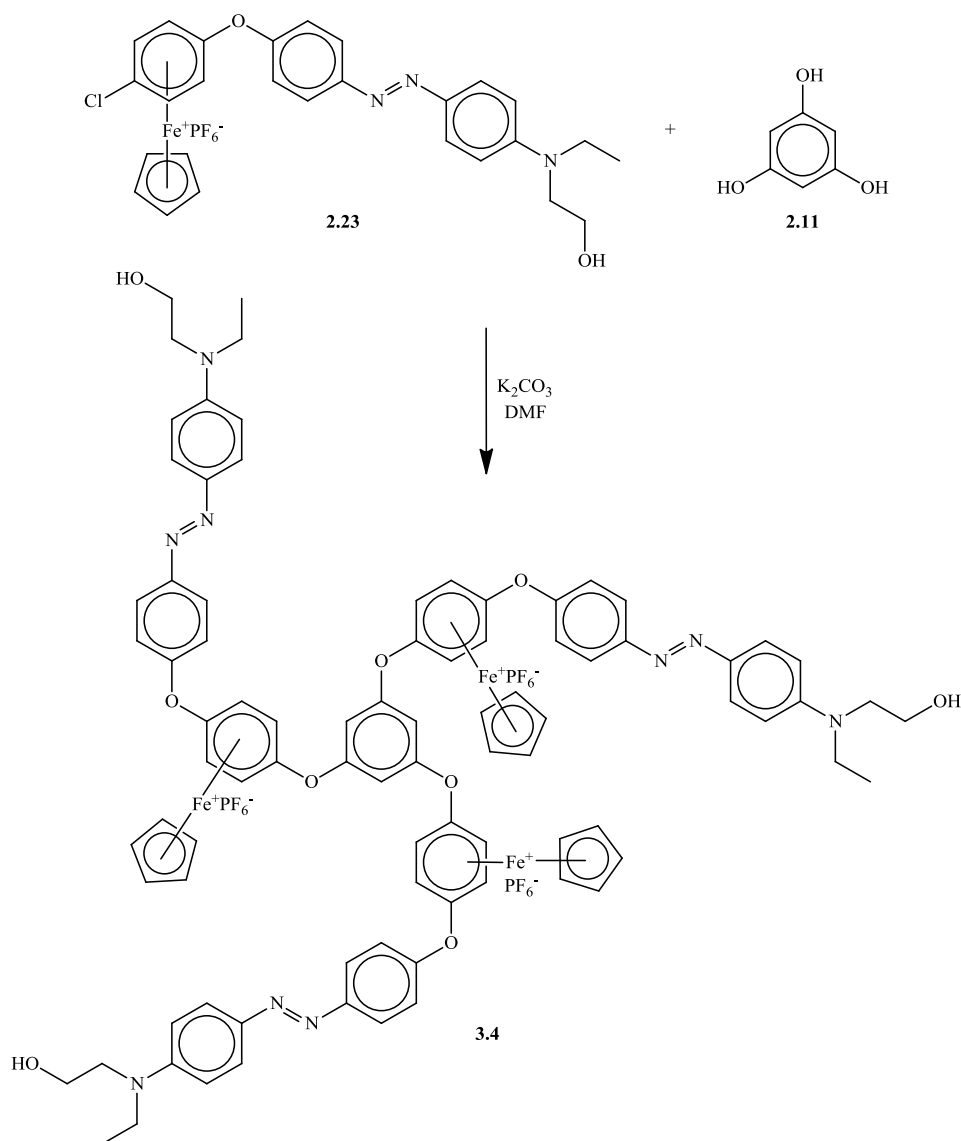
Scheme 3-3: The convergent synthesis of the first generation star-shaped ether 3.4

Compared to Scheme 3-3 as the "arm-first" convergent synthesis, Scheme 3-4 shows the "core-first" divergent synthesis of **3.4** from azo dye **2.15** and three-metal star **2.12**.
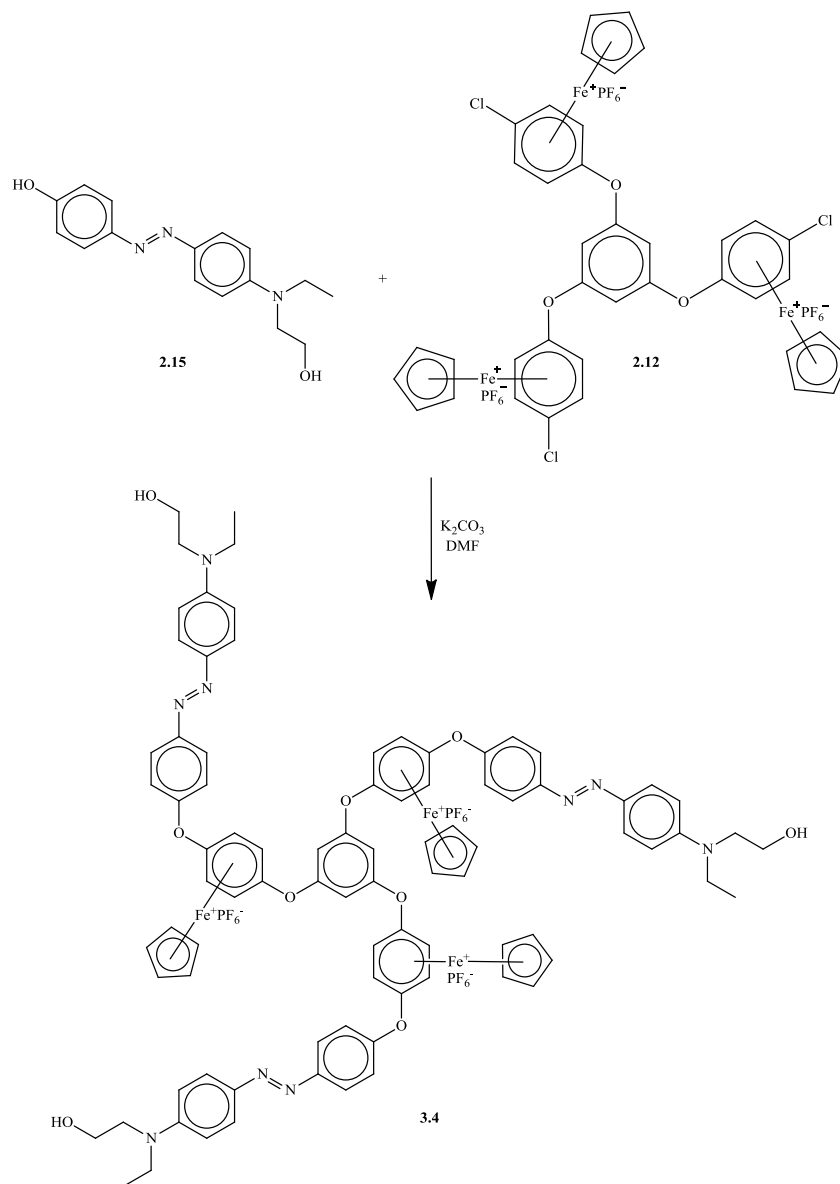
Scheme 3-4: The divergent synthesis of the first generation star-shaped ether 3.4

In comparison of the ^{1}H NMR spectra (Figure 3-8), the product **3.4** formed via convergent synthesis gave a pure product, seen in the ^{1}H NMR spectrum (spectrum 2) with only one Cp peak, while the product **3.4** formed via divergent synthesis resulted in multiple Cp peaks in the ^{1}H NMR spectrum (spectrum 1). The aromatic resonances in spectrum 2 show

up as clearer shifts compared to those in spectrum 1. The ^{1}H NMR spectrum yielded from the

convergent method is clearer due to fewer steric defects in its synthetic route.
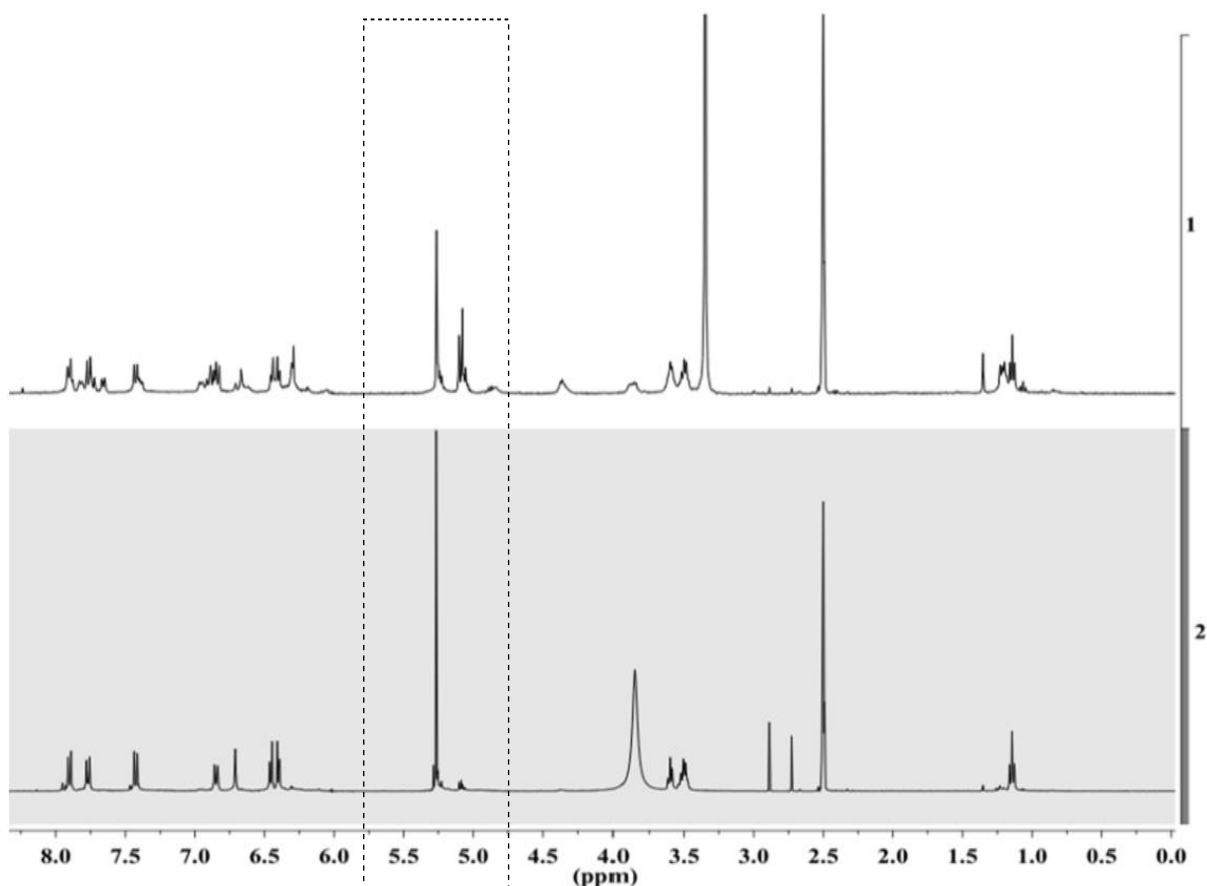
Figure 3-8: 400 MHz ^{1}H NMR comparison of complex 3.4 prepared via divergent

synthesis (spectrum 1) and convergent synthesis (spectrum 2)

The ^{1}H NMR of complex **3.4**, synthesized using the convergent synthetic method

(Scheme 3-3), shows all of the expected resonances (Figure 3-9). The non-complexed arene

resonances appear at 7.91, 7.77, 7.43, 6.85, and 6.71 ppm, while the complexed arene

resonances are found at 6.44 and 6.41 ppm. Compared to the starting material, complex **2.23**,

the complexed aromatic protons shifted from 6.49 ppm and 6.83 ppm to 6.41 ppm and 6.44

ppm, evidence for the formation of the aryl ether bond. The aromatic protons of the

pholoroglucinol show up at 6.71 ppm as a single peak, and the Cp resonance appears at 5.27

64

ppm. The aliphatic methylenes appear as a triplet at 3.60 ppm for the CH_2 alpha to the alcohol group and a multiplet at 3.51 ppm for the CH_2 attached to the nitrogen. Finally, the methyl proton resonance shows at 1.14 ppm.
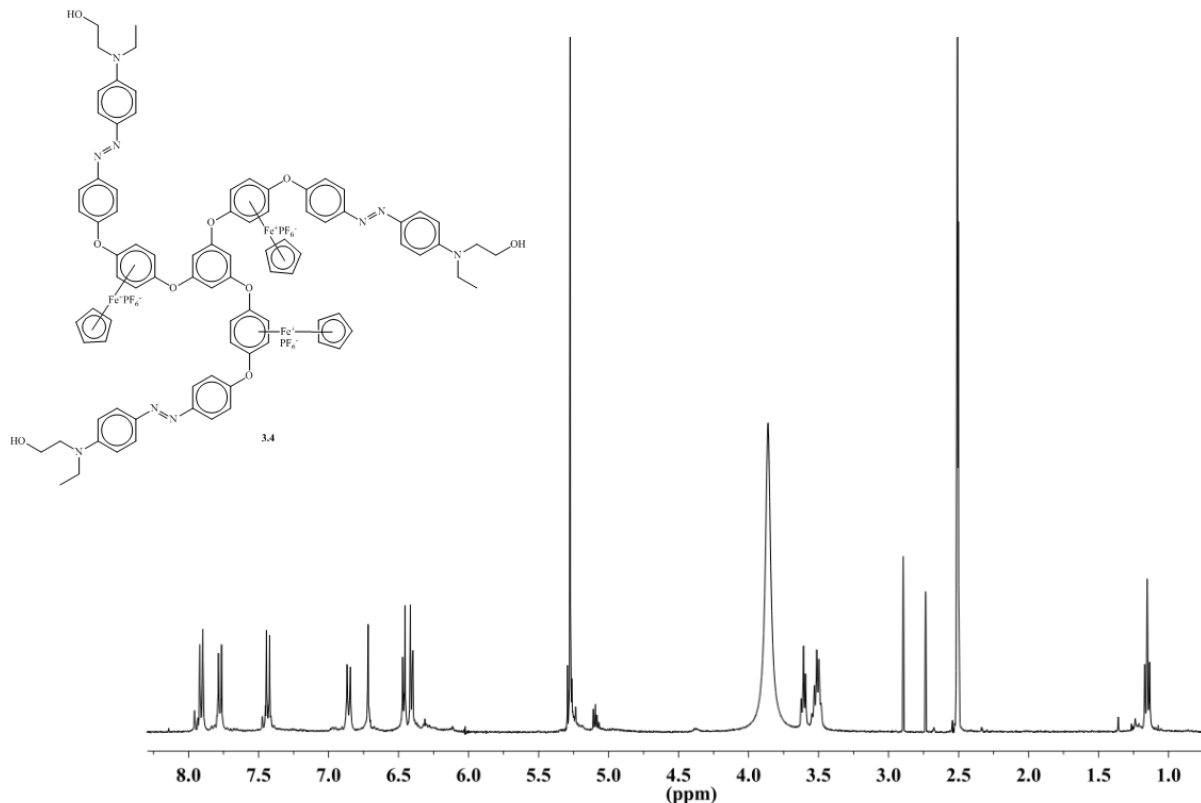
Figure 3-9: 400 MHz ^{1}H NMR spectrum of star-shaped ether core 3.4

The APT ^{13}C spectrum also shows all the expected resonances with quaternary carbons phased up, CH/CH$_3$ carbons phased down, and CH$_2$ carbons phased up. The aryl ether quaternary carbons (C-O-C) appear at 160.8, 155.7, 154.1, 150.8, 150.2, and 142.1 ppm, while the non-complexed arene carbons (CH) are shown at 129.9, 129.6, 125.2, 123.9, 121.0, 111.3, and 105.2 ppm together with the complexed arene carbon (CH) at 75.6 and 75.5 ppm. The Cp peak appears at 78.1 ppm and the methylene carbons appear at 58.3, 52.2, and 45.2 ppm. Finally, the methyl carbon appears at 12.0 ppm.
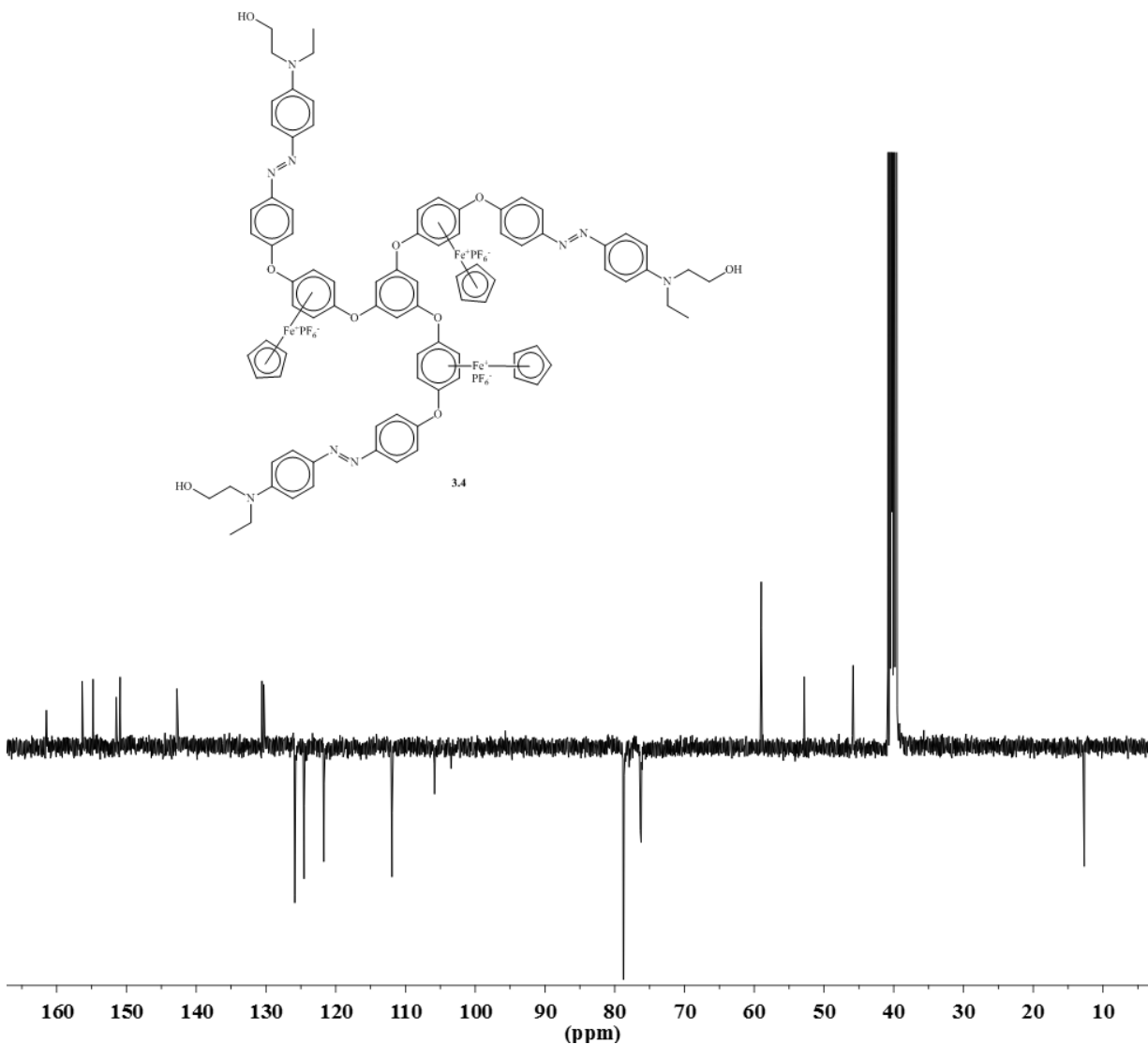
Figure 3-10: 101 MHz APT ^{13}C NMR spectrum for star-shaped ether core 3.4

The further elaboration of complex **3.4** was realized by esterifying the terminal hydroxyl group of the azo dye moieties with ferrocene carboxylic acid **3.5**[94] (Scheme 3-5). As ferrocene carboxylic acid is dissolved in dilute NaOH solution, the reaction is purified by washing with 10% aq NaOH solution to remove any excess ferrocene carboxylic acid. The resulting complexed oligomer (**3.6**) possesses a tri-ether core, which is attached to complexed arene cyclopentadienyliron cations, arylazo dyes, and ferrocene moieties.
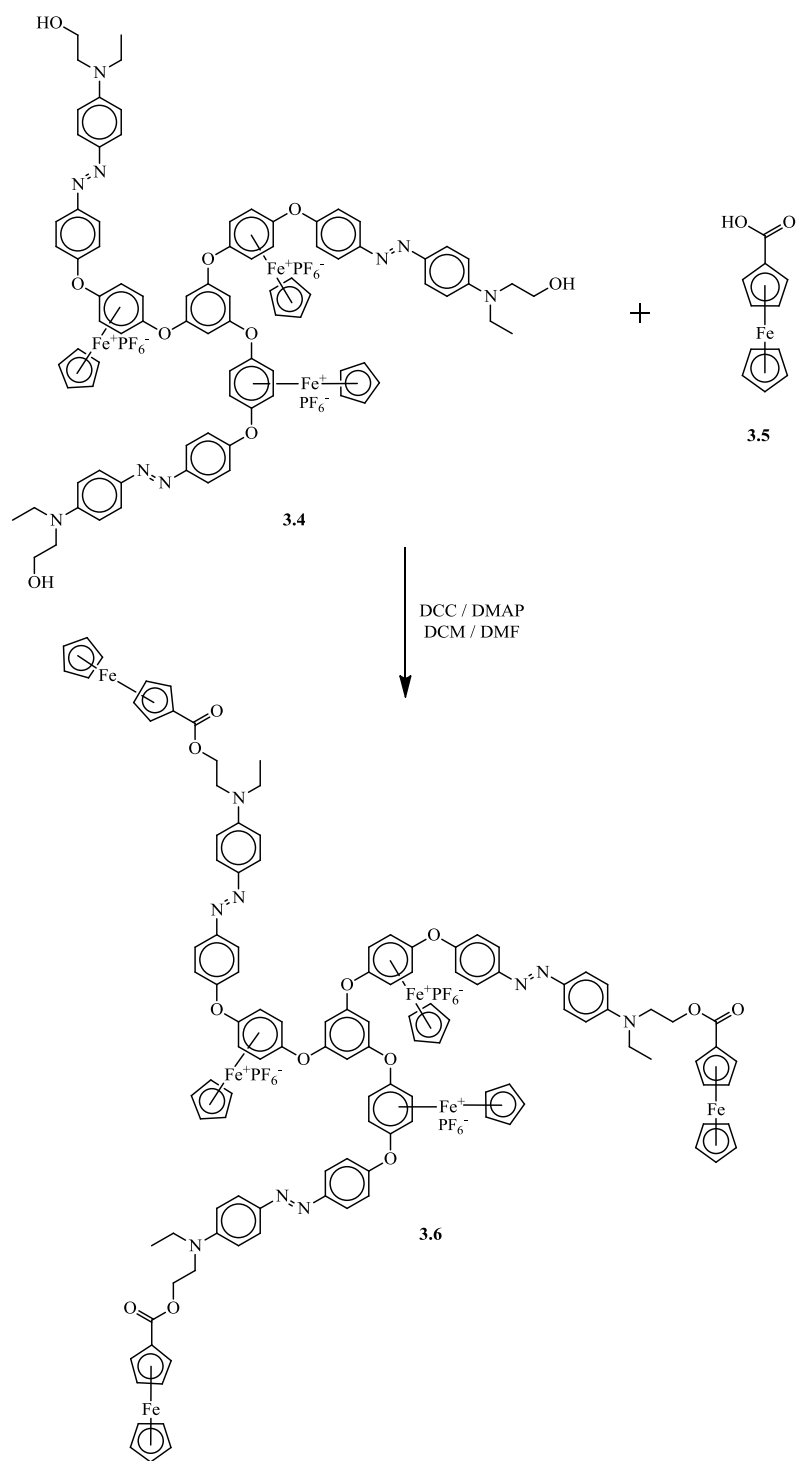
Scheme 3-5: The functionalization of complex 3.6 with ferrocene carboxylic acid

The inclusion of the ferrocene-ester moiety in complex **3.6** was characterized by NMR and IR spectroscopy. The substituted cyclopentadiene ring gives two triplets at 4.73 and 4.48 ppm and the non-substituted cyclopentadiene of the ferrocene ester moiety appears as a singlet

at 4.15 ppm. The resonance of the methylene protons *alpha* to the ester carbonyl group appears at 4.39 ppm, and the methylene attached to the nitrogen on the ester chain appears more down field at 3.78 ppm. The assignment of these methylene protons were confirmed in the gCOSY NMR spectrum (Figure 3-12), which is indicated by the cross peaks at 4.39ppm and 3.78 ppm. The ^{13}C NMR spectrum confirms the presence of the C=O of the ester group at 170.8 ppm. On the other hand, mono-substituted ferrocene show at 71.4, 70.4, 69.8 and 69.6 ppm. (Figure 3-13) IR spectrum shows the C=O of the ester at 1718 cm^{-1}.
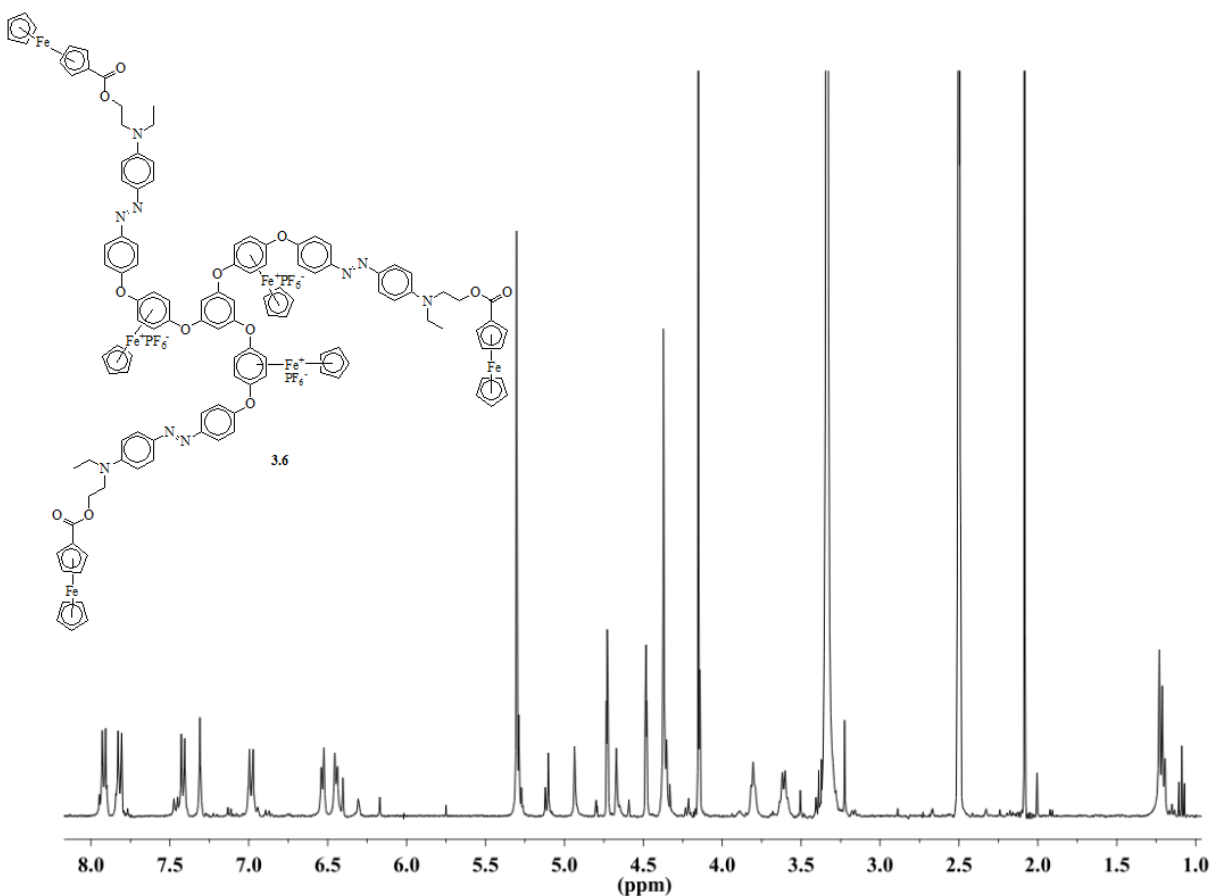
Figure 3-11: 400 MHz ^{1}H NMR spectrum of complex 3.6
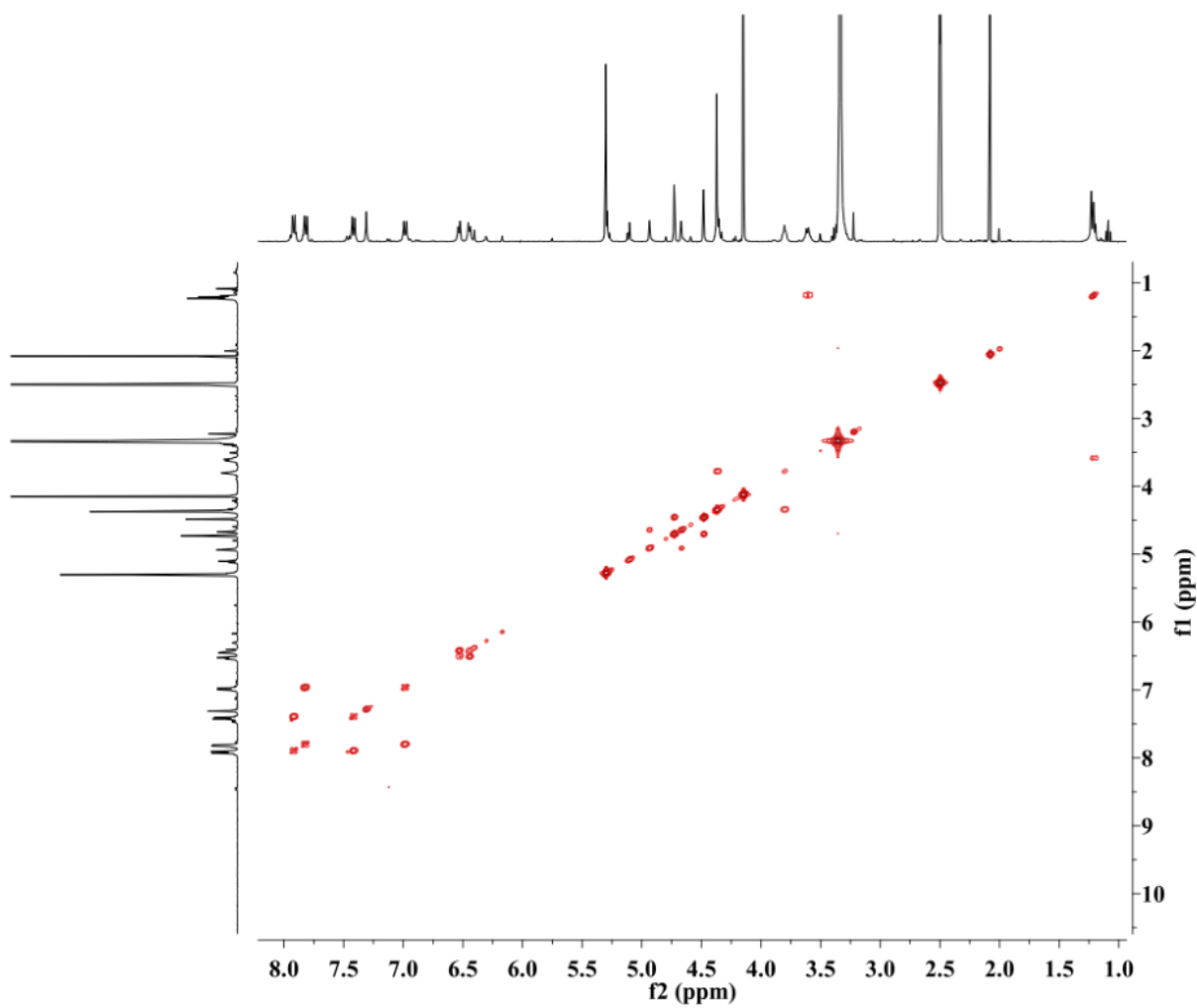
Figure 3-12: ^{1}H-^{1}H gCOSY NMR spectrum of complex 3.6
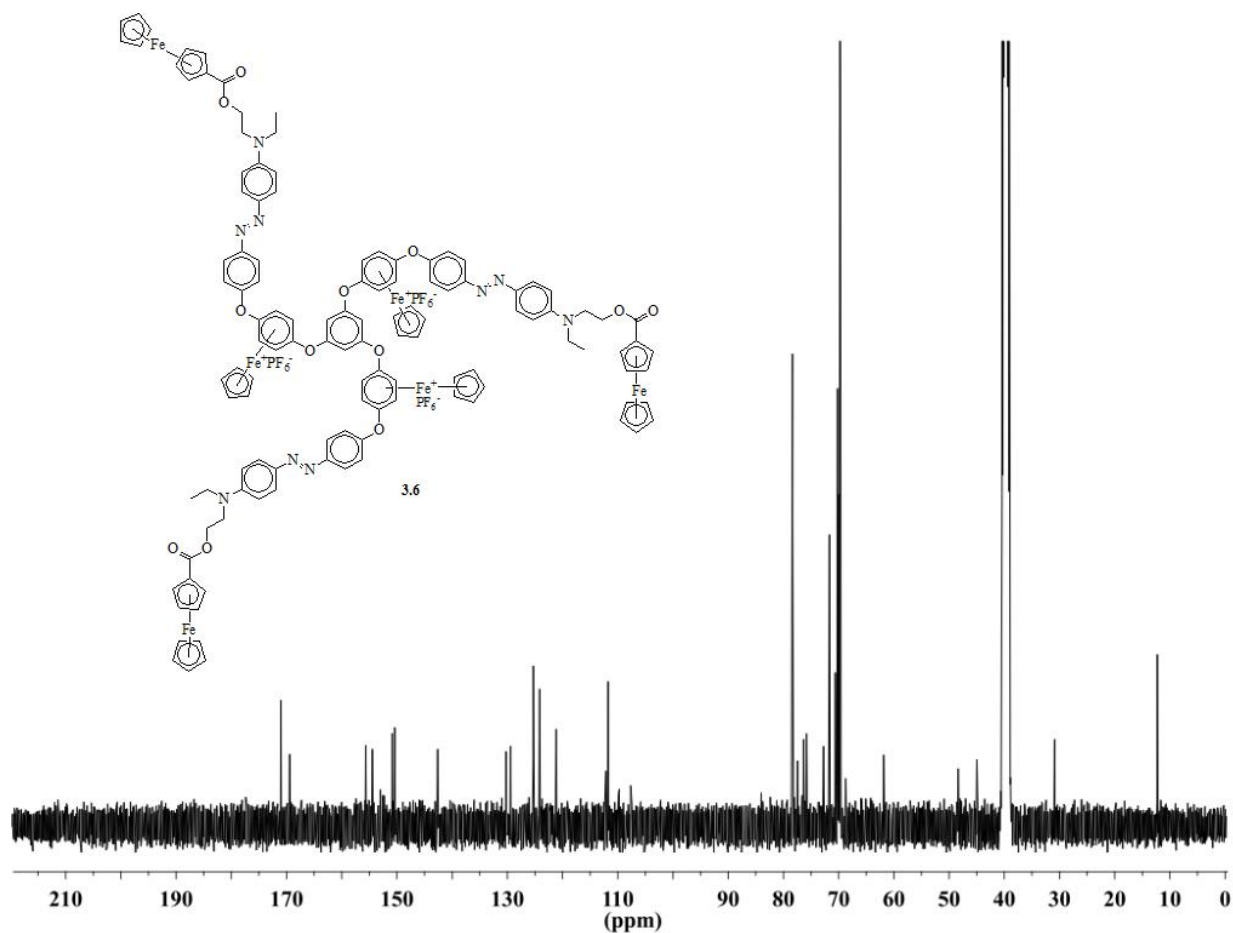
Figure 3-13: 101 MHz ^{13}C NMR spectrum of complex 3.6

The successful esterification reaction gave rise to another more versatile esterification of oligomer **3.4** using bimetallic carboxylic acid complex **2.7** containing a carboxylic acid group and two terminal chloro groups. Scheme 3-6 shows the structure of the three-arm star-shaped molecule (**3.7**) containing six cationic cyclopentadienyliron moieties and six terminal chloro groups. The activated chloro groups can undergo further nucleophilic aromatic substitution reactions to extend the growing chains.
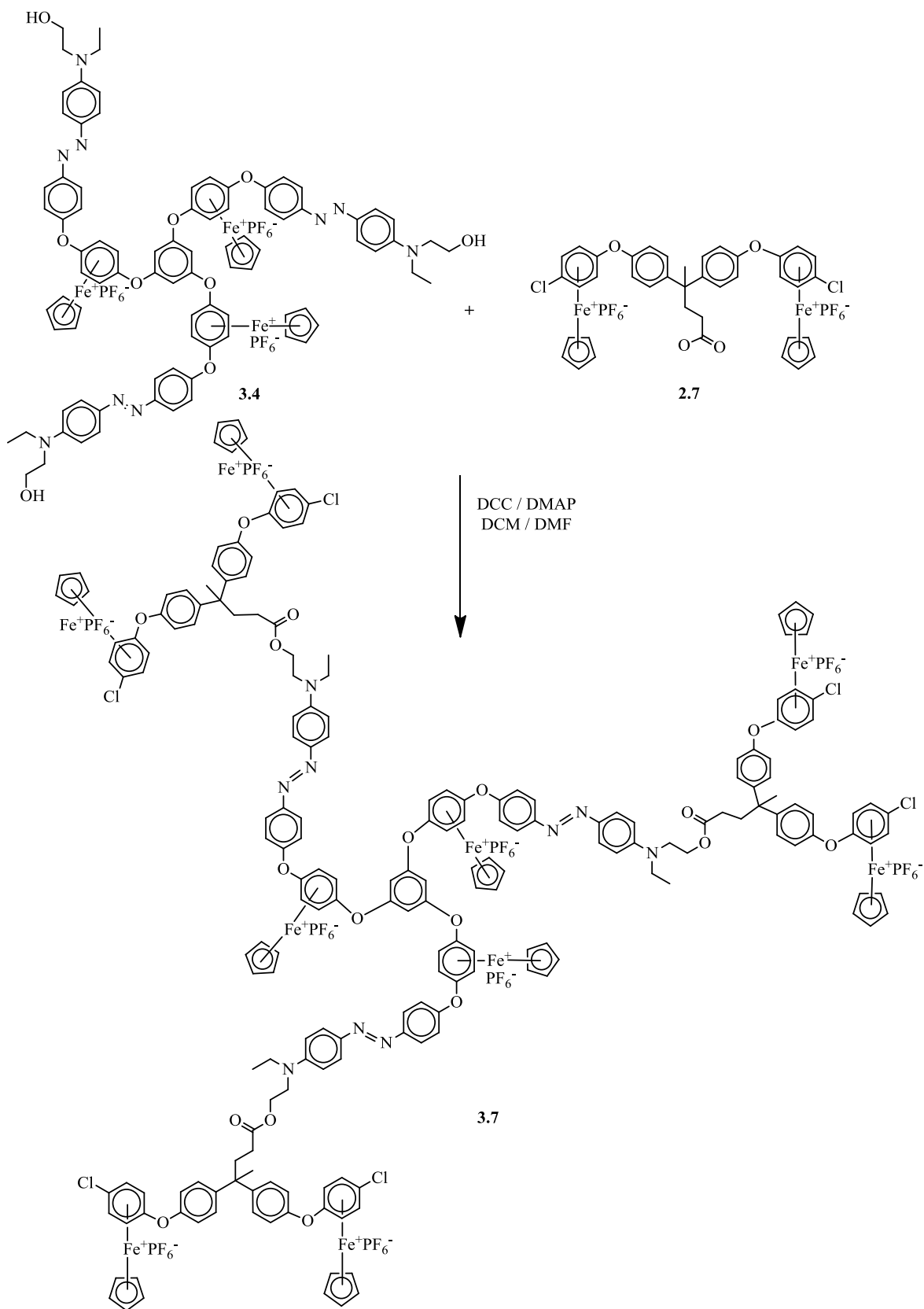
Scheme 3-6: **The formation of star-shaped oligomer 3.7 via an esterification reaction**

The formation of oligomer **3.7** is indicated by ^{1}H NMR spectrum. (Figure 3-14) The methylene protons in the *alpha* position of the ester group of **3.7** appear at 4.21 ppm compared to the methylene protons in the *alpha* position of the hydroxyl group of complex **3.4** at 3.60 ppm. The resonance of the Cp peaks coordinated to the core appear at 5.28 ppm with an integration of 15, while the resonance of the terminal Cp peaks appear at 5.27 ppm with an integration of 30. The complexed arene resonances appear at 6.89, 6.80 and 6.47-6.36 (overlapping) ppm and the non-complexed arene resonances appear at 7.88, 7.79, 7.42, 7.36 and 7.26 ppm. The terminal non-complexed arene resonances appear at 7.36 and 7.26 ppm and integrate to twelve.

The ^{13}C NMR spectrum (Figure 3-14) further confirms the successful synthesis of the product. The resonance at 65.4 ppm is characteristic of an ester CH_2 and the carboxyl carbon and appears at 173.2 ppm. All the other carbon resonances appear as expected. For example, the incorporation of second generation gives rise to the terminal Cp peaks at 79.8 ppm and the terminal complexed aromatics at 87.3 ppm and 76.8 ppm. Additionally, the IR spectrum shows the C=O stretching frequency at 1722 cm^{-1}.
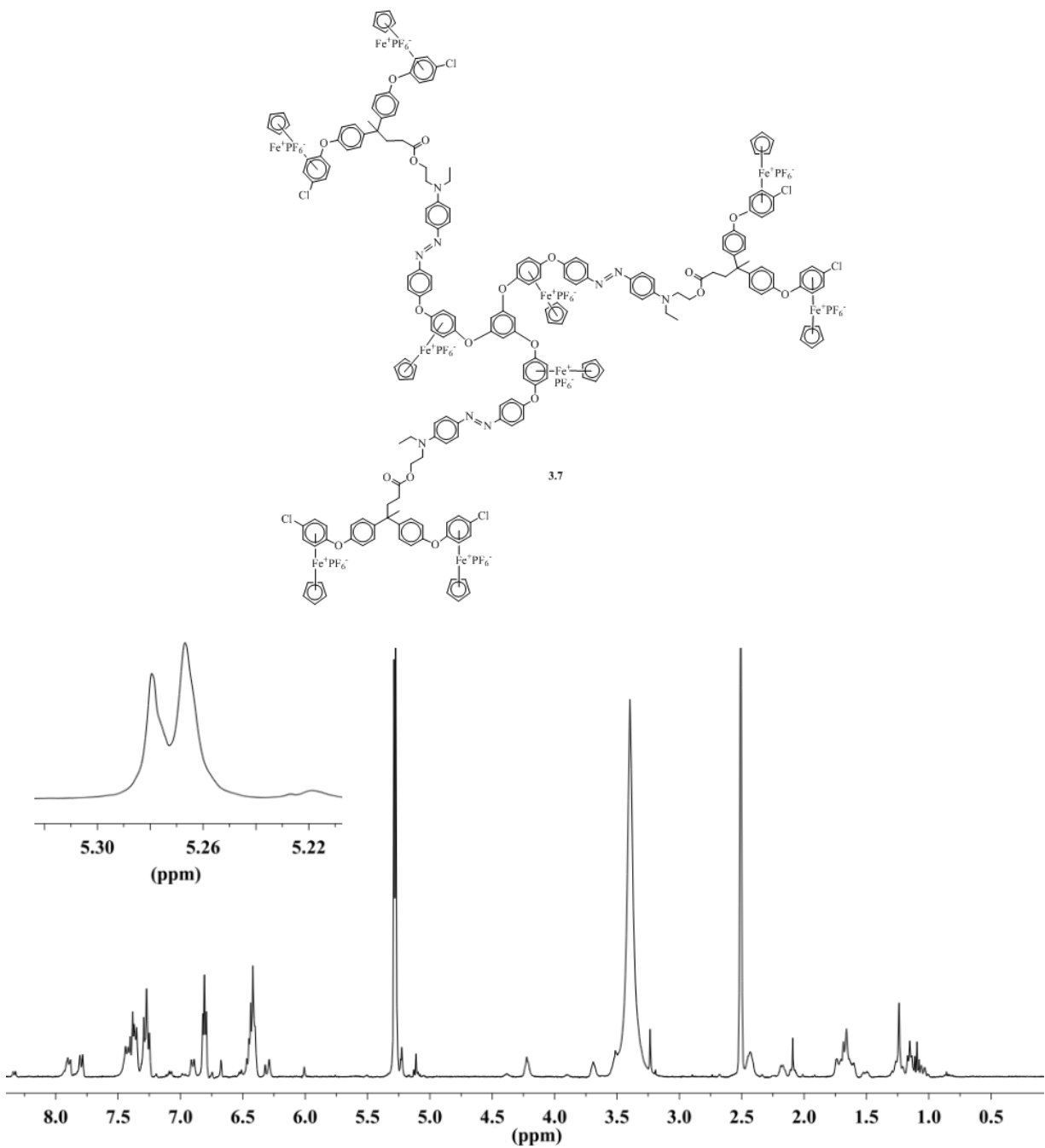
Figure 3-14: 400 MHz ^{1}H NMR spectrum of the star-shaped oligomer 3.7
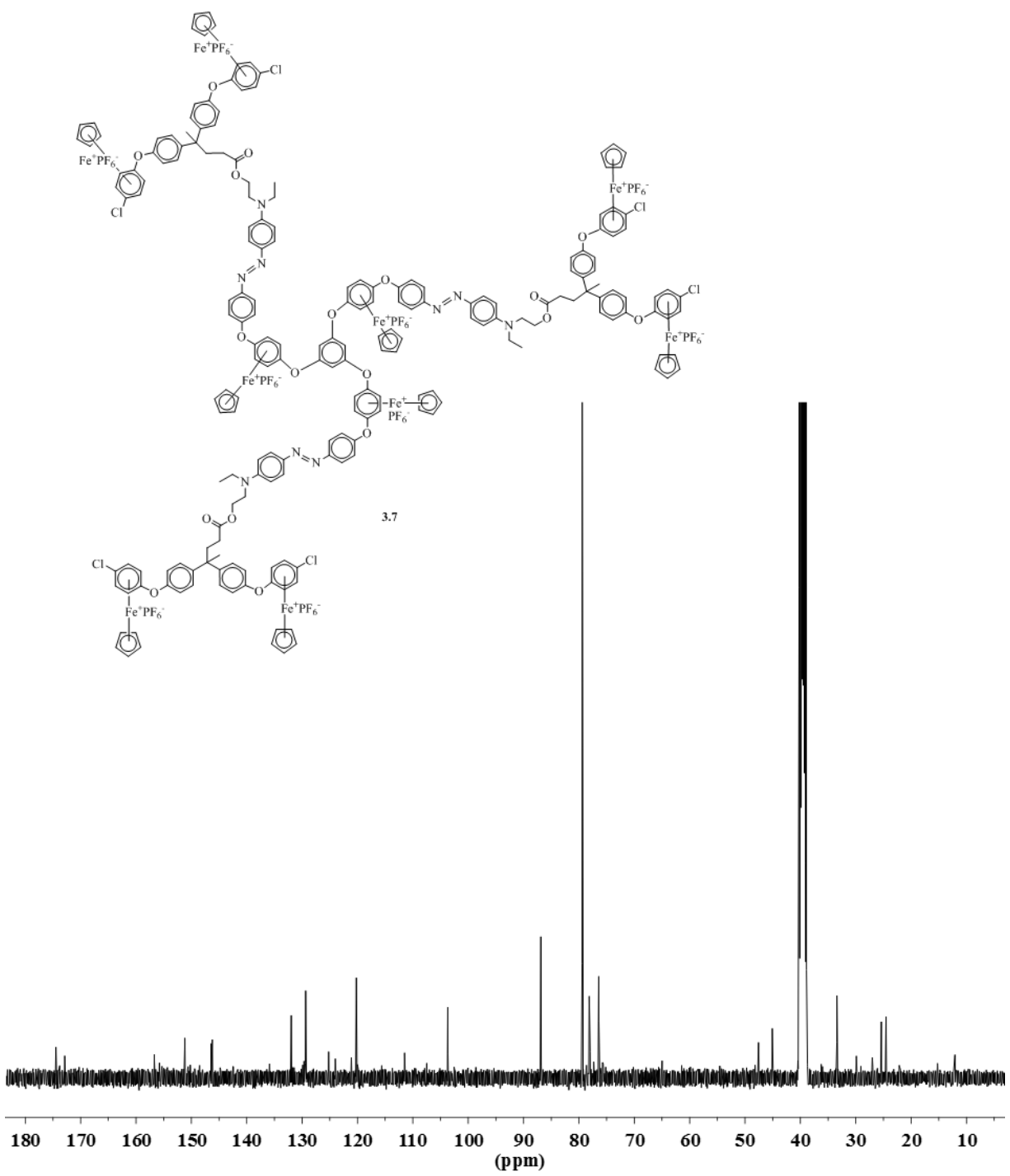
Figure 3-15: 101 MHz ^{13}C NMR spectrum of the star-shaped oligomer 3.7

3.2.2 The synthesis and characterization of tetrairon core oligomers

The synthesis and characterization of the thioether disazo dye **2.19** has been described in Chapter 2. An esterification reaction was performed using the bimetallic carboxylic acid complex **2.7** and disazo dye **2.19** to give the tetrairon core complex **3.8** (Scheme 3-7). This complex is the first example of a disazo dye that allows for the expansion through the divergent approach through nucleophilic aromatic substitution with four terminal chloro groups.
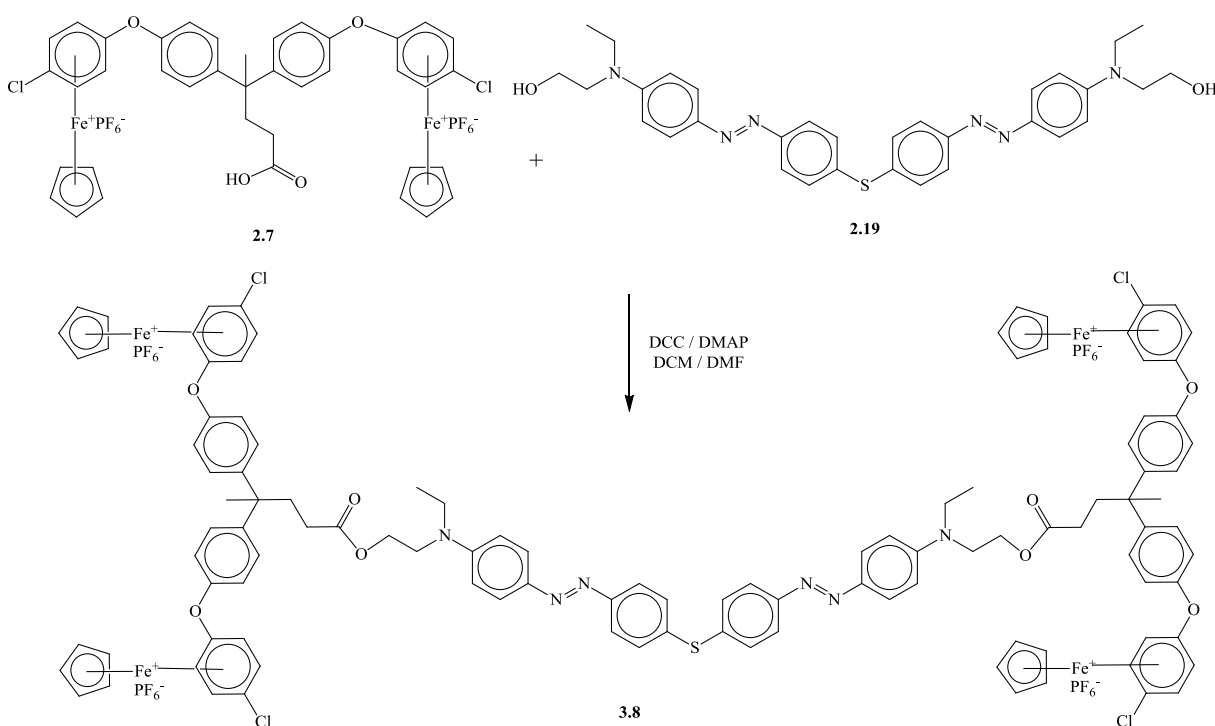
Scheme 3-7: Preparation of tetrairon disazo dye core 3.8

The solubility of tetrairon disazo dye complex **3.8** is enhanced, compared to the thioether disazo dye. For example, the thioether dye is only slightly soluble in acetone and dichloromethane, while complex **3.8** is soluble in both acetone and dichloromethane. This enhanced solubility offers a convenient work-up during purification: the DCU residue is easily filtered out as an undissolved solid in the dichloromethane solution and the excess bimetallic carboxylic complex **2.7** can be washed with 10% aq. NaOH solution.

75
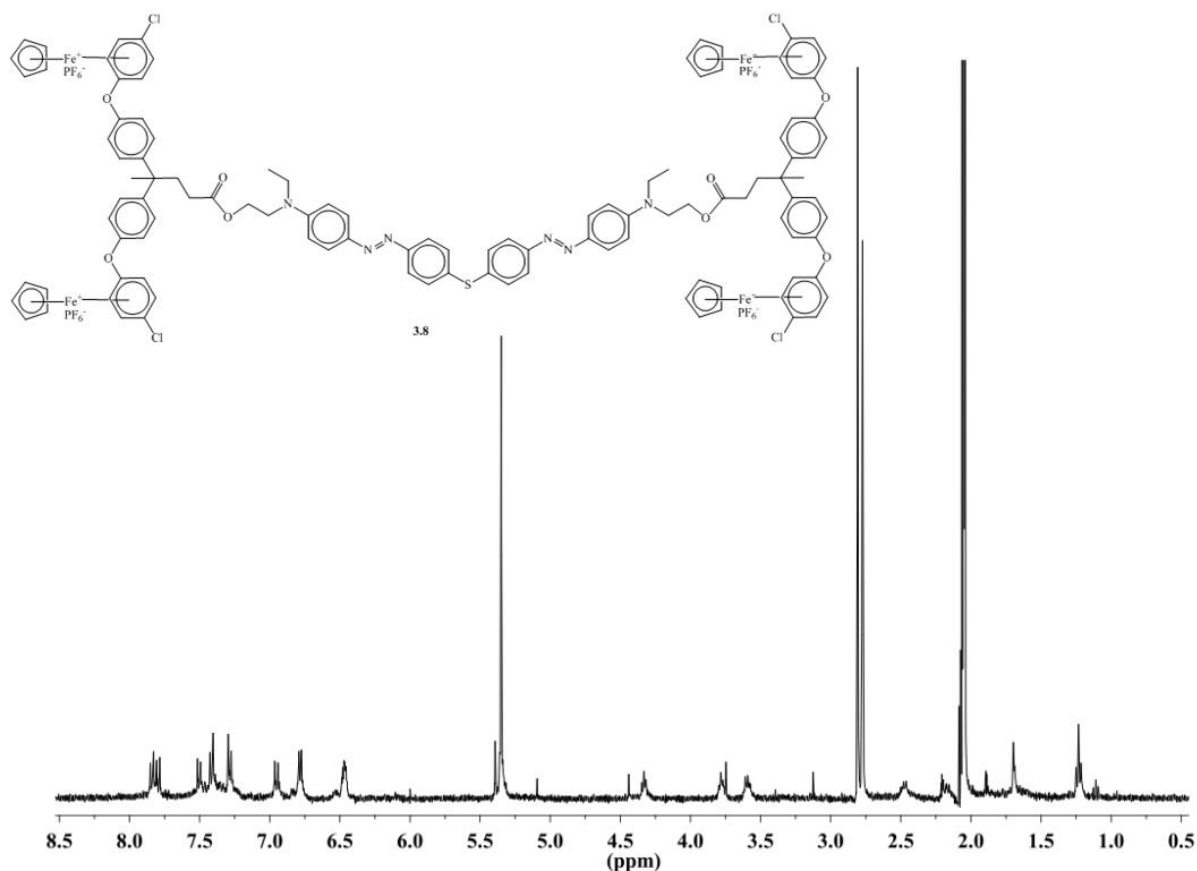
Figure 3-16: 400 MHz ^{1}H NMR spectrum of tetrairon core 3.8

The ^{1}H NMR of the tetrairon disazo dye core (Figure 3-16) shows the methylene protons in the *alpha* position of the ester group appear at 4.33 ppm and all the integrations were as expected. For example, the methyl triplet of the disazo dye core appears at 1.23 ppm and integrates to six protons, while the bisphenol methyl singlet resonance at 1.69 ppm is integrated to eight protons. The ^{13}C NMR spectrum (Figure 3-17) also showed the incorporation of the organoiron complex. The cyclopentadienyliron resonance appears at 80.5 ppm and the complexed arene peaks appear at 87.8 and 77.1 ppm. The ^{13}C NMR spectrum also confirms the formation of the ester as there is an ester carbonyl peak appears at 173.6 ppm. Further support was found in the 2D NMR spectra (Figures 3-18 and 3-19).
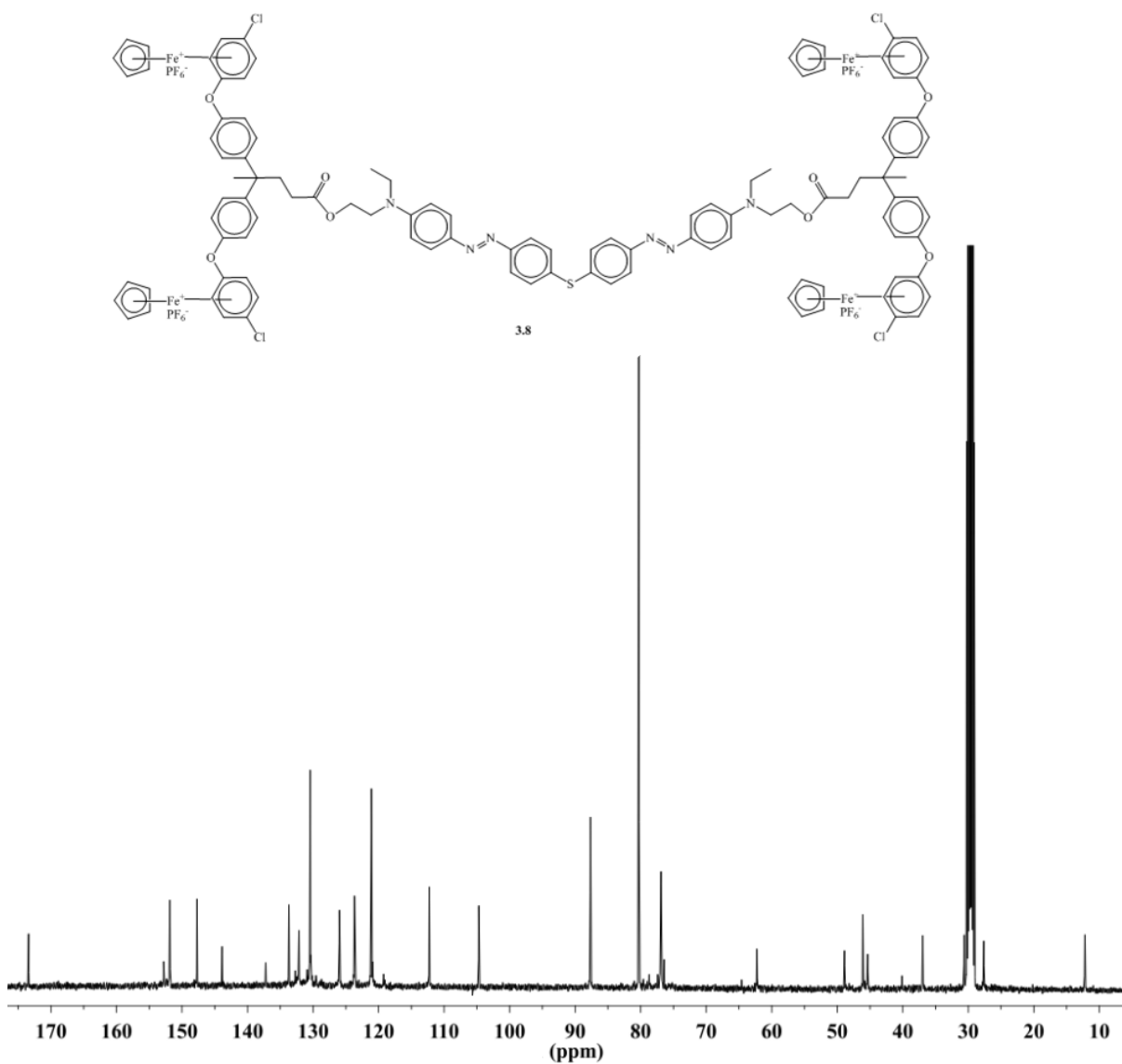
Figure 3-17: 101 MHz ^{13}C NMR spectrum of tetrairon core 3.8
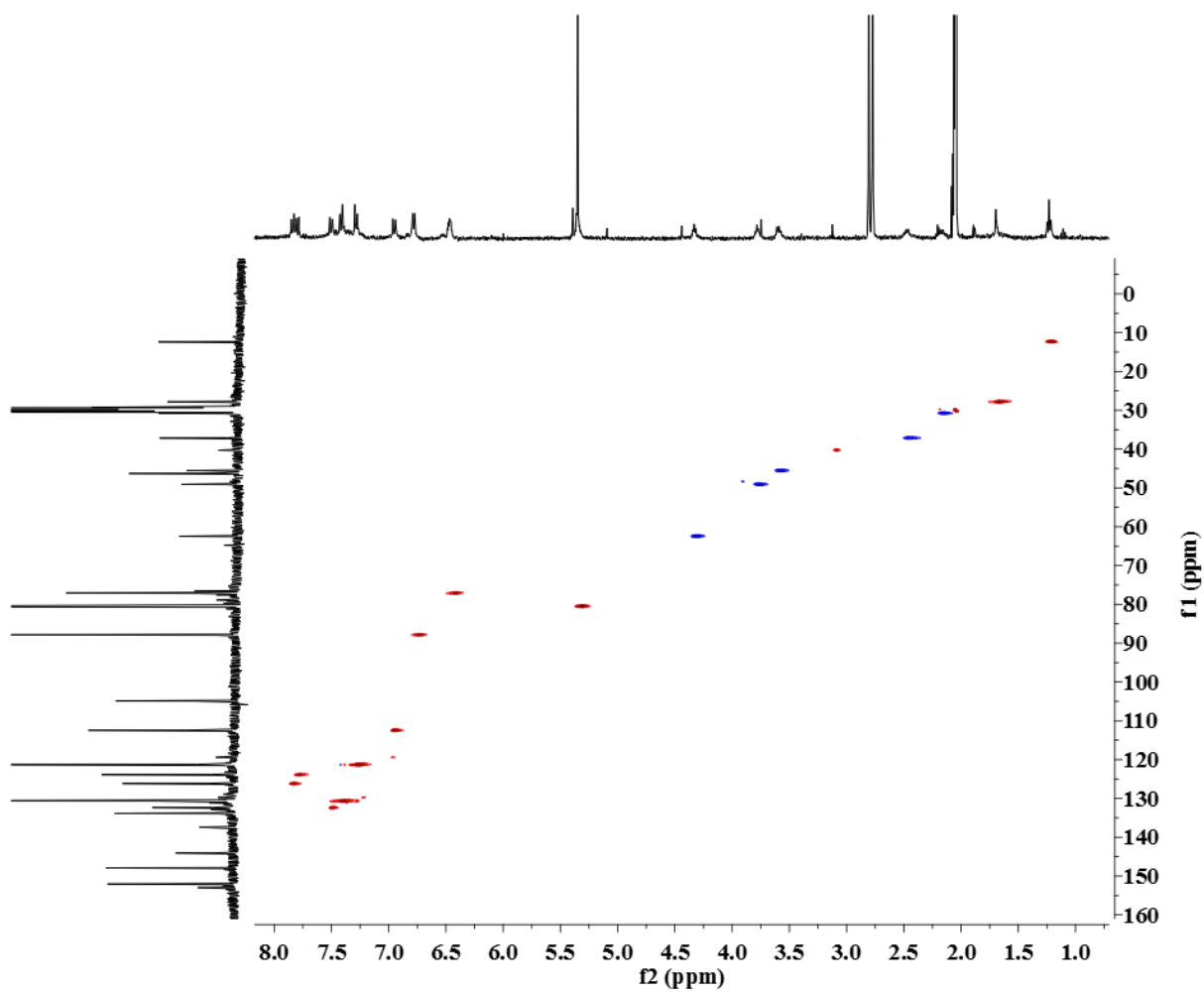
Figure 3-18: ^{1}H-^{13}C gHSQC NMR spectrum of complex 3.8
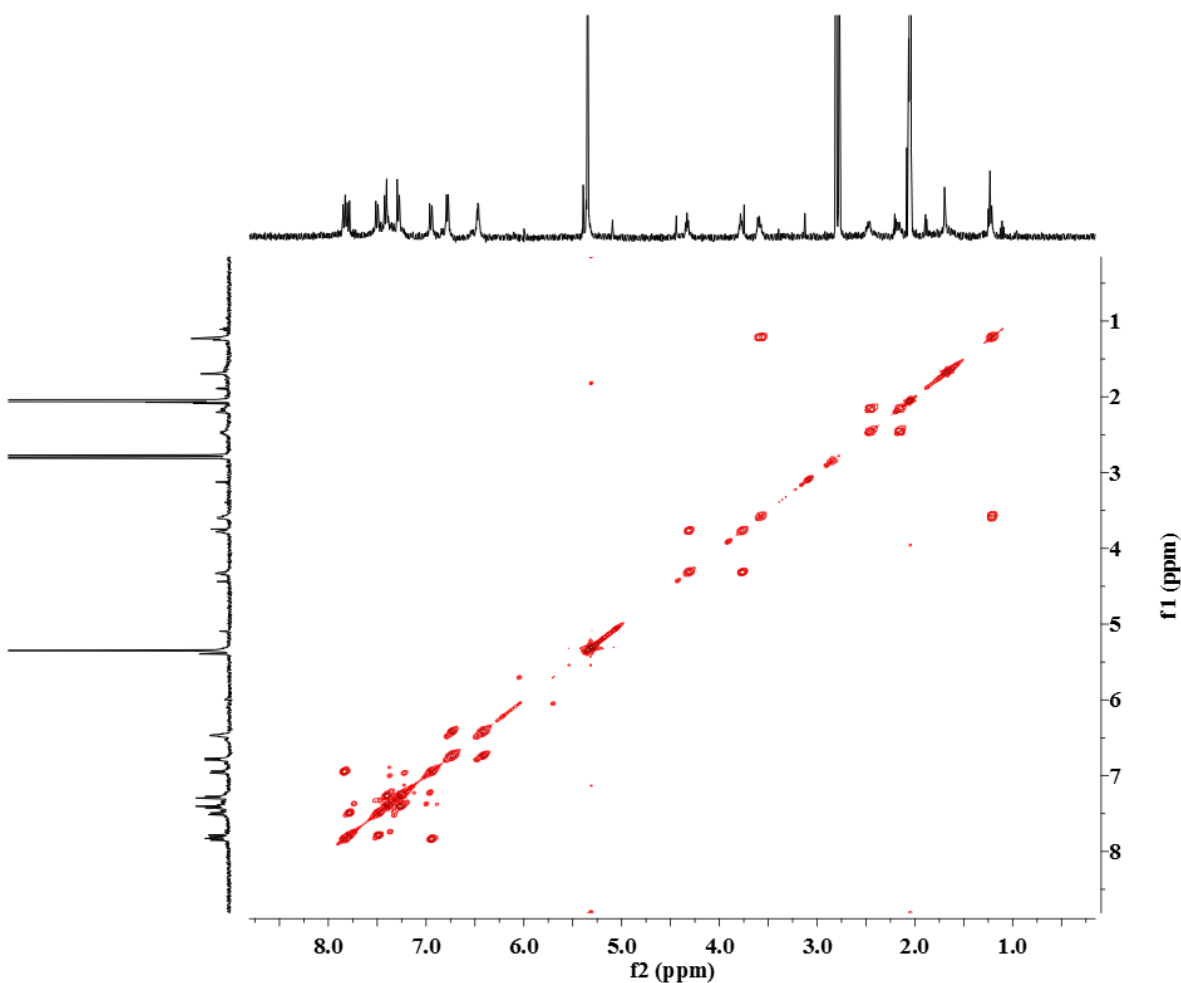
Figure 3-19: ^{1}H-^{1}H gdqCOSY NMR spectrum of complex **3.8**

The UV-vis study (Figure 3-20) of complex **3.8** was performed in acetone and varying concentrations (10:1 v/v) of aqueous hydrochloric acid. Complex **3.8** appeared as an orange-red colour in acetone and exhibited a λ_{max} of 435 nm, due to the π-π* transition of the azo dye. Upon the addition of 4% HCl, the colour changed to a dark purple. The disazo dye group was fully protonated upon the addition of 20% HCl and displayed a bathochromic shift at a λ_{max} of 576 nm. This shift is consistent with other bathochromic shifts that occur in azobenzene chromophores upon protonation.[95,96] When the solution was neutralized with 10% NaOH solution, the colour changed from dark purple back to orange-red.
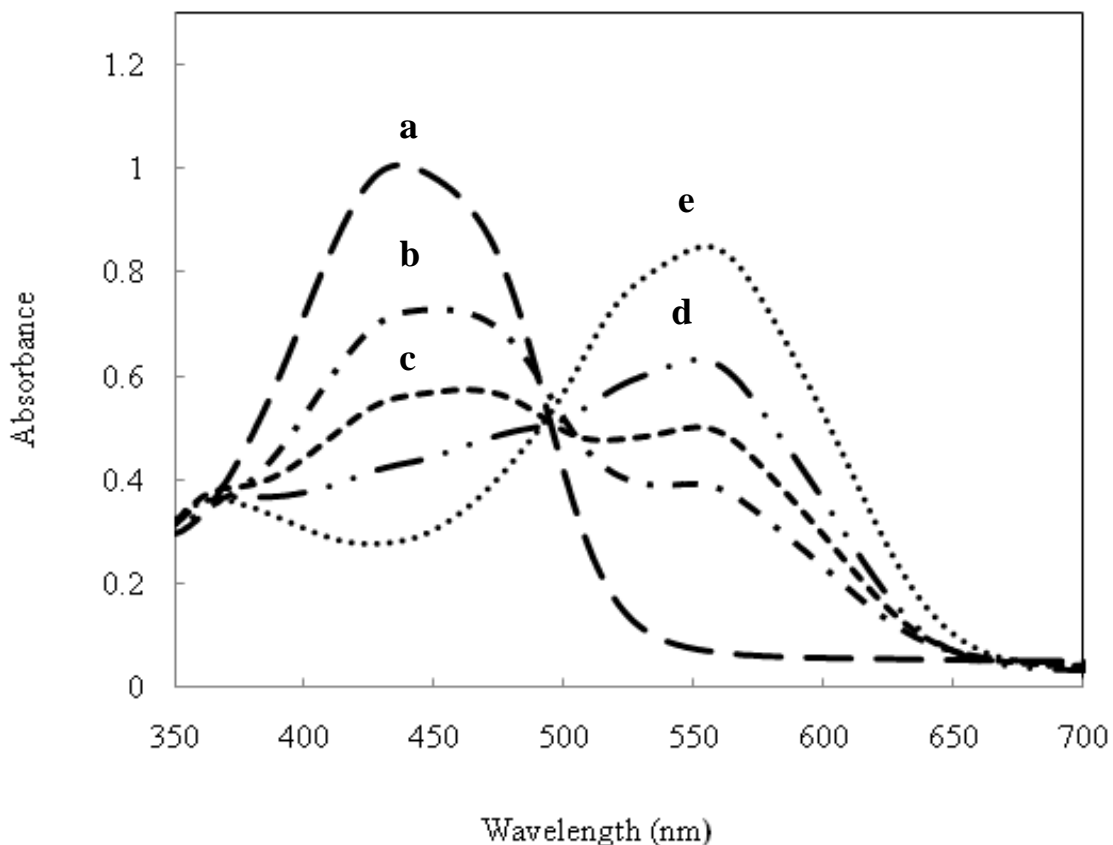
Figure 3-20: UV-vis spectra of disazo dye iron complex 3.8 in (a) acetone, (b) 10:1 acetone/HCl (4%), (c) 10:1 acetone/HCl (8%), (d) 10:1 acetone/HCl (10%), (e) 10:1 acetone/HCl (20%)

As described in Chapter 2, the divergent approach was also employed for the synthesis of a second tetrairon core (complex **2.10**) containing a bridging aliphatic chain instead of disazo dye **2.19**. The four activated terminal chloro groups in complex **2.10** were reacted with four molar equivalents of arylazo dye **2.15** via nucleophilic aromatic substitution (Scheme 3-8). This reaction gave rise to the four-arm star-shaped oligomer **3.9** containing arylazo chromophores.
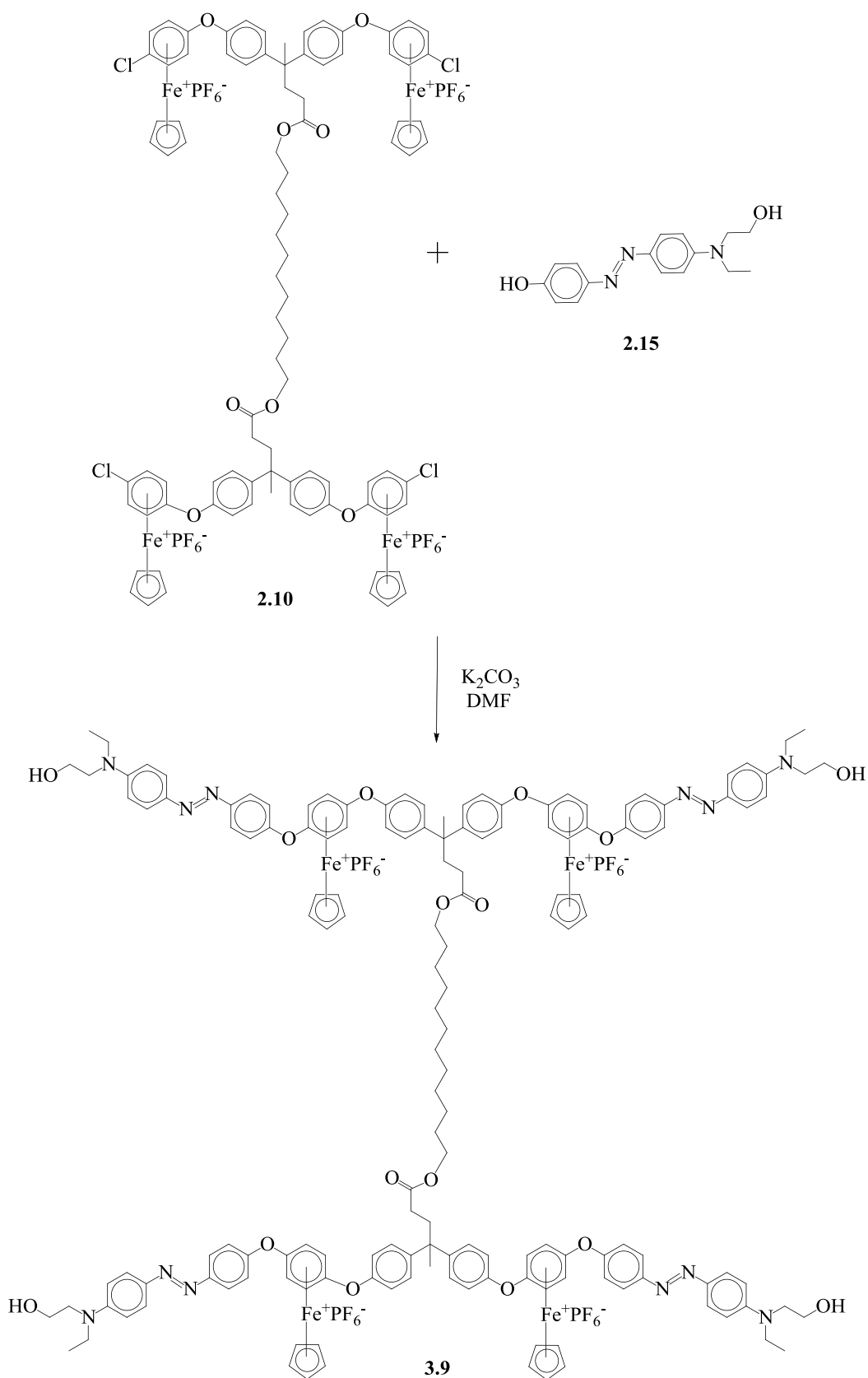
Scheme 3-8: The synthesis of oligomer 3.9 via nucleophilic aromatic substitution
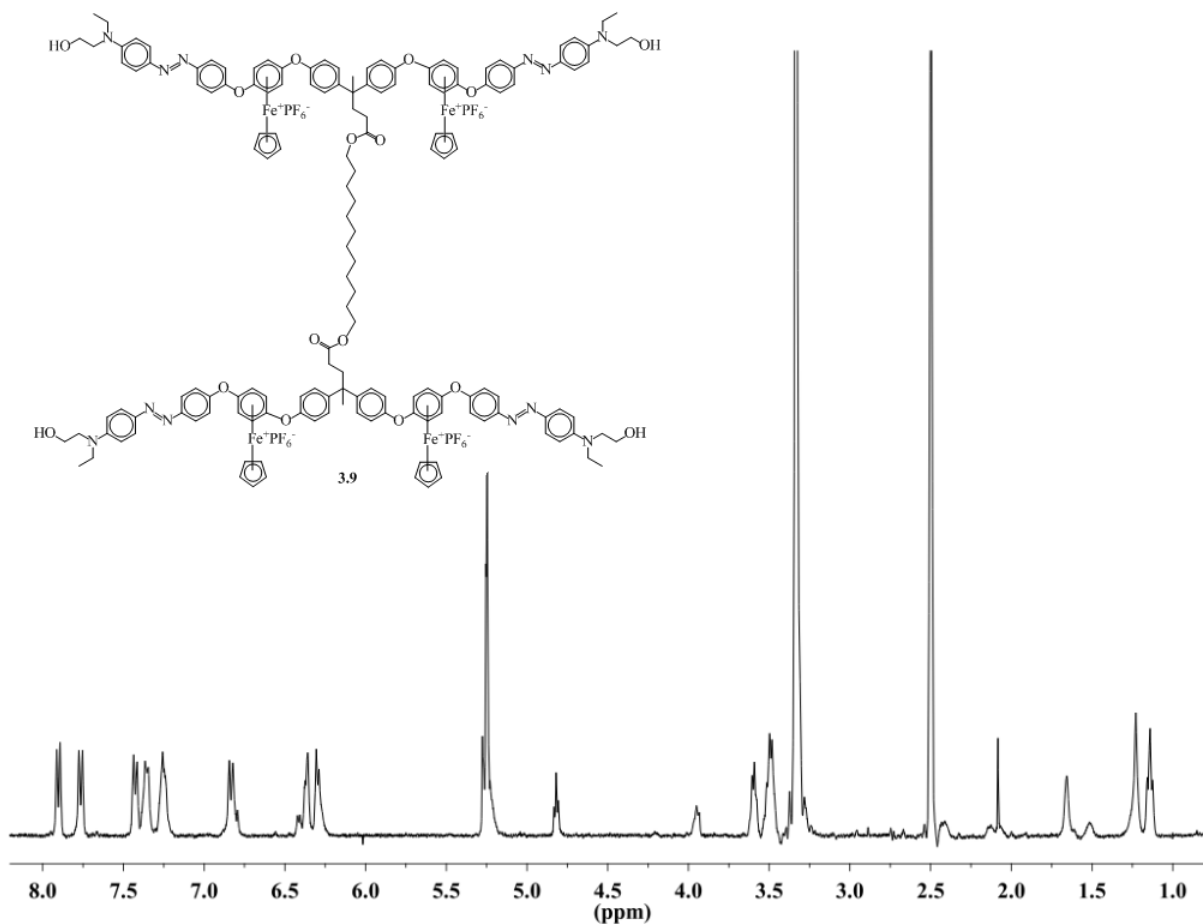
Figure 3-21: 400 MHz ^{1}H NMR spectrum of complex 3.9

The product was analyzed through ^{1}H NMR and ^{13}C NMR spectroscopy. Figure 3-21 shows the ^{1}H NMR spectrum of complex **3.9**. The azo dye aromatic resonances appear as doublets centred at 7.90 ppm, 7.76 ppm and 7.43 ppm. There is one doublet due to the azo dye overlapping with the resonances due to the complexed aromatics (the azo dye should have four sets of doublets). The complexed aromatics appear as a multiplet between 6.39 ppm and 6.25 ppm (due to overlap with the azo dye resonance) and as a doublet at 6.41 ppm. The sharp singlet at 5.25 ppm is due to the cyclopentadienyliron moiety and the multiplet at 3.60ppm (a) is from the CH_2-O of the azo dye aliphatics. The remaining azo dye aliphatics appear at 3.95, 3.49, 2.41 and 1.14 ppm. The singlet at 1.66 demonstrates the CH_3 closed to the iron center. The successful synthesis of **3.9** can be concluded due to the single Cp resonance.

Similarly, the single Cp resonance at 79.5 ppm ^{13}C NMR spectrum indicates the successful formation of complex **3.9**. The azo quaternary carbon resonances clearly appear at 164.2 and 163.8 ppm. The methyl group resonance at 12.1 ppm is another proof of the incorporation of azo dye moiety. (Figure 3-22) The gCOSY NMR spectrum of **3.9** (Figure 3-23) was used to distinguish between the two different methyl groups. The CH$_3$ protons of the ethyl group appear at 1.14 ppm, with a cross peak at 1.14 ppm and 3.49 ppm, confirming that it couples to the CH$_2$ on the nitrogen.
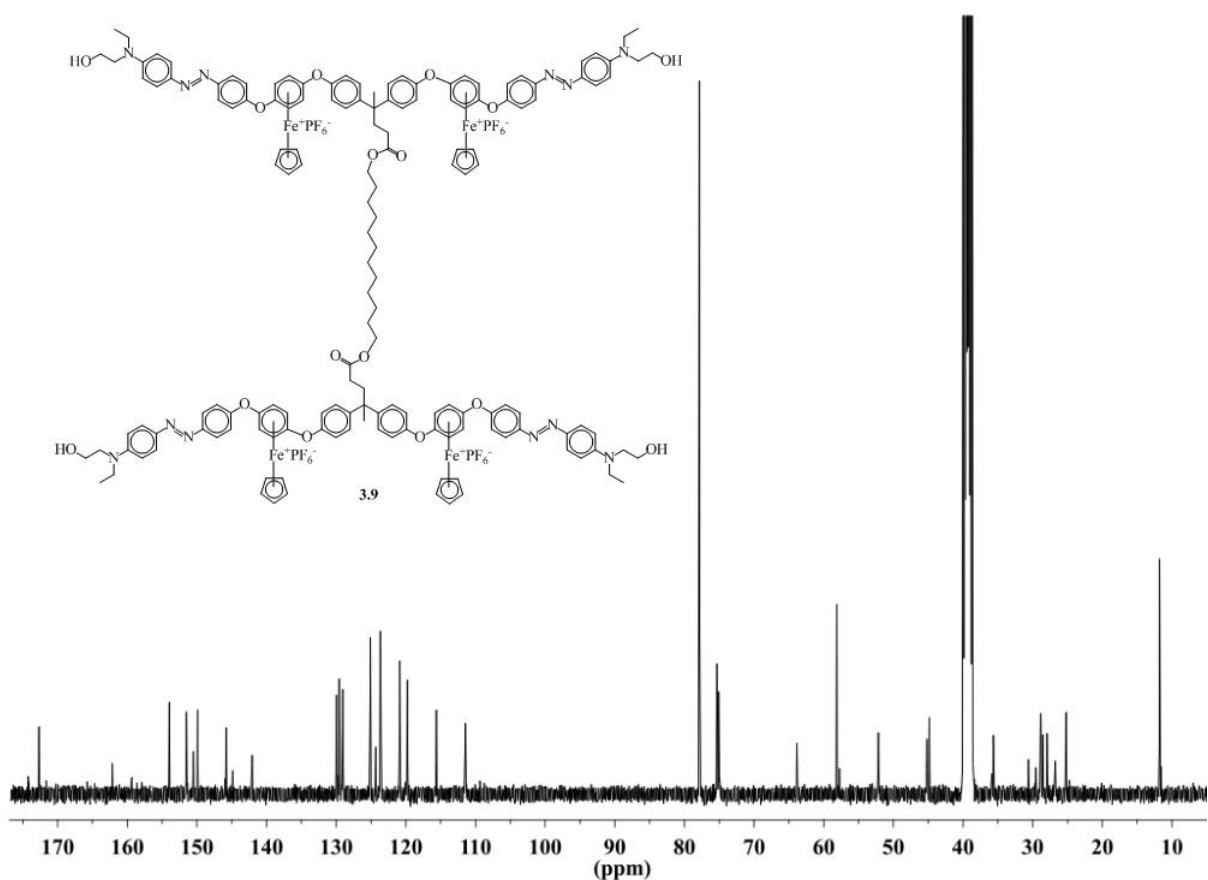
Figure 3-22: 101 MHz ^{13}C NMR spectrum of complex 3.9
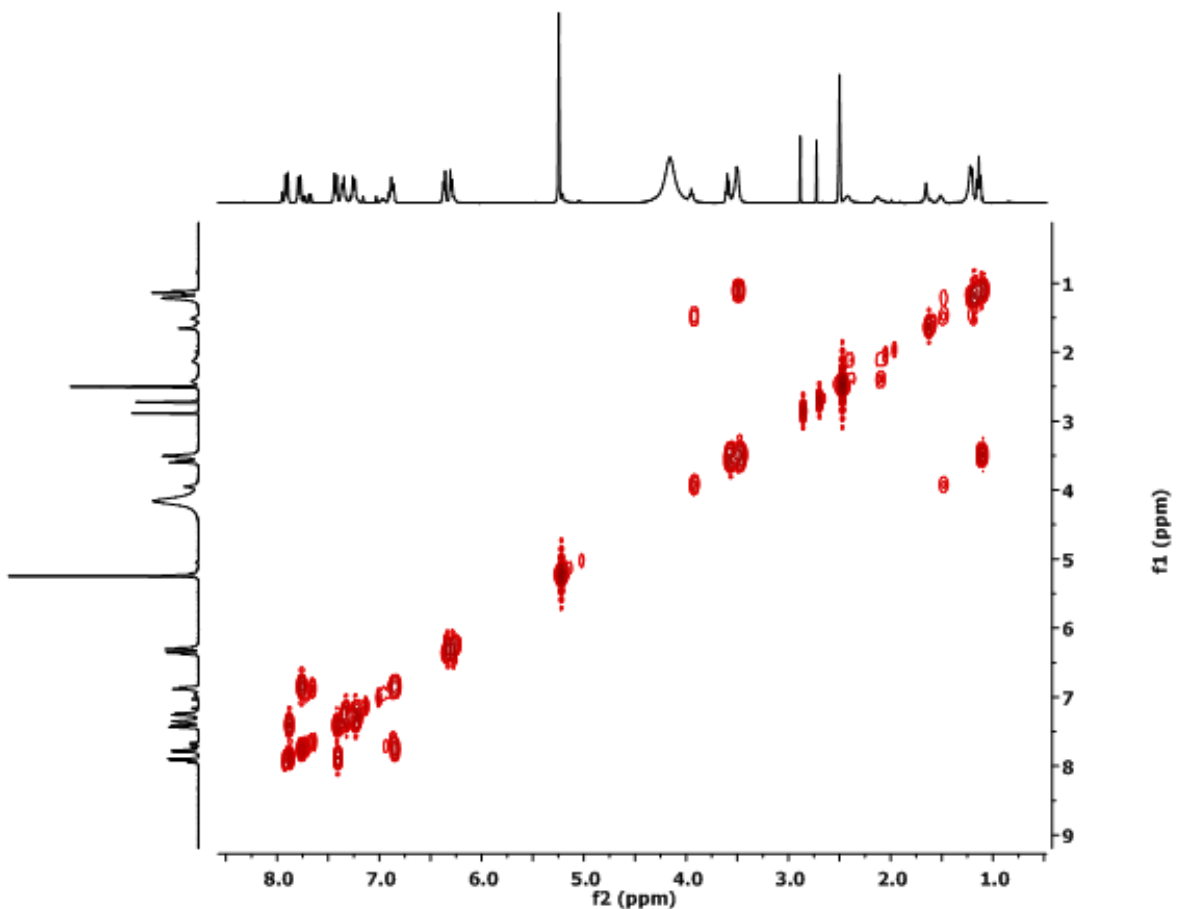
Figure 3-23: ^{1}H-^{1}H gCOSY NMR spectrum of complex 3.9

The first generation star-shaped oligomer **3.9** was synthesized with the intention for further growth in the arms. This was accomplished by reacting the terminal hydroxyl groups of the azo dye moieties with monosubstituted cationic cyclopentadienyliron carboxylic acid **2.5**, to afford the eight-metal four-arm star-shaped oligomer **3.10** with bridging azo dyes (Scheme 3-9).
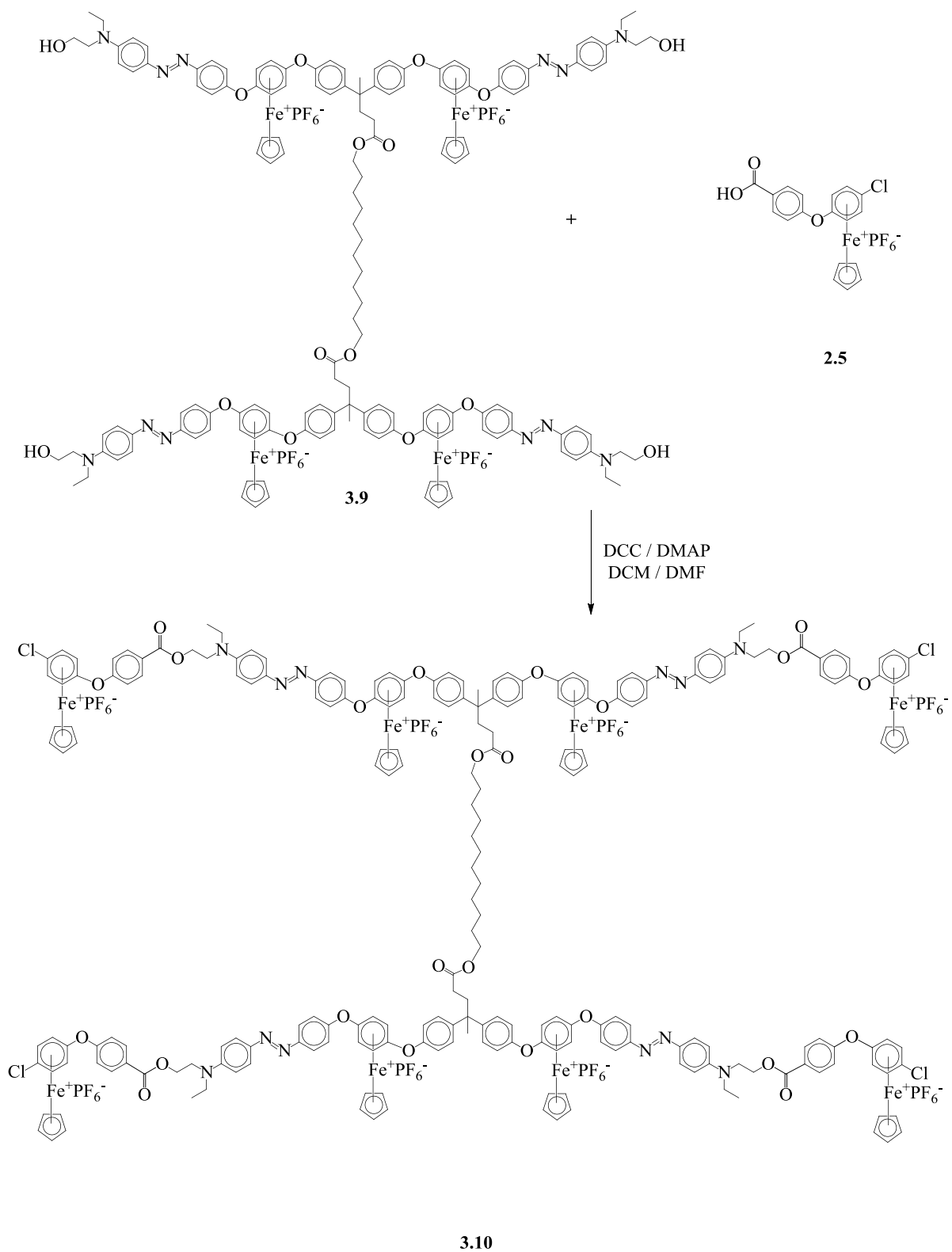
Scheme 3-9: The preparation of octairon star-shaped molecule 3.10 containing arylazo dye moieties

Evidence for the formation of **3.10** was found in the shift of the CH$_2$OH methylene protons in the ^{1}H NMR signal at 3.49 ppm of complex **3.9** to 4.51 ppm in complex **3.10**, as a result of the ester functionality. The presence of the two Cp resonances at 5.29 and 5.25 ppm, is another proof for the incorporation of the terminal Cp.
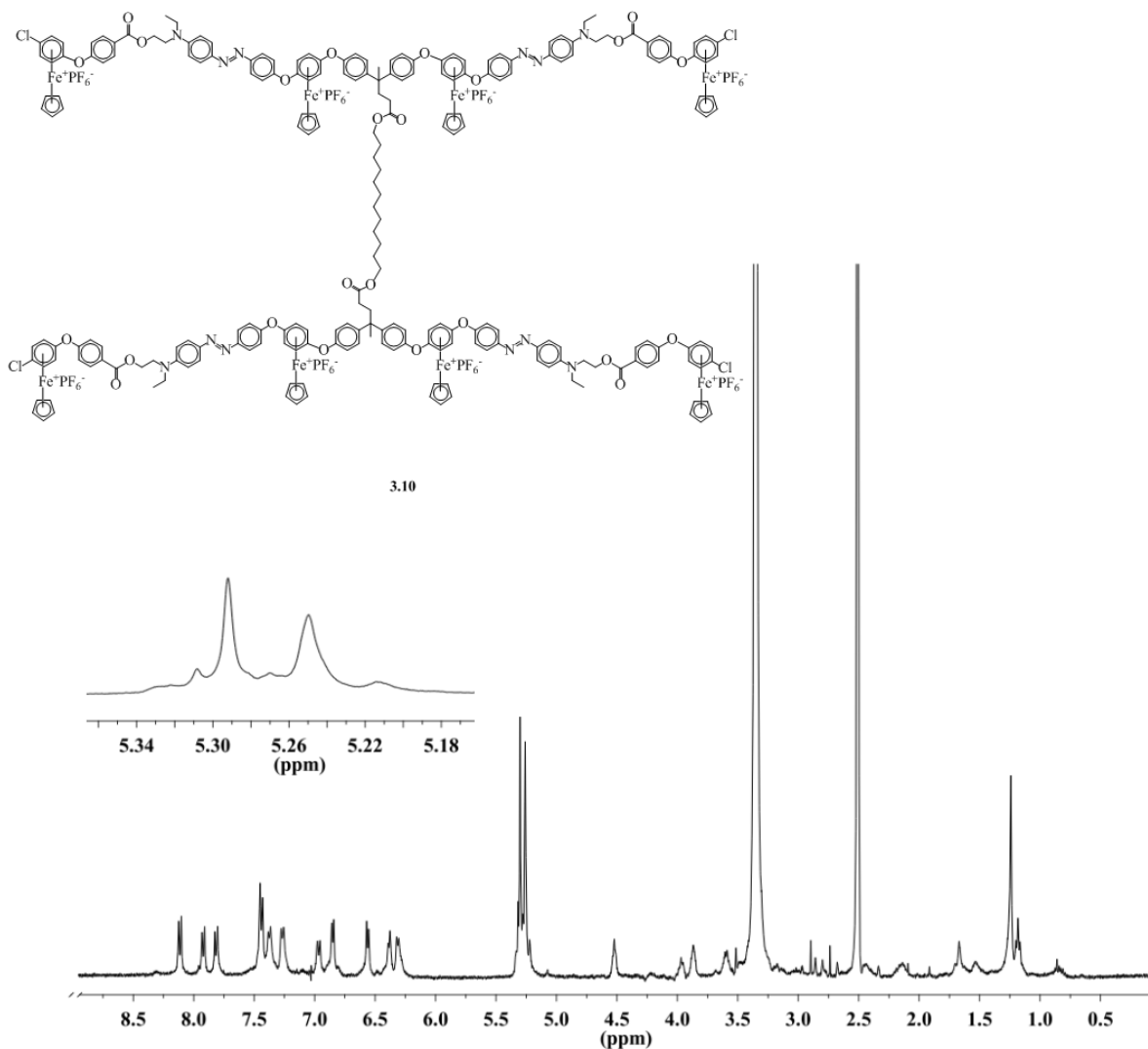
Figure 3-24: 400 MHz ^{1}H NMR spectrum of complex 3.10

The ^{13}C NMR spectrum further supports the synthesis of complex **3.10**. (Figure 3-25) The methylene carbon *alpha* to the ester bond corresponds to the resonance at 62.5 ppm, shifted from 55.0 ppm in complex **3.9**. Furthermore, the terminal Cp carbon resonance appears at 78.0 ppm.
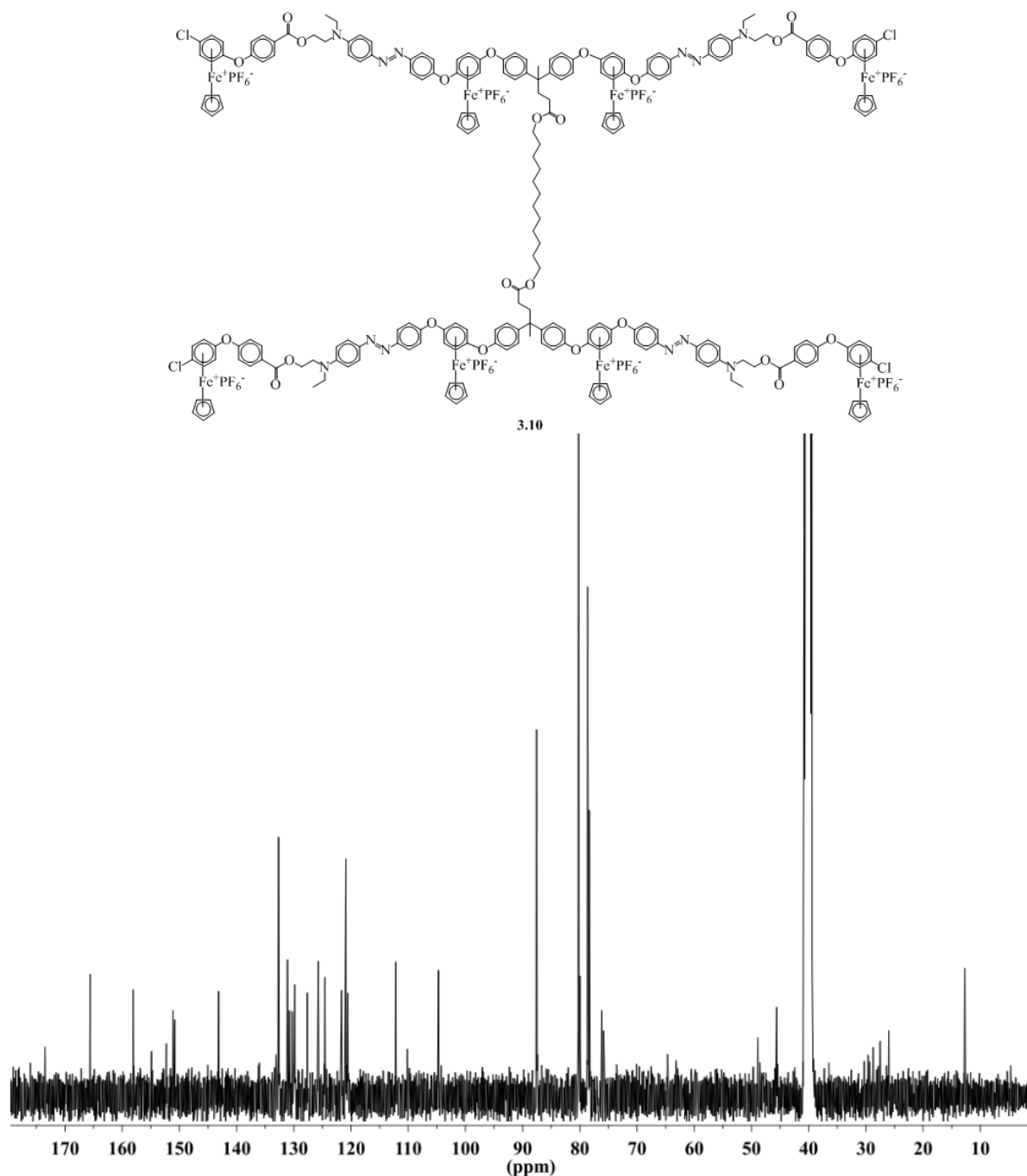
Figure 3-25: 101 MHz ^{13}C NMR spectrum of complex **3.10**

The UV-vis study of arylazo dye-containing oligomer **3.10** (Figure 3-26) was conducted in a similar manner as the disazo dye-containing core **3.8**, but using DMF as the solvent instead of acetone due to lower solubility with orange-red colour. The UV-vis spectra of complex **3.10** displayed similar bathochromic shifts to that of the disazo dye moiety in

compound **3.8**. Complex **3.10** gave an intense absorption peak at λ_{max} = 427 nm in DMF, which was attributed to the π-π* transition. The absorbance decreased as varying concentrations (10%, 20%, 40%) of acidic solution were added to the sample, which was a result of the formation of the diazonium ion. When 60% HCl solution was added to the solution of oligomer **3.10**, the disazo dye groups were fully protonated, displaying an intense absorption peak at a λ_{max} of 558 nm as dark purple colour. Similar to complex **3.8**, the acid-induced colour change is reversible with addition of 10% NaOH aqueous solution.
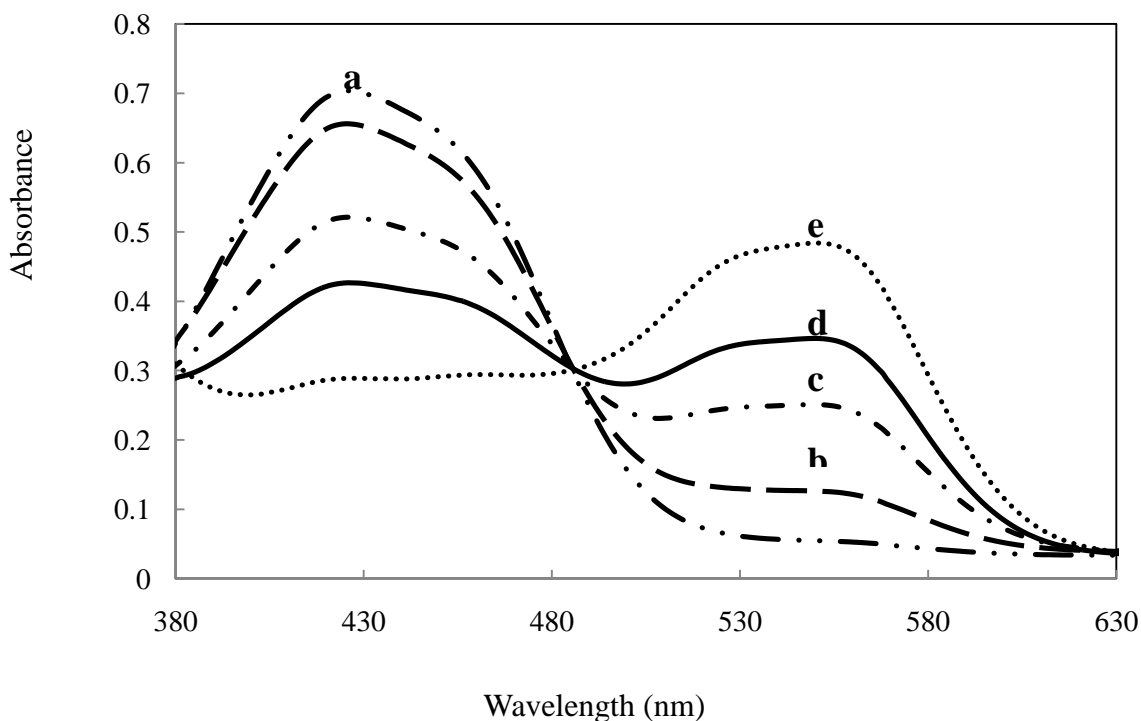
Figure 3-26: UV-vis spectra of star-shaped molecule 3.10 in (a) DMF, (b) 10:1 DMF/HCl (10%), (c) 10:1 DMF/HCl (20%), (d) 10:1 DMF/HCl (40%), (e) 10:1 DMF/HCl (60%)

The electrochemical behaviour of azo dye-containing metal complex **3.10** was studied using cyclic voltammetry as an example of this class of star-shaped oligomers. The cyclic voltammogram of azo dye-containing metal complex **3.10** is shown in Figure 3-27 and all

potentials are referenced to Ag/AgCl. A single reversible redox wave was found corresponding to the conversion from eighteen- to nineteen-electron iron centres. The cyclic voltammogram of complex **3.10** at scan rate $v = 0.1$ V s^{-1} indicated a redox couple at $E_{1/2} =$ -1.53 V, indicating the reduction of the cationic iron moiety and the oxidation of the azo dye, displayed at $E_{pa}= 0.7$ V. Additionally, the reversibility of the redox couple of star-shaped oligomer **3.10** decreased as the temperature increased. At room temperature, the reduction process became completely irreversible.
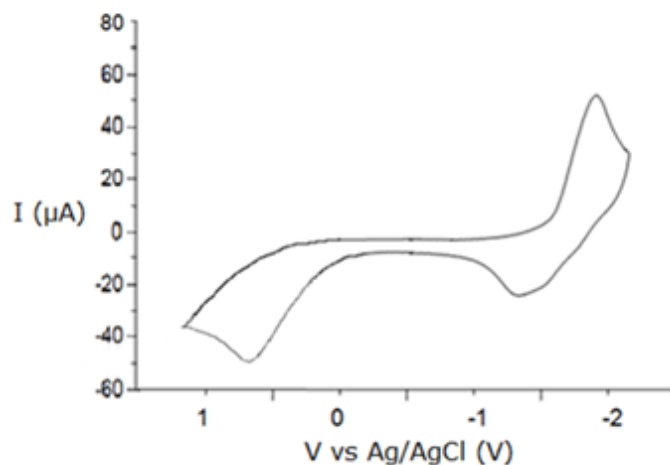
Figure 3-27: Cyclic voltammogram of complex 3.10 using glassy carbon electrode, Ag/AgCl reference electrode, and 1.6x10^{-3} M (analyte) in 0.1 M TEAPF$_6$ in propylene carbonate; $v = 0.1$ V s^{-1} at 238 K

Chapter 4. Experimental

4.1   Materials

Compounds **2.3**, **2.5**, **2.7**, **2.12**, **2.15**, **2.22**, **2.23** and **3.5** were prepared according to previously reported methodologies.[36,52,53,55,86,91,94] All solvents were HPLC grade and purchased from Fisher Scientific. All reagents were purchased from Sigma-Aldrich and used without further purification. All reactions and complexes containing a η^6-dichlorobenzene-η^5-cyclopentadienyliron(II) hexafluorophosphate moiety were kept in the dark to prevent decomposition.

4.2   Characterization

^{1}H and ^{13}C NMR spectral data were collected on a Varian Mercury Plus spectrometer (400 MHz), with an ATB tunable multinuclear probe with a gradient channel. The ^{1}H and ^{13}C NMR were recorded at 400 and 101 MHz, respectively. The chemical shifts were referenced to residual solvent peaks and the coupling constants were reported in Hz. Infrared spectroscopy was performed on an IRPrestige- 21 FTIR by Shimadzu with a MIRacle ATR by PIKE Technologies. A Varian Cary 100 Bio UV–visible spectrophotometer was used to conduct UV–visible measurements using a standard 1 cm^2 quartz cell. Cyclic voltammetry experiments were conducted with an EG&G Princeton Applied Research model 263A potentiostat using a conventional three electrode system. In this study, the working electrode was a glassy carbon disk electrode (ca. 2 mm diameter), the auxiliary electrode was a Pt wire and Ag/AgCl was used as a reference electrode. Temperature was decreased to 238 K using acetone/N$_2$(l) mixture.The concentration of the analyte was $1.69*10^{-3}$ M, while the supporting

electrolyte tetraethyl ammonium hexafluorophosphate (TEAPF$_6$), was 0.1 M. Propylene carbonate was used as solvent and the solution was deaerated with nitrogen prior to use.

4.3 General Procedure for esterification reactions

Compounds containing carboxylic acid functionalities were reacted with compounds containing terminal hydroxyl groups in the presence of N,N-dimethylaminopyridine (DMAP) in DCM/DMF, cooled to 0 ℃, and stirred under N$_2$ for 5 minutes. Dicyclohexylcarbodiimide (DCC) was dissolved in 1-2 mL DCM and added to the stirring mixture at 0 ℃. The solution was stirred in the dark at room temperature under N$_2$ for two days. Dichloromethane was evaporated *in vacuo* and the resulting mixture was poured into 1.2 M HCl, containing equi-metal molar amounts of ammonium hexafluorophosphate (NH$_4$PF$_6$). The resulting precipitate was collected in a sintered glass crucible, washed with water, and dried under reduced pressure. Dicyclohexylurea (DCU) was removed by dissolving the crude product in DCM and placing in the freezer for 30 min, then filtering through a crucible. Purification was achieved by dissolving the product in a minimal amount of acetone and re-precipitating into diethyl ether to afford complex **2.9, 2.10, 3.2, 3.6, 3.7, 3.8,** and **3.10**. The exact ratios for the starting materials are as follows:

Complex 2.9: Complex **2.7** (1 mmol), 1,12-dodecanediol (**2.8**) (1 mmol), DCC (1.5 mmol), and DMAP (1.5 mmol) in 5 mL DCM/5 mL DMF. Yield: 96%.

^{1}H NMR (400 MHz, DMSO-d_6): δ = 7.38 (d, 8.6 Hz, 4H,ArCH), 7.26 (d, 8.6 Hz, 4H,ArCH), 6.81 (d, 6.7 Hz, 4H,*ArCH), 6.42 (d, 6.7 Hz, 4H,*ArCH), 5.27 (s, 10H,Cp),4.38(br s,1H,OH), 3.96 (m, 2H,CH$_2$), 2.44 (m, 2H,CH$_2$), 2.15 (m, 2H,CH$_2$), 1.67 (s, 3H,CH$_3$), 1.53 (m, 2H,CH$_2$), 1.23 (m, 16H,CH$_2$) ^{13}C NMR (101 MHz, DMSO-d_6): δ = 172.8, 156.6, 151.1, 146.2, 131.9,

129.2, 120.1, 103.6, 86.8, 79.3, 76.4, 64.0, 60.7, 47.5, 45.0, 33.4, 32.5, 29.7, 29.1, 29.0, 28.9, 28.7, 28.1, 25.5, 25.3, 24.4. IR (υ/cm^{-1}): 1720 (C=O).

Complex 2.10: Complexes **2.9** (0.5 mmol) and **2.7** (2 mmol), DCC (2.2 mmol), and DMAP (2.2 mmol) in 5 mL DCM/5 mL DMF. Yield: 95%.

^{1}H NMR (400 MHz, DMSO-d_6): δ = 7.37 (d, 8.9 Hz, 8H,ArCH), 7.27 (d, 8.9 Hz, 8H,ArCH), 6.81 (d, 6.7 Hz, 8H,*ArCH), 6.42 (d, 6.7 Hz, 8H,*ArCH), 5.28 (s, 20H,Cp), 3.97 (t, 6.9 Hz, 4H,CH$_2$), 2.43 (m, 4H,CH$_2$), 2.15 (m, 4H,CH$_2$), 1.67 (s, 6H,CH$_3$), 1.51 (m, 4H,CH$_2$), 1.24 (m, 16H,CH$_2$) ^{13}C NMR (101 MHz, DMSO-d_6): δ = 172.8, 151.1, 146.2, 103.6, 86.8, 79.3, 76.4, 64.0, 45.0, 29.4, 29.0, 28.7, 28.1, 27.8, 25.3. IR (υ/cm^{-1}): 1720 (C=O).

Complex 3.2: Complex **2.23** (3 mmol), 1,3,5-benzene tricarboxylic acid (**3.1**) (1 mmol), DCC (3.5 mmol), and DMAP (3.5 mmol) in 10 mL DCM/10 mL DMF. Yield: 84%.

^{1}H NMR (400 MHz, DMSO-d_6): δ = 8.60 (s, 3H,ArCH), 7.90 (d, 8.9 Hz, 6H,ArCH), 7.76 (d, 9.1 Hz, 6H,ArCH), 7.46 (d, 8.9 Hz, 6H,ArCH), 6.93 (d, 9.1 Hz, 6H,ArCH), 6.82 (d, 6.9 Hz, 6H,*ArCH), 6.50 (d, 6.9 Hz, 6H,*ArCH), 5.30 (s, 15H,Cp), 4.57 (br s, 6H,CH$_2$), 3.84 (br s, 6H,CH$_2$), 3.53 (m, 6H,CH$_2$), 1.15 (t, 6.7 Hz, 9H,CH$_3$) ^{13}C NMR (101 MHz, DMSO-d_6): δ = 164.1, 153.7, 150.7, 150.4, 142.5, 133.5, 131.7, 130.7, 125.1, 124.0, 121.4, 111.6, 103.8, 86.8, 79.4, 76.6, 62.9, 47.9, 44.4, 12.0. IR (υ/cm^{-1}): 1734 (C=O).

Complex 3.6: Complexes **3.4** (0.5 mmol) and **3.5** (1.7 mmol), DCC (2 mmol), and DMAP (2 mmol) in 5 mL DCM/5 mL DMF. Yield: 72%.

^{1}H NMR (400 MHz, DMSO-d_6): δ = 7.92 (d, 8.7 Hz, 6H,ArCH), 7.82 (d, 8.9 Hz, 6H,ArCH), 7.42 (d, 8.7 Hz, 6H,ArCH), 7.31 (s, 3H,ArCH), 6.98 (d, 8.9 Hz, 6H,ArCH), 6.53 (d, 6.1 Hz, 6H,*ArCH), 6.44 (d, 6.1 Hz, 6H,*ArCH), 5.30 (s, 15H,Cp), 4.73(t,2.5Hz,6H,*`Cp) 4.48 (t, 1.9Hz,6H,*`Cp), 4.39 (m, 6H,CH$_2$), 4.15 (s, 15H,*Cp), 3.78 (br t, 5.0 Hz, 6H,CH$_2$), 3.62 (br q, 6.7 Hz, 6H,CH$_2$), 1.19 (t, 6.7 Hz, 9H,CH$_3$) ^{13}C NMR (101 MHz, DMSO-d_6): δ = 170.8, 155.4,

154.2, 150.7, 150.2, 130.0, 129.2, 125.1, 124.0, 120.9, 111.9, 111.5, 78.2, 76.1, 75.6, 71.4, 70.4, 69.8, 69.6, 61.6, 48.1, 44.8, 12.0. IR (υ/cm^{-1}): 1718 (C=O).

Complex 3.7: Complexes **3.4** (0.2 mmol) and **2.7** (0.7 mmol), DCC (0.8 mmol), and DMAP (0.8 mmol) in 5 mL DCM/5 mL DMF were reacted. Yield: 69%.

^{1}H NMR (400 MHz, DMSO-d_6): δ = 7.88 (d, 9.1 Hz, 6H,ArCH), 7.79 (d, 9.0 Hz, 6H,ArCH), 7.42 (d, 8.9 Hz, 6H,ArCH), 7.36 (m, 12H,ArCH) 7.26 (m, 12H,ArCH), 6.89 (d, 9.2Hz,6H,ArCH), 6.80 (m, 12H,*ArCH) 6.67 (s, 3H,ArCH), 6.47- 6.36 (m, 24H,*ArCH), 5.28 (s, 15H,Cp), 5.27 (s, 30H,Cp), 4.21 (m, 6H,CH$_2$), 3.68 (m, 6H,CH$_2$), 3.51 (m, 6H,CH$_2$), 2.16 (m, 6H,CH$_2$), 2.08 (m, 6H,CH$_2$), 1.59 (s, 9H,CH$_3$), 1.14 (t, 6.9 Hz, 9H,CH$_3$) ^{13}C NMR (101 MHz, DMSO-d_6): δ = 173.2, 157.0, 151.6, 151.5, 146.8, 146.6, 132.4, 132.3, 129.7, 125.6, 124.4, 121.5, 120.6, 111.9, 104.1, 87.3, 79.8, 78.5, 76.8, 65.4, 61.8, 47.9, 45.5, 33.8, 30.3, 27.4, 25.8, 24.9, 12.5. IR (υ/cm^{-1}): 1722 (C=O).

Complex 3.8: Complexes **2.19** (1.7 mmol) and **2.7** (3 mmol), DCC (3.5 mmol), and DMAP (3.5 mmol) in 10 mL DCM/5 mL DMF. Yield: 56%.

^{1}H NMR (400 MHz, acetone-d_6): δ = 7.84, (d, 9.3 Hz, 4H,ArCH), 7.79 (d, 8.7 Hz, 4H,ArCH), 7.50 (d, 8.7 Hz, 4H,ArCH), 7.41 (d, 8.6 Hz, 8H,ArCH), 7.28 (d, 8.6 Hz, 8H,ArCH), 6.95 (d, 9.3 Hz, 4H,ArCH), 6.78 (m, 8H,*ArCH), 6.47 (d, 8H,*ArCH), 5.35 (s, 20H,Cp), 4.33 (m, 4H,CH$_2$), 3.76 (m, 4H,CH$_2$), 3.60 (m, 4H,CH$_2$), 2.48 (m, 4H,CH$_2$), 2.20 (m, 4H,CH$_2$), 1.69 (s, 6H,CH$_3$), 1.23 (t, 7.0 Hz, 6H,CH$_3$) ^{13}C NMR (101 MHz, acetone-d_6): δ = 173.6, 153.0, 152.0, 152.0, 147.9, 144.1, 137.4, 133.9, 132.3, 130.6, 130.5, 126.1, 123.9, 121.3, 112.4, 104.9, 87.8, 80.5, 77.1, 62.5, 49.1, 46.3, 45.5, 37.1, 27.8, 12.4. IR, υ/cm^{-1}: 1728 (CO).

Complex 3.10: Complex **3.9** (0.2 mmol), 2..5 (0.8 mmol), DCC (1 mmol), and DMAP (1 mmol) in 5 mL DCM/5 mL DMF. Yield: 62%.

^{1}H NMR (400 MHz, DMSO-d_6): δ = 8.10 (d, 9.4 Hz, 8H,ArCH), 7.91 (d, 8.7 Hz, 8H,ArCH), 7.80 (d, 8.7 Hz, 8H,ArCH), 7.43 (m, 16H,ArCH), 7.37 (d, 8.0 Hz, 8H,ArCH), 7.25 (d, 8.0 Hz, 8H,ArCH), 6.96 (d, 8.9 Hz, 8H,ArCH), 6.84 (d, 6.1 Hz, 8H,ArCH), 6.57 (d, 6.1 Hz, 8H,ArCH), 6.38 (m, 8H,*ArCH), 6.29 (m, 8H,*ArCH), 5.29 (s, 20H,Cp), 5.25 (s, 20H,Cp), 4.51 (m, 8H,CH$_2$), 3.96 (m, 4H,CH$_2$), 3.86 (m, 8H,CH$_2$), 3.59 (m, 8H,CH$_2$), 2.44 (m, 4H,CH$_2$), 2.13 (m, 4H,CH$_2$), 1.66 (s, 6H,CH$_3$), 1.53 (m, 4H,CH$_2$), 1.23 (m, 16H,CH$_2$), 1.18 (t, 6.6 Hz, 12H,CH$_3$) ^{13}C NMR (101 MHz, DMSO-d_6): δ = 172.9, 165.0, 157.5, 154.3, 151.7, 150.5, 150.2, 142.5, 132.0, 130.5, 130.1, 129.7, 129.2, 127.0, 125.1, 124.0, 121.0, 120.3, 119.9, 111.6, 104.1, 86.9, 79.6, 78.0, 77.7, 75.5, 75.2, 64.0, 62.5, 48.3, 45.0, 29.7, 29.0, 28.7, 28.1, 26.9, 25.4, 12.1. IR (v/cm^{-1}): 1720, 1728 (C=O).

4.4 General procedure for Nucleophilic Aromatic Substitution

Complexes containing organoiron moieties with terminal chloro groups were reacted with compounds containing phenolic groups in the presence of excess K$_2$CO$_3$ in DMF and stirred in the dark under N$_2$ for 18 h. The resulting mixtures were precipitated into 1.2 M HCl, containing equi-metal molar amounts of NH$_4$PF$_6$ and filtered through a sintered glass crucible, washed with water and dried under reduced pressure. The crude products were dissolved into a minimal amount of acetone and purified via re-precipitation into diethyl ether to afford complexes, **3.3**, **3.4** and **3.9**. The exact ratios for the starting materials are as follows:

Complex 3.3: Complex **3.2** (0.5 mmol), hetarylazo dye **2.22** (1.75 mmol), K$_2$CO$_3$ (3.5 mmol) in 12 mL DMF. Yield: 78%.

^{1}H NMR (400 MHz, DMSO-d_6): δ = 8.50 (s, 3H,ArCH), 7.92 (d, 8.3 Hz, 3H,ArCH), 7.87 – 7.82 (m, 12H,ArCH), 7.69 (d, 8.6 Hz, 6H,ArCH), 7.39 (d, 8.8 Hz, 6H,ArCH), 7.33 (d, 8.3 Hz, 3H,ArCH), 6.98 (d, 8.8 Hz, 6H,ArCH), 6.86 (d, 8.6 Hz, 6H,ArCH), 6.76 (d, 6.7 Hz,

6H,*ArCH), 6.43 (d, 6.8 Hz, 6H,*ArCH), 5.24 (s, 15H,Cp), 4.51 (br s, 6H,CH$_2$), 3.78 (br s, 6H,CH$_2$), 3.47 (m, 6H,CH$_2$), 3.35 (s, 9H,OCH$_3$), 1.10 (t, 6.8 Hz, 9H,CH$_3$) ^{13}C NMR (101 MHz, DMSO-d_6): δ = 174.8, 164.2, 163.8, 153.7, 150.8, 150.5, 144.6, 142.6, 137.7, 133.7, 131.8, 130.4, 128.5, 126.9, 125.2, 124.1, 123.8, 122.4, 121.5, 120.6, 116.9, 111.7, 103.9, 86.8, 79.5, 78.1, 76.7, 63.3, 55.0, 48.1, 44.7, 12.1. IR (v/cm^{-1}): 1732 (C=O).

Complex 3.4: Complex **2.23** (3.5 mmol), phloroglucinol (**2.11**) (1.0 mmol), K$_2$CO$_3$ (7 mmol) in 20 mL DMF. Yield: 80%.

^{1}H NMR (400 MHz, DMSO-d_6): δ = 7.91 (d, 9.0 Hz, 6H,ArCH), 7.77 (d, 9.2 Hz, 6H,ArCH), 7.43 (d, 9.0 Hz, 6H,ArCH), 6.85 (d, 9.2 Hz, 6H,ArCH), 6.71 (s, 3H,ArCh), 6.44 (d, 6.9 Hz, 6H,*ArCH), 6.41 (d, 6.9 Hz, 6H,*ArCH), 5.26 (s, 15H,Cp), 3.60 (m, 6H,CH$_2$), 3.51 (m, 12H,CH$_2$), 1.14 (t, 7.0 Hz, 9H,CH$_3$) ^{13}C NMR (101 MHz, DMSO-d_6) δ = 160.8, 155.7, 154.1, 150.8, 150.2, 142.1, 129.9, 129.6, 125.2, 123.9, 121.0, 111.3, 105.2, 78.1, 75.6, 75.5, 58.3, 52.2, 45.2, 12.0.

Complex 3.9: Complexes **2.10** (3.5 mmol) and **2.15** (1.0 mmol), K$_2$CO$_3$ (7 mmol) in 20 mL DMF. Yield: 86%.

^{1}H NMR (400 MHz, DMSO-d_6) δ = 7.90 (d, 8.6 Hz, 8H,ArCH), 7.76 (d, 8.6 Hz, 8H,ArCH), 7.43 (d, 8.8Hz, 8H, ArCH), 7.37 (m, 8H,ArCH), 7.26 (m, 8H,ArCH), 6.82 (d, 7.9Hz, 8H,ArCH), 6.41(d,6.7Hz,8H,*ArCH)6.39-6.25 (m, 16H,*ArCH overlap ArCH), 5.25 (s, 20H,Cp), 4.82 (t, 5.4 Hz, 4H,OH), 3.95 (m, 4H,CH$_2$), 3.60 (m, 8H,CH$_2$), 3.49 (m, 16H,CH$_2$), 2.41 (m, 4H,CH$_2$), 2.10 (m, 4H,CH$_2$), 1.66 (s, 6H,CH$_3$), 1.52 (m, 4H,CH$_2$), 1.23 (m, 16H,CH$_2$), 1.14 (t, 6.3 Hz, 12H,CH$_3$) ^{13}C NMR (101 MHz, DMSO-d_6): δ = 174.83, 164.2, 163.8, 153.7, 150.8, 150.5, 144.6, 142.6, 137.7, 131.8, 130.8, 128.5, 126.9, 125.2, 124.1, 123.8, 122.4, 121.5, 120.6, 116.9, 111.7, 103.9, 86.9, 79.5, 78.0, 76.7, 64.0,55.0, 48.1, 43.4, 37.5, 30.8, 21.4, 12.1. IR (v/cm^{-1}): 1721 (C=O).

4.5   General procedures for arylazo dye synthesis

The amine was dissolved in a solution of 5 mL conc. HCl in 20 mL water and cooled to 0-5 °C. Sodium nitrite ($NaNO_2$) was dissolved in 10 mL water and added dropwise to the stirring mixture, ensuring that the reaction mixture remained cooled to 0-5 °C and stirred for 1 h. Sulfamic acid was added to the solution to remove any traces of nitrous acid. Subsequently, the coupling reagent was dissolved in glacial acetic acid (20 mL) and water (50 mL), and transferred to the diazo solution. The reaction was stirred overnight and sodium acetate (NaOAc) was added in small amounts until a pH of 4-5 was achieved. The reaction continued to stir for 48 h, and the resulting precipitate was collected in a Buchner funnel, washed with water, and dried under reduced pressure. The exact ratios for the starting materials are as follows:

Azo dye 2.17: Compound **2.13** (10 mmol), **2.16** (10 mmol), and $NaNO_2$ (10 mmol).Yield: 64%.

^{1}H NMR (400 MHz, acetone-d_6) δ=7.76(d, 4.3Hz, 2H, ArCH), 7.74 (d, 3.6Hz, 2H, ArCH), 6.96 (d, 8.9Hz, 2H, ArCH), 6.86 (d, 9.6Hz, 2H, ArCH), 3.82 (m, 4H, CH_2), 3.68 (t, 5.6Hz, 4H, CH_2). ^{13}C NMR (101 MHz, acetone-d_6): δ=160.0, 151.4, 147.6, 144.3, 125.2, 124.8, 116.5, 112.5, 60.3, 55.1. IR (v/cm^{-1}): 3430 (OH).

Thioether disazo dye 2.19: Compound **2.18** (15 mmol), **2.14** (30 mmol), and $NaNO_2$ (30 mmol). Yield: 67%.

^{1}H NMR (400 MHz, DMSO-d_6): δ = 7.78 (d, 8.4 Hz, 4H, ArCH), 7.76 (d, 9.2 Hz, 4H, ArCH), 7.49 (d, 8.4 Hz, 4H, ArCH), 6.83 (d, 9.2 Hz, 4H, ArCH), 3.59 (m, 4H, CH_2), 3.49 (m, 8H, CH_2), 1.14 (t, 6.4 Hz, 6H, CH_3). ^{13}C NMR (101 MHz, DMSO-d_6): δ = 151.6, 150.8, 142.2, 135.7, 131.3, 125.2, 122.8, 111.2, 58.3, 52.1, 45.1, 12.0. IR (v/cm^{-1}): 3337 (OH).

4.6 Synthesis of hetarylazo dye 2.22 [91]

2-Amino-6-methyloxybenzothiazole **2.21** (25 mmol) and 25 mL 50% H_2SO_4 were combined and stirred for 20 min at room temperature. The reaction was cooled to $0-5$ °C and $NaNO_2$ (25 mmol) was added portion-wise to the amine while it was on ice. The reaction was stirred for 1 h at $0-5$ °C. Phenol **2.20** (25 mmol) was dissolved in 20 mL HCl (conc.) and 100 mL H_2O and cooled to $0-5$ °C. The diazonium solution was poured into the coupler solution, and 200 mL H_2O added. The resulting mixture was stirred for 30 min. The crude precipitate was isolated by filtration and allowed to dry. The solid was suspended in 250 mL H_2O and NH_4OH added until the solution was basic. The product was collected by filtration and allowed to dry .Yield: 37.5%

^{1}H NMR (400 MHz, DMSO-d_6): δ = 7.98 (d, 8.2 Hz, 1H, ArCH), 7.93 (d, 7.9Hz, 2H,ArCH), 7.88 (s, 1H,ArCH), 6.83 (dd, 8.2Hz, 2.09 Hz, 1H,ArCH), 7.01 (d, 8.9Hz, 2H,ArCH), 2.47 (s, 2H,OCH_3). *consistent with previously reported structure, therefore ^{13}C NMR was not performed.

Chapter 5. Conclusions and future work

In conclusion, the preparation of novel star-shaped organoiron oligomers containing bridging azo chromophores was accomplished using both convergent and divergent methods via metal-mediated nucleophilic aromatic substitutions and ester condensation reactions with tri- and tetra-functional core molecules. For the first generation star, the convergent method is used with less steric defects, while the second generation is afforded via divergent method with less steric hindrance. Characterization of these oligomers was performed using spectroscopic analysis such as one- and two-dimensional NMR and infrared spectroscopies. UV-visible studies were conducted for complexes **3.8** and **3.10** as examples. Upon the addition of HCl, complexes **3.8** and **3.10** exhibited bathochromic shifts over 130 nm and the colour changed from red to purple. Upon the addition of sodium hydroxide, the complexes underwent a reversible colour change. The cyclic voltammetric study of star-shaped oligomer **3.10** containing eight iron centres showed that the eighteen- to nineteen-electron iron centers were reversibly reduced at $E_{1/2} = $ -1.53 V.

In addition, this thesis established a series of star-shaped organoiron oligomers containing bridging azo chromophores that can be used in higher generations of dendrimer divergent synthesis. In theory, by utilizing the repeating metal-mediated nucleophilic aromatic substitutions and ester condensation reactions, the organoiron moieties and the azo dyes could be added infinitely. However, in reality, the divergent synthesis usually faces the problems of low reaction yield and difficulty in purification. In future studies, with the increasing number of branches, the proper ratio of reagents, and the reaction conditions could be further studied, along with modification of the purification methods.

Another extension for the project is to form hyperbranched polymers based on the star-shaped oligomers prepared in this thesis. Using A_2+B_x polymerization, star-shaped molecules

are able to react with common diols, dithiols or dichloroarenecomplexes to yield hyperbranched polymers that find applications in coatings, cross-linking and melt additives, nanoporous materials, catalysis, and soluble functional supports.[36] Therefore, continuing work will be focused on the synthesis of hyperbranched azo chromophore-containing organoiron polymers, the variation of starting materials, and the difference between azo chromophores containing organoiron hyperbranched polymers and the organoiron hyperbranched polymers in solubility, thermal stability, and viscosity.

References

1. Carraher, C. E. In *Introduction to Polymer Chemistry;* CRC Press Taylor & Francis: Boca Raton FI, 2007; pp 1-503.

2. Flory, P. J. In *Principles of Polymer Chemistry*; Cornell U.P.: New York, 1953; p 672.

3. Morris, K. In *The History of PVC*; Maclaren: London, 1969.

4. Tomalia, D. A. *Mater. Today* **2005**, *8*, 34.

5. Newkombe, G.R.; Moorefield, C. N.; Vőegtle, F. In *Dendrimers and Dendrons*: *Concepts*, *Syntheses*, *Applications*; Wiley-VCH: Weinheim, 2001.

6. Martin, I.K.; Twyman, L.J. *Tetrahedron Lett.* **2001**, *42,* 1119-1121.

7. Fréchet, J.M.J. *Science* **1994**, *263,* 1710-1715.

8. An, S.G.; Cho, C.G. *Macromol. Rapid Commun.* **2004**, *25,* 618-622.

9. Fritz, V.; Gabriele, R.; Nicole, W. In *Dendrimer Chemistry*; Wiley-VCH: Weinheim, 2009.

10. Buhleier, E.; Wehner, W.; Vőegtle, F. *Synthesis* **1978**, 155-158.

11. Tomalia, D.A.; Baker, H.; Dewald, J.; Hall, M.; Kallos, G.; Martin, S.; Roeck, J.; Ryder, J.; Smith, P. *Macromolecules* **1986**, *19*, 2466-2468.

12. Rempp, P.; Herz, J.E. In *Encyclopedia of Polymer Science and Engineering*, *Ed. 2*; Wiley: New York, 1989; p 793.

13. Shen, X.; Liu, H.; Li, Y.; Liu, S. *Macromolecules* **2008**, *41,* 2421-2425.

14. Rein, D.; Lamps, J.P.; Lutz, P.; Papanagopoulos, D.; Tsitsilianis, C. *Acta Polymerica* **1993**, *44,* 225-229.

15. Fréchet, J.M.J., Tomalia, D.A. In *Dendrimers and Other Dendritic Polymers*; Wiley: New York, 2002.

16. Wooley K.L.; Hawker, C.J.; Fréchet, J.M.J. *J. Am. Chem. Soc*. **1991**, *113,* 4252-4261.

17. Klopsch, R.; Franke, P.; Schlüter, A.D. *Chem. Eur. J.* **1996**, *2,* 1330-1334.

18. L'Abbe', G.; Forier, B.; Dehaen, W. *Chem. Commun.* **1996**, 2143-2144.

19. Stoddart, F.J.; Welton, T. *Polyhedron* **1999**, *18,* 3575-3591.

20. Astruc, D.; Boisselier, E.; Ornelas, C. *Chem. Rev.* **2010**, *110*, 1857.

21. Dandliker, P.J.; Diederich, F.; Gross, M.; Knobler, C.B.; Louati, A.; Sanford, E.M. *Angew. Chem., Int. Ed. Engl.* **1994**, *33,* 1739-1741.

22. Issbemer, J.; Vöegtle, F.; De Cola, L.; Balzani, V. *Chem. Eur. J.* **1997**, *3,* 706-712.

23. Serroni, S.; Campagna, S.; Puntoriero, F.; Loiseau, F., Ricevuto, V.; Passalacqua, R.' Galletta, M. *C. R. Chimie* **2003**, *6,* 883-893.

24. Newkome, G.R.; Cardullo, F.; Constable, E.C.; Moorefield, C.N.; Thompson, A.M.W.C. *J. Chem.* Soc., *Chem. Commun.* **1993**, 925-927.

25. Alonso, B.; Armada, P.G.; Losada, J.; Cuadrado, I.; Gonzalez, B.; Casado, C.M. *Biosens. Bioelectron.* **2004**, *19,* 1617-1625.

26. Mond, L; Langer, C. *J. Chem. Soc., Trans.* **1891**, *59,* 1090-1093.

27. Pearson, A.J. In *Iron Compounds in Organic Synthesis*; Academic Press: London, 1994.

28. Kealy, T.J., Pauson, P.L. *Nature* **1951,** *168,* 1039-1040.

29. Astruc, D.; Hamon, J.R.; Althoff, G.; Roman, E.; Batail, P.; Michaud, P.; Mariot, J.P.; Varret, F.; Cozak, D. *J. Am. Chem. Soc.* **1979**, *101,* 5445-5447.

30. Trujillo, H.; Casado, C.M.; Astruc, D. J. *Chem. Soc.*, *Chem. Commun.* **1995**, 7.

31. Casado, C.M.; Wagner, T.; Astuc, D. *J. Organomet. Chem.* **1995**, *502,* 143-146.

32. Gill, T.P.; Mann, K.R. *Inorg. Chem.* **1983**, *22,* 1984-1986.

33. Valério, C.; Alonso, E.; Ruiz, J.; Blais, J.C.; Astruc, D. *Angew. Chem. Int. Ed. Engl.* **1999**, *38,* 1743-1747.

34. Valerio, J.; Ruiz, E.; Alonso, P.; Boussaguet, J.; Guittard, J.C.; Blais, D.; Astruc. Bull. *Soc. Chim. Fr.* **1997**, *134,* 907-909.

35. Astruc, D. *Pure Appl. Chem.* **2003**, *75*, 461-481.

36. Abd-El-Aziz**,** A.S.; Carruthers, S.A.; Todd**,** E.K.; Afifi, T.H.; Gavina**,** J.M.A. *J. Polym. Sci. Part A: Polym. Chem.* **2005**, *43,* 1382-1396.

37. Froehling, P.E. *Dyes Pigments* **2001**, 48, 187-195.

38. Neckers, D.C. In *Mechanistic Organic Photochemistry*; Reinhold: New York, 1967.

39. Zollinger, H. In *Azo and Diazochemistry;* Interscience: New York, 1961.

40. Griffiths, J. *J. Chem. Soc. Rev.* **1972**, *1,* 481-493.

41. Hartley, G.S. *J. Chem. Soc.* **1938**, 633-642.

42. Irjer, M.; Hiramo, K.; Hashimoto, S.; Hayashi, K. *Macromolecules* **1981**, *14,* 262-267.

43. Tawa, K.; Kamada, K.; Sakaguchi, T.; Ohta, K. *Appl. Spectrosc.* **1998**, *52,* 1356.

44. Viswanathan, N.K.; Kim, D.Y.; Bian, S.P.J. *Mater. Chem.* **1999**, *9,* 1941-1955.

45. Wu, Y.; Demachi, Y.; Tsutsumi, O.; Kanazawa, A.; Shiono, T.; Ikeda, T. *Macromolecules* **1998**, *31,* 349-354.

46. Irie, M. *Adv. Polym. Sci.* **1990**, *94,* 27-67.

47. Archut, A.; Vögtle, F.; De Cola, L.; Azzellini, G.C.; Balzani,V.; Ramanujam, P.S.; Berg, R.H. *Chem.Eur. J.* **1998**, *4,* 699-705.

48. Archut, A.; Azzellini, G. C; Balzani, V; De Cola, L; Vögtle, F. *J. Am. Chem. Soc.* **1998**, *120*, 12187-12191.

49. Gopalan, P.; Katz, H.E.; Mcgee, D.J.; Erben, C.; Zielinski, T.; Bousquet, D.; Muller, D.; Grazul, J.; Olsson, Y. *J. Am. Chem. Soc.* **2004**, *126,* 1741**-**1747.

50. Abd-El-Aziz, A.S.; Afifi, T.H.; Budakowski, W.R.; Friesen, K.J.; Todd, E.K. *Macromolecules* **2002**, *35*, 8929-8932.

51. Abd-El-Aziz, A.S.; Manners, I. *J. Inorg. and Organomet. Polym. and Mater*. **2005**, *15*, 157-195.

52. Abd-El-Aziz, A.S.; Okasha, R.M.; Afifi, T.H.; Todd, E.K. *Macromol. Chem. Phys.* **2003**, *204*, 555-563.

53. Abd-El-Aziz, A.S.; Okasha, R.M.; Shipman, P.O.; Afifi, T.H. *Macromol. Rapid Commun.* **2004**, *25*, 1497-1503.

54. Abd-El-Aziz, A.S.; Shipman, P.O.; Shipley, P.R. *Macromol. Rapid Commun*. **2010**, *31*, 459-466.

55. Coffield, T.H.; Sandel, V.; Closson, R.D. *J. Am. Chem. Soc.* **1957**, *79,* 5826.

56. Nesmeyanov, A.N.*;* Vol'kenau, N.A.*;* Bolesova, I.N. *Dokl Akad Nauk SSSR.* **1963**, *149,* 615-618.

57. Nesmeyanov, A.N.; Vol'kenau, N.A.; Bolesova, I.N. *Tetrahedron Lett.* **1963**, *25,* 1725-1729.

58. King, R.B. In *Arene Complexes, The Organic Chemistry of Iron;* Academic Press: New York, 1981, Vol. 2, pp 155-187.

59. Astruc, D.; Dabard, R. *Tetrahedron* **1976**, *32*, 245-249.

60. Astruc, D. In *Organometallic Chemistry and Catalysis;* Springer-Verlag: New York, 2007; p 608.

61. Tsierkezos, N. *Journal of Solution Chemistry* **2007**, *36,* 289-302.

62. Bond, A.M.; Oldham, K.B.; Snook, G.A. *Anal. Chem.* **2000**, *72,* 3492-3496.

63. Nesmeyanov, A.N.; Vol'kenau, N.A.; Petrovskii, P.V.; Kotova, L.S.; Petrakova, V.A.; Denisovich, L.T. *J. Organomet. Chem.* **1981**, *210,* 103-113.

64. Abd-El-Aziz, A.S., Bernardin, S. *Coordination Chemistry Reviews*. **2000**, *203,* 219-267.

65. Haslam, E. *Tetrahedron 1980*, *36*, 2409-2433.

66. Neises, B.; Steglich, W. *Angew. Chem. Int. Ed.*, **1978**, *17,* 522-524.

67. Abd-El-Aziz, A.S.; Corkery, T.C.; Todd, E.K.; Afifi, T.H.; Ma, G Z. *J. Inorg. Organomet. Polym.* **2003**, *13,* 113-130.

68. Abd-El-Aziz, A.S.; Todd, E.K.; Afifi, T.H. *Macromol. Rapid Commun.* **2002**, *23,* 113-117.

69. Abd-El-Aziz, A.S.; May, L.J.; Edel, A.L. *Macromol. Rapid Commun.* **2000**, *21,* 598-602.

70. Moroni, M.; Le Moigne, J.; Luzzati, S. *Macromolecules* **1994**, *27,* 562-57.

71. Yamaguchi, I.; Osakada, K.; Yamamoto, T. *Macromolecules* **1998**, *31,* 8731-8736.

72. Teetsov J., Fox M.A. *J. Mater. Chem.* **1999**, *9,* 2117-2122.

73. Zollinger, H. In *Azo and Diazo Chemistry;* Interscience Publishers: New York, 1961.

74. Allen, R.L.M. In *Colour Chemistry*; Appleton-Century-Crofts: New York, 1971.

75. Mehta, H.P.; Peters, A.T. *Dyes Pigm.* **1981**, *2,* 259-269.

76. Mehta, H.P.; Peters, A.T. *Dyes Pigm.* **1982**, *3,* 71-78.

77. Hallas, G.; Towns, A.D. *Dyes Pigm.* **1997**, *33,* 319-336.

78. Abd-El-Aziz, A.S.; Afifi, T.H. *Dyes Pigm.* **2006**, *70,* 8-17.

79. Yazdanbakhsh, M.R.; Giahi, M.; Mohammadi, A. *J. Mol. Liq.* **2009**, *144,* 145-148.

80. Hepworth, J.D.; Mason, D.; Hallas, G.; Marsden, R. *Dyes Pigm.* **1985**, *6,* 389-396.

81. Marcandalli, B.; Bellobono, I.R.; Selli, E.; Polissi, A. *Dyes Pigm.* **1987**, *8*, 239-251.

82. Ya, Q.; Dong, X.; Chen, W.; Duan, X. *Dyes Pigm.* **2008,** *79,* 159-165.

83. Rangnekar, D.W.; Chaudhari, M.B. *Dyes Pigm.* **1989**, *10,* 173-181.

84. Hallas, G.; Towns, A.D. *Dyes Pigm.* **1997**, *33,* 319-336.

85. Annen, O.; Egli, R.; Hasler, R.; Henzi, B.; Jakob, H.; Matzinger P. *Rev. Prog. Color. Relat. Top.* **1987**, *17,* 72-85.

86. Zollinger, H. In *Diazo Chemistry I*; VCH: New York, 1994.

87. Yazdanbakhsh M.R; Mohammadi,A. *J. Mol. Liq.* **2009**,*148*,35-39.

88. Okada, Y.; Motomura, H.; Morita, Z. *Dyes and Pigments*, **1992**, *20,* 123 -135.

89. Seferoğlu, Z.; Ertan, N.; Yılmaz, E.; Uraz, G. *Color. Techn.* **2008**, *124,* 27-35.

90. Venkataraman, K. In *The Analytical Chemistry of Synthetic Dyes*; Wiley-Interscience Publication: New York, 1978.

91. Prajapati, A.K.; Bonde, N.L. *J. Chem. Sci.* (Bangalore, India) **2006**, *118,* 203-210.

92. Strohm, E .The Design of Organoiron-based Linear and Star-Shaped Molecules Containing Photoconductive Aryl- and Hetaryl-Azo Dyes. Chem 449. Thesis, The University of British Columbia, Kelowna, 2010.

93. Abd-El-Aziz, A. S.; Strohm, E.; Ding, M.; Okasha,R.M.; Afifi, T. H.; Sezgin,S.;Shipley,P. *J. Inorg. Organomet. Polym. and Mater*.**2010**,*20*,592-603.

94. Szafran, Z.; Pike, R. M.; Singh, M. M. In *Preparation and use of ferrocene;* Microscale inorganic chemistry: A complete laboratory experience; John Wiley & Sons, Inc.: New York, US, 1991; pp 302-313.

95. Tawa, K.; Kamada, K.; Sakaguchi, T.; Ohta, K.; Yasumatsu, D.; Sekkat, Z.; Kawata, S. *Macromolecules* **2001**, *34*, 8232-8238.

96. Abd-El-Aziz, A. S.; Okasha, R. M.; Afifi, T. H. *J. Inorg. Organomet. Polym. and Mater*. **2004**, *14*, 269-278.